Aus dem Institut für Chirurgische Forschung
(im Walter-Brendel-Zentrum für Experimentelle Medizin, WBex)
der Ludwig-Maximilians-Universität München
ehem. Vorstand Prof. Dr. med. Ulrich Pohl
kommis. Vorstand Prof. Dr. med. dent. Reinhard Hickel

The role of the potassium channels $K_V1.3$ and $K_{Ca}3.1$ in arteriogenic smooth muscle cell proliferation

Dissertation
zum Erwerb des Doktorgrades der Naturwissenschaften (Dr. rer. nat.)
an der Medizinischen Fakultät
der Ludwig-Maximilians-Universität München

Vorgelegt von
Amelia Caballero Martínez

aus
Murcia, Spanien

2018

Mit Genehmigung der Medizinischen Fakultät

der Universität München

Betreuerin:	PD Dr. rer. nat. Elisabeth Deindl
Zweitgutachter :	Prof. Dr. Jürgen Bernhagen
Dekan:	Prof. Dr. med. dent. Reinhard Hickel
Tag der mündlichen Prüfung:	11.04.2019

Table of contents

Index of figures

Index of tables

Introduction

1. Introduction

1.1. Vascular remodelling

The vascular system is not a static vessel's network, but rather constantly changing to adapt to the body's and tissue's needs and maintain vascular homeostasis. In response to short-term alterations in hemodynamic forces exerted by the flowing blood or to humoral factors, especially oxygen, vessels adjust blood flow and flow distribution, regulating lumen diameters through vasoconstriction or vasodilation. However, when these alterations become longstanding, the vasculature responds by modifying its basal structure, changing the vascular network through the generation (angiogenesis) or elimination of vessels (pruning), and/or by remodelling the vessel's wall (Zakrzewicz, Secomb et al. 2002).

Vascular remodelling processes can result in increased (outward remodelling) or decreased lumen diameters (inward remodelling) and can develop in both physiological and pathological situations. Involved mechanisms are fibrosis, hyperplasia of the intima and media layers, changes in the extracellular matrix (ECM) and in case of pathological remodelling, endothelial dysfunction and/or arterial calcification (van Varik, Rennenberg et al. 2012). By switching to a synthetic phenotype, smooth muscle cells (SMCs) play a crucial role in some of these mechanisms. By migrating and proliferating in the intima they contribute to intimal thickening and by releasing elastolytic enzymes and synthesizing new matrix components, to the restructuring of the ECM (Doran, Meller et al. 2008, van Varik, Rennenberg et al. 2012).

In pathological remodelling, damage of the endothelium (endothelial dysfunction) occurring during angioplasty or the formation of atherosclerotic plaques often derive in inward remodelling that can result in stenosis of the vessel followed by ischemia in the downstream tissues (Patel, Waltham et al. 2010). Interestingly, to counterbalance ischemic damage in obstructive vascular diseases, vasculature spontaneously develops a physiological adaptive response: the outward remodelling of collateral arteries or arteriogenesis.

Arteriogenesis happens near the obstruction site and defines the growth of arterial anastomosis, or collateral arteries, bypassing the obstructed artery. The redirected blood from a feeding artery into the collaterals increases the hemodynamic forces that drive their development into physiological bypasses. Grown collateral arteries can indeed restore 30 to 40 % of the blood perfusion (Schaper 2009). Hence, therapeutic arteriogenesis represents the only option to mitigate ischemic symptoms of an obstructed artery.

To better understand arteriogenic remodelling, a basic knowledge of the structure and function of an artery wall is required and will be introduced next.

1.1.1. Artery wall

Vessels are composed of up to three different tissue layers or tunics, that from the vessel lumen to the outside are called tunica intima, media and adventitia (**Figure 1.1**). While capillaries are composed of a tunica intima solely, arteries and veins possess all three layers.

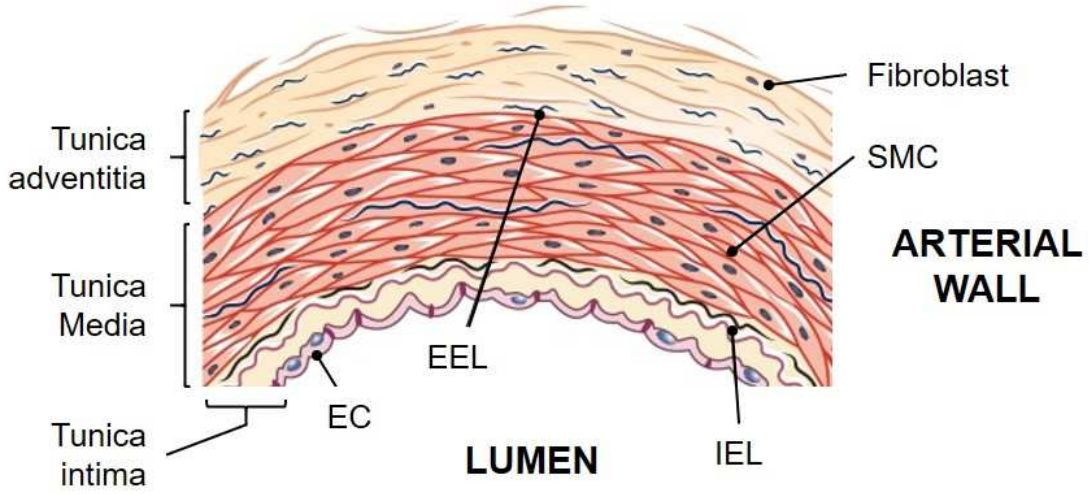

Figure 1.1: Schematic representation of an artery wall

Artery wall composed of the three tunics: intima, media and adventitia. The intima is formed usually by a single-cell lining of endothelial cells (ECs) and a basement membrane underneath. The media is composed of several layers of smooth muscle cells (SMCs) embedded in elastin sheets with collagen fibers and thin layers of proteoglycan-rich extracellular matrix (ECM). The adventitia is composed of fibroblasts in collagen-rich ECM. The interna elastic lamina (IEL) and the externa elastic lamina (EEL) separate the intima from the media and the media from the adventitia, respectively. Modified from (Hammes 2015).

The intima, or endothelium, is a single-cell lining of endothelial cells (ECs) covering the internal vessel surface, with a basement membrane underneath, constituted by connective tissue and elastin and collagen fibers. The tunica media is formed by one or more concentric layers of SMCs supported by elastin sheets with collagen fibers and thin layers of proteoglycan-rich ECM in-between. Finally, the outer adventitia is a layer of connective tissue composed of collagen-rich ECM and fibroblasts that holds the vessel in the tissue surrounding. In conductive arteries, between the intima and the media and between the media and the adventitia are located the internal and external elastic laminae (IEL and EEL), respectively, which provide structure to the vessel and allow the vessel to stretch.

1.1.1.1 ECs

ECs not only act as a transport barrier between the blood and the rest of the vessel, they regulate the equilibrium between thrombosis and haemostasis by separating their anticoagulant luminal surface with the strongly thrombogenic macromolecules of the basement membrane underneath (Félétou 2011). ECs also exert important functions in the control of lumen diameter, leukocytes trafficking and wound healing (Félétou 2011).

Due to blood flow, ECs are exposed to hemodynamical forces, one perpendicular to the wall - the blood pressure - and the other being parallel to the wall, and representing a frictional force at the surface of the endothelium, the fluid shear stress (FSS) (Davies 1995). Changes in FSS are sensed by ECs and are mechanotransduced via activation of cell membrane proteins, mechanosensitive ion channels, focal adhesion and integrins, G-protein linked receptors and/or mitogen-activated protein kinase (MAPK) signalling (Davies 1995). One of the most important physiological consequences of FSS changes sensed by ECs is the regulation of lumen diameter by the secretion of relaxing and contractile factors acting on the SMC layer underneath (Davies 1995). However, in response to long-term changes in FSS the endothelium initiates arterial remodelling processes (Resnick, Yahav et al. 2003). Hence, while decreased blood flow and FSS lead to inward remodelling, increased flow and FSS results in enlargement of the lumen diameters as happens during arteriogenesis (Resnick, Yahav et al. 2003, Schaper and Scholz 2003).

1.1.1.2 SMCs

The principal function of differentiated SMCs is the regulation of lumen diameter and blood flow through vasoconstriction and vasodilation, in part in response to endothelial-released relaxing and contracting factors, or by sensing circumferential wall stress (CWS) (Jacobsen and Holstein-Rathlou 2012). CWS is directly proportional to the intravascular pressure and inversely proportional to wall thickness. Long-term changes in CWS can also induce vascular remodelling processes to preserve vascular homeostasis. To increased CWS, the media responds by thickening and vice versa (Jacobsen and Holstein-Rathlou 2012). SMCs retained plasticity allow them to dedifferentiate into a synthetic, high proliferative phenotype in response to a variety of environmental cues (Owens, Kumar et al. 2004). Proliferative SMCs are strongly involved in arterial remodelling by contributing to the thickening of the intima and restructuring of the ECM. Due to their pleiotropic functions, proliferative SMCs are targets for treatments of coronary artery disease as well as targets in therapeutic arteriogenesis (Grundmann, Piek et al. 2007, Stefanini and Holmes 2013) .

1.1.1.3 Function of vessels wall

The function of the vessel will determine the composition of its wall. Near the heart, elastic arteries are characterized by big lumen diameters and thick tunica intima with a substantial IEL and several sheets of SMCs layers in the tunica media. Their high elasticity helps stabilize blood pressure oscillations from pumping. Elastic arteries branch into muscular arteries, with lower percentage of elastic fibers but thicker tunica media and play an important role in vasoconstriction.

Arteries branch to arterioles of around 30 µm of diameter which walls are much thinner, with a tunica media of one or two SMC layers. SMCs in arterioles are slightly contracted, leading to a basal arteriolar vasoconstriction, called vascular tone, regulated under neural and chemical control (Jackson 2000). Hence, arterioles are referred to as resistance vessels since they considerably slow down blood flow causing a rise in blood pressure.

Arterioles eventually end into small capillaries. Through the thin capillary walls composed solely of an intima layer, gases, nutrients and metabolites are exchanged between blood and tissue. Finally, the less-oxygenated blood is returned to the heart from capillaries via venules and veins.

1.1.2. Collateral circulation

Arterioles occasionally end into a conductive artery without capillary branching in-between, building so arterio-arteriolar anastomoses. These arterioles are called collateral arteries and can be found in both the heart and the peripheral circulation.

The existence of a collateral circulation is known since the 18th century (Ziegler, Distasi et al. 2010). Repetitively during history, cardiologists have described the existence of such anastomoses in the heart bypassing obstructed arteries and correlating with better outcomes. Due to low resolution techniques unmasking small arterioles, the origin and formation of these grown collateral arteries have been for long subject of debate. Were they formed *de novo* or were they growing from pre-existing arteriolar anastomoses? In the 1960's, by using more sensitive techniques, Fulton and Baroldi concurrently demonstrated in post-mortem heart angiograms that collaterals had developed from pre-existing arteriolar connections (Baroldi, Mantero et al. 1956, Fulton 1963). In fact, collateral arteries are nowadays well characterized (Faber, Chilian et al. 2014).

Histologic- and morphologically, there is no difference between an arteriole and a collateral artery at rest. Like arterioles, collaterals are composed of a tunica intima, a prominent IEL,

a tunica media with one or two layers of SMCs and a tunica adventitia (Scholz, Ziegelhoeffer et al. 2002). Their diameters vary depending on the species, in mice, they are usually smaller than 50 µm (Ziegler, Distasi et al. 2010). Even so, resting collateral arteries can be distinguished from normal arterioles in that blood enters the collaterals from the two anastomotic ends simultaneously and is drained from branches localized along the collateral length. A pulsatile collateral flow prevents haemostatic thrombosis and results in almost no net flow near the midpoint of the collateral. It is thought that collaterals optimize regional metabolic control of oxygen delivery in healthy tissues and serve as scaffolds for delivery of blood flow to parenchymal tissue between adjacent artery trees (Faber, Chilian et al. 2014).

1.1.3. Arteriogenesis

Since the identification of arteriogenesis as a remodelling process occurring in pre-existent arteriolar anastomoses and differing from angiogenesis - the sprouting or splitting of pre-existing capillaries - (Schaper, De Brabander et al. 1971), extensive research has been performed in the field. Several *in vivo* models, especially the femoral artery ligation (FAL) model have considerably contributed to identify underlying molecular mechanisms and cellular players (Limbourg, Korff et al. 2009, Schaper 2009).

Following the obstruction of a feeding artery, a pressure gradient is established between the prestenotic high-pressure bed and the poststenotic low-pressure bed, leading to a rise in blood flow and flow velocity through the collaterals (**Fig 1.2, A** and **B**) (Pipp, Boehm et al. 2004). As a consequence, FSS, a force proportional to the flow velocity and exerted onto ECs rises and is mechanotransduced by the endothelium into diverse biochemical signalling pathways initiating the arteriogenic process (Schaper and Scholz 2003). Collateral vasodilation occurs and is mediated by nitric oxide (NO), prostacyclin and endothelium-derived hyperpolarization factor (EDHF) (Unthank, Nixon et al. 1996, Schaper and Scholz 2003, Troidl, Troidl et al. 2009). However, since FSS is inversely proportional to the cube of the radius, small increases in lumen diameter due to vasodilation and arterial remodelling lead to a substantial drop of its value. Hence, other mechanisms contribute to further arterial remodelling such as an increase in CWS and the recruitment of perivascular cells (Schaper and Scholz 2003).

An early FSS-induced upregulation of endothelial adhesion molecules, such as Intercellular adhesion molecule 1 (ICAM-1) and Vascular cell adhesion molecule 1 (VCAM-1) as well as vascular endothelial growth factor (VEGF-A) participate in the recruitment of leukocytes,

principally monocytes (Scholz, Ito et al. 2000). Besides macrophages, a role of mast cells which degranulate around growing collateral arteries further supports leukocytes recruitment and cell proliferation by releasing growth factors (GFs) and cytokines (Chillo, Kleinert et al. 2016). Platelets activation also mediates leukocyte recruitment by facilitating leukocytes adhesion to the activated endothelium (Chandraratne, von Bruehl et al. 2015). Monocyte chemoattractant protein 1 (MCP-1) chemotaxis gradient generated by SMCs upon increase in CWT and stretch further guides monocytes towards the vessel's wall (Demicheva, Hecker et al. 2008) (**Fig 1.2, B**).

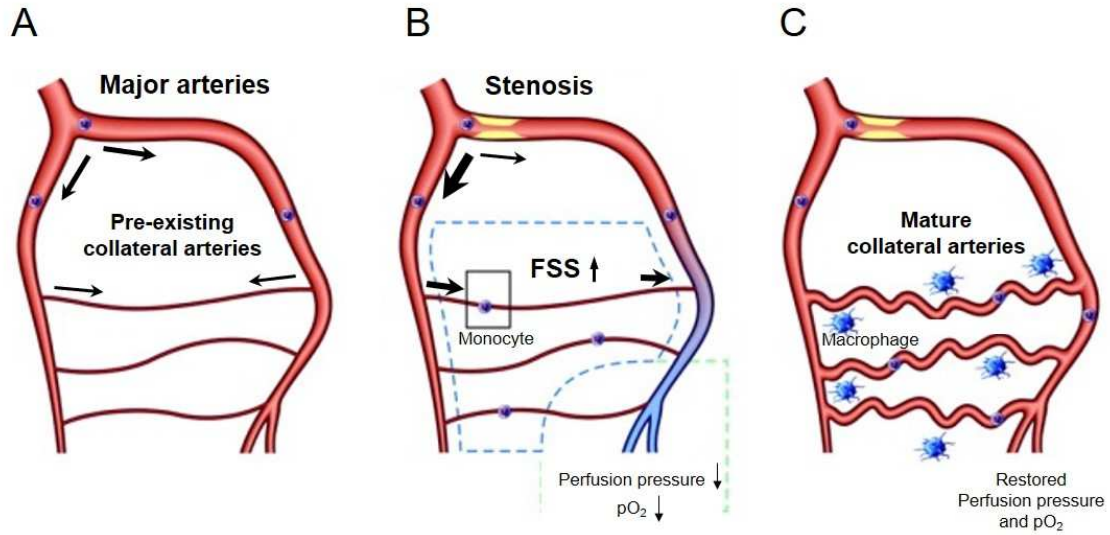

Figure 1.2: Arteriogenesis

A. Pre-existing collateral arteries as arterio-arteriolar anastomosis. **B**. In the presence of an arterial obstruction, the formation of a pressure gradient in the extremes of the collateral arteries establishes an increased blood flow from a supplying artery. Blood flow is accompanied by a rise in FSS sensed by the EC layer, inducing a vasodilation first, followed by recruitment of monocytes. **C**. Collateral arteries grow in diameter and length and act as physiological bypasses restoring blood perfusion of the downstream tissue and palliating so ischemic-damage. Modified from (Schirmer, van Nooijen et al. 2009).

Macrophages and mast cells orchestrate then collateral growth by secreting GFs and matrix proteases, inducing proliferation of ECs and SMCs and degrading the IEL and basal membrane to provide room for the proliferating cells (Arras, Ito et al. 1998, Heil, Eitenmuller et al. 2006, Schaper 2009, Chillo, Kleinert et al. 2016). Recently, we demonstrate a role of vascular arginase in recruitment of M2 macrophages through the regulation of *Icam-1* expression in collateral arteries (Lasch, Caballero-Martinez et al. 2016). M2 macrophages localize within the adventitial space of growing collaterals where they might be involved in matrix rebuilding and new space formation for the growing collateral (Troidl, Jung et al. 2013). Depending on the species, collateral arteries can increase their diameter 2 to 20-fold and their tissue mass up to 50-fold. The grow in diameter

and in length gives mature collaterals their characteristic tortuosity (Schaper 2009) (**Fig 1.2, C**). As collateral vessels mature, SMCs re-synthesize the wall matrix building the platform for the grown collateral vessel. Matrix proteins also contribute to the re-differentiation of SMCs, that finally rearrange into circulatory layers and establish cell-to-cell contacts (Schaper 2009).

1.2. Epidemiology of cardiovascular diseases (CVDs)

1.2.1. CVDs and atherosclerosis

Cardiovascular diseases (CVDs) constitute the major cause of mortality worldwide (WHO 2015). Indeed, in 2015, the World Health Organisation (WHO) estimated that annually 17.7 million people die from CVDs, representing 31 % of all global death.

The most common disorders are coronary heart disease (CHD), cerebrovascular disease and peripheral artery disease (PAD), diseases affecting arteries supplying heart muscle, the brain or arms and legs, respectively.

The main cause of CVDs is atherosclerosis, a chronical arterial disease characterized by lipid deposition and oxidation at the luminal layer of the vascular vessels that can cause the narrowing of the vessels to even stenosis or to thrombotic events. The disease is influenced by unmodified factors such as hyperlipidaemia diseases or genetic susceptibility (genetic history), but also by life habits such as smoking, physical inactivity, obesity, diabetes mellitus and hypertension (Herrington, Lacey et al. 2016).

The severity of the symptomatology will depend on localization and sequential events of the plaque. The lipid deposits are phagocytosed by macrophages that transform into foam cells. In an advanced stage, these accumulations develop into fibroatheromas characterized by the disruption of the intimal structure, an enrichment in collagen-rich fibrous tissue and apoptosis and necrosis of the underlying macrophages and SMCs layers (Bentzon, Otsuka et al. 2014). The slow narrowing of a coronary artery usually leads to stable angina pectoris. While if the narrowing occurs in a leg artery, it generates intermittent arterial claudication mostly during exercise. This relatively slow reduction of the vessel lumen occurs due to the growth of the fibrous tissue forming the fibrotic cap or to an aberrant proliferation of SMCs leading to neointima hyperplasia (Bentzon, Otsuka et al. 2014). However, a more dramatic situation appears when the rupture of the fibrotic cap or the exposure of the highly haemorrhagic necrotic core leads to thrombus formation, that can suddenly partially or even totally obstruct the affected artery or a nearby artery (Bentzon, Otsuka et al. 2014).

Thrombotic obstruction of a supplying brain artery can lead to ischemic stroke, while the obstruction of a coronary artery can cause myocardial infarction or even heart failure. In PAD, thrombotic obstruction can lead to rest pain and even gangrene and amputation (Ziegler, Distasi et al. 2010).

1.2.2. Current treatments for atherosclerotic-driven CVDs

In high-income countries, mortality rates for CVDs have decreased in the last decades due to changes in health habits - such as smoking cessation, healthy diet and exercise activity - and treatment improvements (Herrington, Lacey et al. 2016).

Besides vasodilators and anti-thrombotic drug treatments, physicians have developed two different revascularization strategies to free obstructed arteries in CVDs: angioplasty and bypass surgery. Angioplasty is a nonsurgical procedure used to open an artery at the site of an atherosclerotic plaque, whereby a balloon with or without stent is introduced through a catheter and inflated at the obstructed site. Stents contribute to stabilize artery wall and the new generation of drug-eluding stents (DES), releasing anticoagulant or intimal growth inhibitors, has proven to significantly reduce the risk of thrombus formation and in-stent restenosis (Haas, Lloyd et al. 2012). An alternative to angioplasty is bypass surgery, usually preferred in patients with several atherosclerotic arteries. This technique consists in the implantation of vessel grafts circumventing the obstructed zone of the affected artery. The efficacy and safety of coronary bypass surgery and coronary angioplasty with DES deployment have been compared by several randomized trials, showing no clear advantages for the one over the other (Al Ali, Franck et al. 2014, Fanari, Weiss et al. 2015).

However, revascularization therapies are not always recommended in patients with CHDs as they do not always result in clear survival benefits over medical therapy alone (Fox, Garcia et al. 2006). Hence, while revascularization improves survival in acute coronary syndromes, no prognostic benefits have been observed with coronary angioplasty in stable coronary artery disease usually performed to relieve symptomatic (Degen, Millenaar et al. 2014, Al-Lamee, Thompson et al. 2018). Patients with high-procedure morbidity and mortality, with a non-significant coronary stenosis (with less than 50 %) or with mild or with no symptoms of ischemia, are usually treated with medical therapy alone (Fox, Garcia et al. 2006). However, all these patients may benefit from another therapeutic option, the pharmacological induction of arteriogenesis.

1.2.3. Limitations of physiological arteriogenesis

Atherosclerosis-driven CVDs, sometimes remain asymptomatic due to the development of collateral arteries into physiological bypasses. In CHDs, numerous studies demonstrate a protective role of good versus poor coronary collateralization (Meier, Schirmer et al. 2013). Patients with a good collateralization tend to have smaller infarcts, improved ventricular function, fewer future cardiovascular events and improved survival (Berry, Balachandran et al. 2007, Meier, Hemingway et al. 2012).

Nevertheless, only a third of patients with hemodynamically significant atherosclerotic lesions still develop sufficiently grown coronary collaterals as to prevent signs of myocardial ischemia (Meier, Schirmer et al. 2013). Similarly, limitations of collateral growth are found in PAD patients too (Murrant 2008). Heterogeneity in the arteriogenic response against cardiovascular obstruction can be explained by the existence of both inherited and risk factors. Studies in a mice model for arteriogenesis have identified genetic differences between mouse strains as well as aging as factors influencing collateral density during embryonic development (collaterogenesis) and/or collateral growth in adulthood (Scholz, Ziegelhoeffer et al. 2002, Chalothorn and Faber 2010, Epstein, Lassance-Soares et al. 2012). Several genetic determinants have been identified in patients with CHD too, principally through analysis of monocytes transcriptomes (Chittenden, Sherman et al. 2006, Schirmer, Fledderus et al. 2008, Meier, Antonov et al. 2009, de Marchi 2014). In addition, factors known to induce atherosclerosis such as hypercholesterolemia, hypertension, hyperglycemia or obesity, could at the same time hamper collateral artery growth (de Groot, Pasterkamp et al. 2009).

Besides the above-mentioned factors, arteriogenesis also displays physiological limitations. Typically, only 30 to 40 % of functional blood flow can be restored by grown coronary and peripheral collaterals, respectively (Schaper 2009). This growth arrest has been explained by the rapid decrease in FSS, once the diameter of the collateral lumen increases as a consequence of the outward remodelling (Schaper 2009). Indeed, the study of Pipp et al with the arteriovenous shunt model, resulting into a constant raised FSS and in an impressive collateral artery growth demonstrated that anatomical restraints can be transcended. Hence, therapeutic stimulation of collateral growth may improve the formation of a strong collateral network in patients with CVDs (Pipp, Boehm et al. 2004).

1.2.4. Therapeutic arteriogenesis

Several strategies have been followed to induce arteriogenic growth in patients (Hakimzadeh, Verberne et al. 2014). One has been the induction of increased shear stress in collaterals by means of physical exercise (Haas, Lloyd et al. 2012, Mobius-Winkler, Uhlemann et al. 2016). However, this kind of therapy is not suitable in patients with end-stage obstructive arterial disease who are unable to perform exercise training.

Another strategy has been based on the versatile role of monocytes recruited to the growing collaterals, fomenting vascular cell proliferation and matrix remodelling through the release of GFs and matrix degradation enzymes (Fung and Helisch 2012). Several compounds targeting monocytes recruitment and/or activation have been carried out in experimental settings with relative success. Despite the promising outcomes of such therapies, large randomized clinical trials have failed to show clear beneficial effects (Hakimzadeh, Verberne et al. 2014).

SMCs have also been targets in arteriogenesis by promoting their proliferation with GFs such as Fibroblast growth factor 2 (FGF-2) (Yang, Deschenes et al. 1996, Rissanen, Markkanen et al. 2003, de Paula, Flores-Nascimento et al. 2009). While in preclinical studies, FGF-2 could improve arteriogenesis, in a clinical trial, the beneficial effects in CHD patients were limited (Simons, Annex et al. 2002). Probably the time point of FGF administration is likely to be critical, as expression of the FGF-receptors is induced during a brief time window in the early phase of arteriogenesis (Deindl, Hoefer et al. 2003).

Besides GFs, several potassium (K^+) channels have been involved in SMCs phenotypic modulation and proliferation. Hence, K^+ channel inhibitors have been used to target SMCs proliferation in intima hyperplasia following angioplasty or allograft vasculopathy (Tharp, Wamhoff et al. 2008, Chen, Lam et al. 2013, Cidad, Novensa et al. 2014). The characterization of K^+ channels involved in arteriogenic SMC proliferation might open new ways to foster arteriogenesis in CVD patients.

1.3. SMCs in arteriogenesis

SMCs play a crucial role in arteriogenesis, not only as a principal cellular component of the vessel wall but also as a source of chemokines, proteolytic enzymes and new ECM components (Schaper 2009). To accomplish these new tasks, SMCs undergo a dedifferentiation process toward a synthetic/high-proliferative phenotype (Owens, Kumar et al. 2004).

1.3.1. SMC phenotypic modulation

SMCs differentiate during embryogenesis in cells with a clear function, the regulation of the vascular tone. SMC-specific contractile and contractile-associated proteins allow a fast modulation of cell morphology, that in a synchronized manner leads to changes in the lumen diameter of the vessels (Owens, Kumar et al. 2004). The expression regulation of SMC contractile genes is complex and involves both transcription factors (TFs) and transcriptional coactivators. SMCs contractile proteins have highly conserved CArG cis-element in their promoter recognized by the TF serum response factor (SRF). SRF however is not exclusive of the SMC lineage, since it also regulates the expression of cardiac- and skeletal-specific genes and early response and structural genes (Mack 2011). Specificity is achieved by Myocardin and Myocardin related transcription factors (MRTF) A and B, a family of transcriptional coactivators considered as the master regulators of the SMC lineage. The binding of Myocardin or MRTFs and additional coactivators to SRF regulates the SRF-dependent transcription of important SMC effector proteins like α-smooth muscle actin (α-SMA), smooth muscle myosin heavy chain (SMMHC), or smooth muscle 22 alpha (SM22-α) among others (Yoshida, Sinha et al. 2003, Wang and Olson 2004, Wang, Wang et al. 2004, Mack 2011).In adulthood however, diverse stimuli such as GFs, several matrix components or matrix degradation products secreted during vascular growth or vascular injury stimulate SMC phenotypic modulation (PM) toward a proliferative phenotype (Owens, Kumar et al. 2004, Mack 2011). Receptor tyrosine kinase (RTK) engagement and subsequent activation of the MAPK signalling pathway results in the phosphorylation of Myocardin and its consequent release from DNA binding. SRF is then recruited to a member of the ternary complex factor (TCF) family that recognizes E26 transformation-specific (Ets) box sequences in the promoters of early growth genes. So Myocardin and TCF members compete for SRF to control contractile gene versus early growth genes (Mack 2011).

1.3.2. Factors inducing SMC proliferation in arteriogenesis

GFs and their signalling through RTKs are strong SMCs mitogenic factors during arteriogenesis too. In a rabbit FAL model, Deindl et al. reported a strong expression of fibroblast growth factor receptor 1 (FGFR-1) in growing collateral arteries as early as 3h after FAL, mostly restricted to SMCs. Moreover, treatment with polyanethole-sulfonic acid (PAS), that blocks the binding of FGFR-1 with fibroblast growth factors (FGFs), resulted in poorer collateral artery growth (Deindl, Hoefer et al. 2003).

FGF-2 is the most relevant FGF in SMC proliferation. Monocytes, which adhere to the activated endothelium as early as 12h post ligation, strongly express FGF-2 (Arras, Ito et al. 1998, Scholz, Ito et al. 2000, Deindl, Hoefer et al. 2003). Mast cells are another source of FGF-2 as well as of platelet-derived growth factor ß (PDGF-BB), another strong SMC-mitogenic GF (Chillo, Kleinert et al. 2016). Consistently, application of FGF-2 following coronary artery stenosis boosted collateral artery growth in the canine heart and resulted in higher blood flow recovery after FAL (Lazarous, Scheinowitz et al. 1995, Yang, Deschenes et al. 1996). Interestingly, the combined administration of FGF-2 and PDGF-BB as well as transfer of both genes has been beneficial in promoting angiogenesis and arteriogenesis in the FAL model (Cao, Brakenhielm et al. 2003, de Paula, Flores-Nascimento et al. 2009). Moreover, FGF-2 induces platelet-derived growth factor receptor PDGFR-α and -ß expression and together enhance stabilization of collateral arteries (Kano, Morishita et al. 2005). Nonetheless, since deletion of FGF-2 in mice did not affect collateral growth in the FAL model (Sullivan, Doetschman et al. 2002), other FGFs might have similar functions, such as FGF-4 (Rissanen, Markkanen et al. 2003).

The relevance of RTK engagement and MAPK activation during arteriogenesis is reflected by the upregulation and activation of the MAPK members extracellular-signal regulated kinases 1 and 2 (ERK-1 and -2) (Eitenmuller, Volger et al. 2006). ERK activation in turn leads to an upregulation of the pro-arteriogenic TF early growth response 1 (EGR-1) expression. The role of EGR-1 in arteriogenesis has been studied in *Egr1* knockout mice undergoing FAL. Interestingly, EGR-1 deficiency leads to lower hind-limb perfusion recovery and poorer arteriogenesis, partially due to an inhibition of SMCs PM and proliferation (Pagel, Ziegelhoeffer et al. 2012).

Besides GFs, the matrix surrounding SMCs also regulates SMC phenotype. Hence, the proteolytic cleavage of the IEL and the basement membrane by matrix metalloproteinases (MMPs), release collagen I, fibronectin (FN) and elastin-derived peptides, which are

inducers of SMC PM and proliferation (Mochizuki, Brassart et al. 2002, Schaper 2009, Mack 2011). Collagen I and FN signal through integrin receptors and the nonreceptor tyrosine kinase focal adhesion kinase (FAK) leading to activation of the MAPK and Rho A signalling pathways regulating migration and proliferation of collateral SMCs (Eitenmuller, Volger et al. 2006, Mack 2011).

1.3.3. SMCs and matrix remodelling

In early arteriogenesis, SMCs, together with recruited monocytes, secrete MMPs and contribute to the disruption of the basement membrane that facilitate their migration and proliferation, as well as the fragmentation of the IEL that enable the vascular wall to expand and enlarge (Cai, Kocsis et al. 2004). As the collateral vessels grow and the final diameter is attained, SMCs reconstitute the IEL producing ECM, collagen and elastin (Schaper and Scholz 2003). Moreover, collagen IV and laminin regulate SMCs differentiation towards a contractile phenotype (Mack 2011).

1.4. K^+ channels and cell proliferation

SMC PM and proliferation have not only been correlated with changes in the expression of contractile proteins and early growth genes, but also with changes in the composition of K^+ channels (Cidad, Moreno-Dominguez et al. 2010). Moreover, *in vivo* and *in vitro* blockade of several K^+ channels inhibit SMC proliferation (see below).

K^+ channels are transmembrane proteins that specifically conduct K^+ ions across the membrane down their electrochemical gradient. They play an important role in cellular processes such as cell proliferation, cell volume regulation, hormone secretion and formation of action potentials in excitable cells (MacKinnon 2003).

1.4.1. Membrane potential

Due to their hydrophobic interior, cell membranes are non-permeable to ions. Through ion channels and ion pumps, cells control the permeation of the membrane to each type of ions and create ion gradients across it. This way, cells generate in an energy invested process a voltage called membrane potential (MP), that facilitates the transport of nutrients and proteins or generates electrical driving forces for the movement of ions, crucial e.g. during action potentials in excitable cells (Wright 2004).

While K^+ ions are concentrated in the interior of the cell, in the extracellular space are more abundant Na^+, Cl^- and Ca^{2+} ions. The membrane is relatively permeable to K^+ ions and

almost no permeable to Cl^- and Na^+ ions. The high membrane permeability to K^+ which leads to the constant efflux of positive charges through them, strongly influence the MP which is near the equilibrium potential for K^+, -84 mV (Wright 2004). Permeability is conferred by the amount of leakage channels expressed by the cell, a type of channels characterized by being always open.

Besides leakage channels, there are other channels that can be in a closed or opened state, the voltage- and ligands-gated ion channels. Gating of these channels can change very quickly the MP through the movement of ions towards their electro-chemical gradients. For example, an influx of Ca^{2+} or Na^+ leads to depolarisation of the membrane while K^+ ions efflux through K^+ channels leads to membrane hyperpolarisation.

1.4.2. Structure and types of K^+ channels

The structure of K^+ channels can be divided in two parts: a pore-forming structure, responsible for the transportation of K^+ ions, and a regulatory part which senses diverse stimuli and regulate the pore-forming structure.

The pore-forming structure is a tetrameric structure of four identical protein subunits, called α-subunits. Depending on the K^+ channel type, this α-subunit is a transmembrane protein containing two, four or six α-helices, that arrange around the central ion-conducting pore (Kuang, Purhonen et al. 2015). All identified K^+ channels belong to a unique protein family, that conserve a segment in their protein sequence called K^+ signature sequence, TVGYG. This segment constitutes a structural element called selectivity filter (SF), responsible for the discrimination between K^+ and Na^+ ions, allowing only the transportation of K^+ ions with a selectivity over Na^+ of more than 1000. Furthermore, K^+ ions are conducted very efficiently at rates approaching the diffusion limit (MacKinnon 2003, Kuang, Purhonen et al. 2015).

Ion flux rates through the channels are tightly regulated by gating and/or inactivation of the pore-forming structure. There are mainly two mechanisms of K^+ channel gating: by voltage or by ligand binding. Voltage-gated K^+ channels (K_V) are opened by energetically coupling changes in the membrane electric field with a conformational change in a voltage sensor domain of the channel (MacKinnon 2003). The other K^+ channels are ligand opened, by which opening of the pore is energetically coupled to the binding of a ligand. This ligand can be an ion, phospholipids or a binding protein in inwardly rectifying K^+ channels (Kir); ions, pH, lipids and regulatory proteins in tandem pore domain K^+ channels (K2P) or cAMP, Ca^{2+} and NADP in ligand-activated K^+ channels (Kligand) (Kuang, Purhonen et al. 2015).

K^+ channel gating is also modulated by auxiliary subunits that form heteromultimeric complexes with Kv α-subunits. Auxiliary subunits also regulate channel assembly and exit from the endoplasmic reticulum (ER) and trafficking to and from the cell membrane (Pongs and Schwarz 2010).

1.4.3. Mechanisms of K^+ channel-mediated cell proliferation

One of the most important functions assigned to K^+ channels is the regulation of cell cycle progression and cell proliferation. Hence, blockade of K^+ channels with broad spectrum-blockers inhibits cell proliferation. Moreover, expression or activity of several K^+ channels change during cell cycle (Blackiston, McLaughlin et al. 2009).

In eukaryotes, cell division can be divided in four different phases: a first growth phase (G1), a DNA replication phase (S), a second growth phase (G2) and a cell division phase or mitosis (M). Correct progression through cell cycle is controlled by several mechanisms to assure completion of one phase before proceeding to the next. One of these mechanisms controls changes in MP during transitions: depolarization towards G0/G1 and membrane hyperpolarizations during the G1/S and G2/M transitions (Pardo 2004, Urrego, Tomczak et al. 2014). K^+ channels gating results in efflux of K^+ ions and creates an electrical gradient that derives in membrane hyperpolarization. Membrane hyperpolarization in turn regulates cell cycle progression through 3 different mechanisms. Through activation of Cl^- ion channels involved in cell volume regulation, through changes in membrane potential themselves and through the generation of a driving-force for Ca^{2+} entry. Ca^{2+} ions act as second messengers and activate important signalling pathways involved in cell division (see **Fig 1.3**) (Cartin, Lounsbury et al. 2000, Urrego, Tomczak et al. 2014).

Interestingly, as shown in **Figure 1.3**, besides K^+-current dependent mechanisms, non-canonical, permeation-independent mechanisms of cell progression have been described for several K^+ channels. It has been shown that not only broad-spectrum K^+ channels inhibitors but also channel specific blockers can inhibit cell proliferation. This denotes that specific channels and not only a general change in K^+ current are involved in cell-cycle-regulation through specific actions of the channel itself. Indeed, the channels éther-a-gogo (eag), voltage-gated K^+ channels $K_V1.10$ and $K_V1.3$ and the Ca^{2+}-gated K^+ channel $K_{Ca}3.1$, among others, are still able to influence proliferation even in the absence of K^+ permeation (Pardo 2004, Millership, Devor et al. 2011, Cidad, Jimenez-Perez et al. 2012). K^+ channels may act as scaffold proteins and activate signalling pathways following channel gating. Moreover, K^+ channel activity is highly regulated by intracellular auxiliary subunits that act as scaffold

proteins too (Sole, Roura-Ferrer et al. 2009, Pongs and Schwarz 2010). The signalling cascades and interaction partners involved are now starting to be identified.

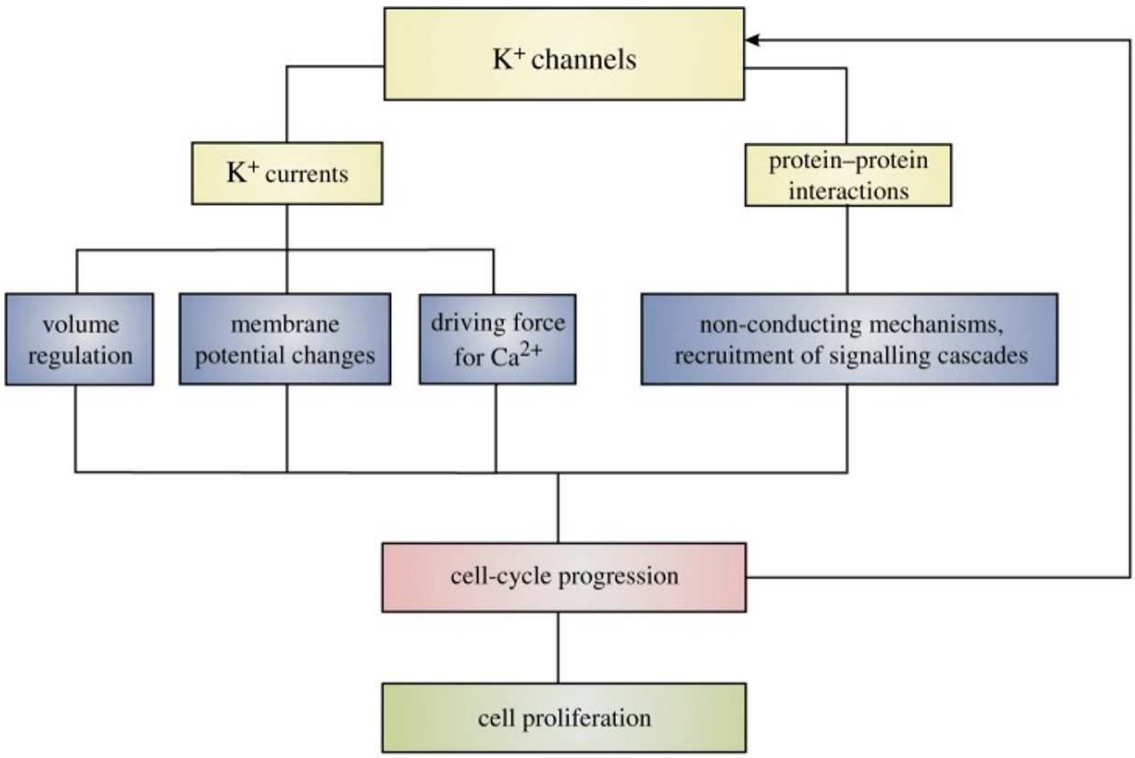

Figure 1.3: K^+ channels and their mechanisms of cell proliferation

K^+ channels have different mechanisms to regulate cell cycle progression and cell proliferation. Besides permeation-dependent mechanisms, K^+ channels can act as scaffold proteins activating downstream signalling cascades. Modified from (Urrego, Tomczak et al. 2014).

1.4.4. K^+ channels in SMC proliferation

Several *in vitro* and *in vivo* studies report changes in ion transport and ion channel configuration during SMC PM and proliferation in different contexts (Neylon, Lang et al. 1999, Miguel-Velado, Moreno-Dominguez et al. 2005, Beech and Cheong 2006, Beech 2007, Cidad, Moreno-Dominguez et al. 2010). This evidence a function of several K^+ channels in the induction and control of the cell division in SMCs too.

While the expression of channels involved in the SMC contraction such as Ca^{2+}-gated K^+ channel $K_{Ca}1.1$ (BK_{Ca}), $Ca_V1.2$, and several K_V1 channels is repressed in proliferating SMCs, two K^+ channels, the voltage-gated K^+ channel $K_V1.3$ and the Ca^{2+}-gated K^+ channel $K_{Ca}3.1$, among others, have been repeatedly found upregulated in proliferative SMCs *in vitro* and in neointima hyperplasia models. Moreover, their specific blockade could hinder SMC proliferation (Cidad, Moreno-Dominguez et al. 2010, Cheong, Li et al. 2011).

1.4.4.1 Role of K_V1.3 in SMC proliferation

In SMCs, an upregulation of K_V1.3 has been detected in cultured SMCs compared to fresh isolated ones and in *in vivo* pathological situations characterized by endothelial dysfunction and neointima hyperplasia (Cidad, Moreno-Dominguez et al. 2010, Cheong, Li et al. 2011).

Furthermore, small interference RNA (siRNA)-mediated K_V1.3 downregulation as well as treatment with two specific K_V1.3 channel blockers, Margatoxin and PAP-1 (Garcia-Calvo, Leonard et al. 1993, Schmitz, Sankaranarayanan et al. 2005), resulted in an inhibition of SMC migration and proliferation *in vitro* (Cidad, Moreno-Dominguez et al. 2010). Contrarily, transfection of human embryonic kidney cells (HEK-293) with K_V1.3 together with the auxiliary subunit K_Vß2, resulted in an increased proliferation that was reverted by treatment with Margatoxin or PAP-1 (Cidad, Jimenez-Perez et al. 2012).

In cultured organ segments of saphenous veins with induced intima hyperplasia, K_V1.3 blockade with Margatoxin or correolide compound C, another K_V1.3-specific channel blocker (Felix, Bugianesi et al. 1999), reduced SMC proliferation too (Cheong, Li et al. 2011).

The mechanisms of K_V1.3-mediated cell proliferation are still unclear. K_V1.3 blockade with Margatoxin or correolide compound C resulted in partial inhibition of K^+ efflux in depolarized proliferating SMCs and to a significant suppression of Ca^{2+} entry under blockade with Margatoxin. So, K_V1.3-mediated hyperpolarization could influence Ca^{2+} entry and Ca^{2+}-dependent gene expression in proliferative SMCs (Cheong, Li et al. 2011). In contrast, Cidad et al. observed that Margatoxin-mediated inhibition of SMC proliferation could not be reverted by high concentrations of K^+ in the medium and hypothesized that K_V1.3 could exert its role through permeation-independent mechanisms and independent on Ca^{2+} entry (Cidad, Moreno-Dominguez et al. 2010). Indeed, a non-conducting voltage-sensitive K_V1.3 channel mutant showed similar pro-proliferative effects than the wild type K_V1.3 channel in transfection experiments on HEK-293 cells. Hence, a conformational change of the channel driven by membrane depolarization was sufficient to activate channel-mediated cell proliferation (Cidad, Jimenez-Perez et al. 2012).

1.4.4.2 The role of $K_{Ca}3.1$ in SMC proliferation

Similar to $K_V1.3$, several *in vitro* reports stated an upregulation of $K_{Ca}3.1$ in SMC of different origins too, following stimulation with RTK ligands such as epidermal growth factor (EGF), PDGF-BB or tumor growth factor-ß (TGF-ß) (Neylon, Lang et al. 1999, Kohler, Wulff et al. 2003, Si, Grgic et al. 2006, Tharp, Wamhoff et al. 2006, Shepherd, Duffy et al. 2007, Toyama, Wulff et al. 2008, Bi, Toyama et al. 2013). *In vivo*, $K_{Ca}3.1$ expression is induced in several models of intima hyperplasia (Kohler, Wulff et al. 2003, Tharp, Wamhoff et al. 2008) .

The role of the $K_{Ca}3.1$ channel in SMC proliferation has also been evidenced through channel blockade with the specific blocker TRAM-34 (Wulff, Miller et al. 2000). Bi et al demonstrated that PDGF-BB-induced SMC proliferation *in vitro* is mediated by $K_{Ca}3.1$ since treatment with TRAM-34 or downregulation of the channel via siRNA reverted this effect (Bi, Toyama et al. 2013). Moreover, *in vivo* blockade of $K_{Ca}3.1$ with TRAM-34 could reduce neointima hyperplasia in a balloon catheter injury rat model of the carotid artery (Kohler, Wulff et al. 2003). Similarly, in a porcine model of postangioplasty restenosis, coating the balloon with TRAM-34 prevented $K_{Ca}3.1$ induction and significantly reduced intima hyperplasia 14 and 28 days post-surgery (Tharp, Wamhoff et al. 2008). Toyama et al also reported an inhibition of SMCs proliferation in Apolipoprotein E knockout mice, a genetic model of atherosclerosis, when mice were treated with TRAM-34 (Toyama, Wulff et al. 2008).

$K_{Ca}3.1$-mediated SMC proliferation seems to involve Ca^{2+}-mediated signalling but also non-permeation mechanisms. Hence, $K_{Ca}3.1$-blockade by TRAM-34 inhibits PDGF-BB induced rise in $i[Ca^{2+}]$, responsible for the expression of cyclins involved in cell proliferation and Ca^{2+}-dependent TFs, such as cAMP response element-binding protein (CREB) (Bi, Toyama et al. 2013). In contrast, the transfection of HEK-293 cells with a $K_{Ca}3.1$ pore-mutant, unable neither to conduct K^+ ions nor to promote Ca^{2+} entry, increased cell proliferation with respect to mock-transfected cells. Intriguingly, transfection with a non-functional trafficking mutant localized in a ring surrounding the nucleus also increased proliferation. Hence, not either its localization at the cell membrane was essential for its cell proliferation induction (Millership, Devor et al. 2011).

1.5. The voltage-gated K^+ channel $K_V1.3$

The voltage-gated K^+ channels (K_V) constitute a family of K^+ ion specific channels which are activated by changes in the voltage of the cell membrane, usually upon depolarization. It comprehends many different channels grouped in 12 subfamilies based on sequence homology of the hydrophobic transmembrane cores of the α-subunit (Gonzalez, Baez-Nieto et al. 2012). $K_V1.3$ belongs to the delayed rectifier, shaker subfamily of K_V channels characterized by a slow inactivation of the channel in the presence of a maintained membrane depolarization. $K_V1.3$ is ubiquitously expressed in mammals and can be found in both excitable and non-excitable cells (Blunck and Batulan 2012).

1.5.1. Structure and gating of Kv1.3

As a typical K_V channel, $K_V1.3$ is composed out of four α-subunits, each having six transmembrane α-helices, S1-S6, connected by five linker regions. Both the amino (NH_2)- and carboxy (COOH)-termini are located intracellularly (**Fig 1.4, A**). The subunits tetramerize so that the α-helices S5-S6 of all the monomers co-assemble to the center of the structure to form the ion-conducting pore. Surrounding the central pore rearranged the voltage-sensing domains (VSD), each formed by the S1-S4 segments (**Fig 1.4, B**). On the extracellular entrance of the pore, the S5-S6 linker forms a membrane re-entering small helix (P-loop) that contains the selectivity filter (SF) (**Fig 1.4, C**) (Blunck and Batulan 2012). K^+ permeation through the channel is controlled by the SF gate and the S6 bundle crossing (BC) gate (**Fig 1.4, C**). Upon depolarization of the membrane potential, the VSD undergoes conformational change, which leads to the widening of the BC gate. In $K_V1.3$, with a C-type inactivation, opening of the pore subsequently triggers closing of the SF gate preventing ions from passing through (Blunck and Batulan 2012).

Other functional domains in $K_V1.3$ channel have been described. The intracellular T1 domain located at the NH_2-terminus is responsible for its interaction with K_Vß-subunits that regulate channel gating (McCormack, McCormack et al. 1999, Gulbis, Zhou et al. 2000). Additionally, the tertiary topology of the COOH-terminus is responsible for the interaction with the auxiliary subunit potassium voltage-gated channel subfamily E member 4 (KCNE4) that regulates $K_V1.3$ endoplasmic reticulum (ER) retention and trafficking to the cell membrane (Sole, Roig et al. 2016).

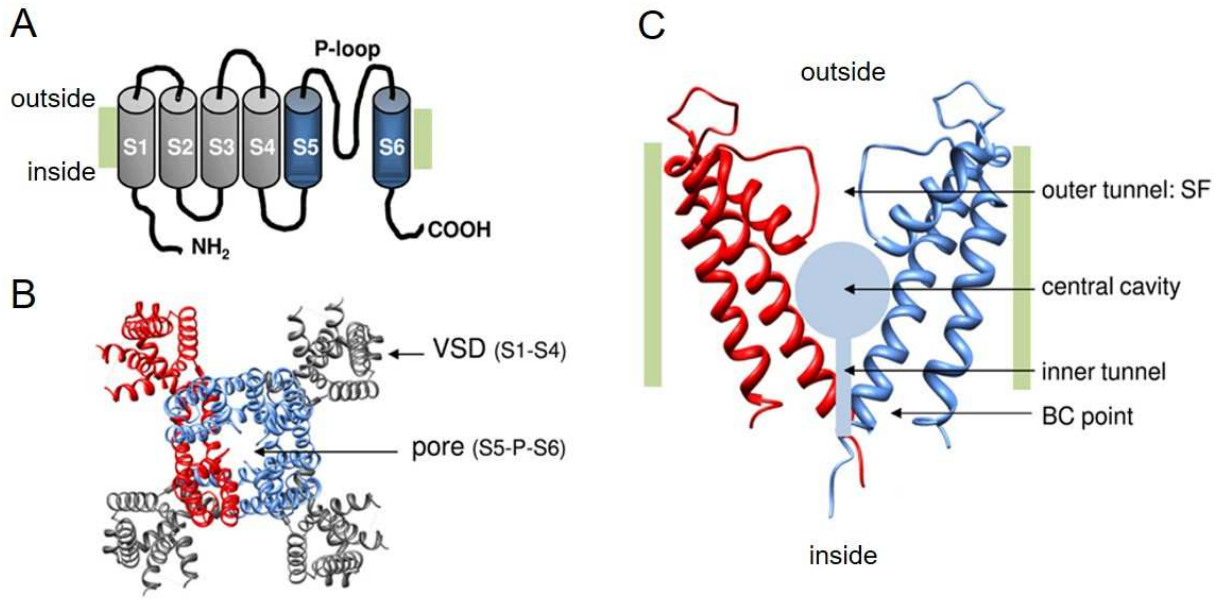

Figure 1.4: Structure of voltage-gated K^+ channels

A. Cartoon of an K_V channel α-subunit composed of 6 transmembrane segments (S1-S6) and one P-loop. In grey are represented the voltage-sensing domains (S1-S4) and in blue the 2 pore-forming domains (S5-S6). The amino and carboxy termini are intracellular. **B**. 3D structure of the $K_V1.2$ channel, viewed from the extracellular site. Four α-subunits forms a typical K_V channel. One subunit is red. **C**. Side view of the pore region formed by the segments S5, S6 and the P-loop. The selectivity filter (SF) allows the passage of K^+ ions. The bundle crossing (BC) of the S6 helices (BC gate) forms a barrier K^+ ions. Taken from (Labro and Snyders 2012).

1.5.2. Functions of $K_V1.3$

Its role as inducer of cell division has been reported in many different cell types pointing to a conserved role of the channel in the process. Kv1.3 role in cell proliferation was first observed in T cells where it plays an important role in T-cell-receptor signalling-mediated proliferation (Cahalan and Chandy 2009). By now its mitogenic role has been observed in several other cell types such as oligodendrocytes (Chittajallu, Chen et al. 2002), microglia (Kotecha and Schlichter 1999), ECs (Erdogan, Schaefer et al. 2005) and SMCs (Cidad, Moreno-Dominguez et al. 2010, Cheong, Li et al. 2011, Cidad, Jimenez-Perez et al. 2012, Tian, Yue et al. 2013, Cidad, Novensa et al. 2014).

The characterization of $K_V1.3$ knockout mice has revealed a role of $K_V1.3$ in olfactory sensing, insulin metabolism and control of body weight. $K_V1.3$ plays a key role in the establishment of a membrane potential in the neurons of the olfactory bulb. It also participates in the structure of the olfactory bulb glomeruli and modulates the capacity to detect odorant molecules by changing the expression of scaffold proteins involved in downstream signalling pathways (Fadool, Tucker et al. 2004). Interestingly, channel activity is inhibited by insulin through activation of RTKs (Fadool, Tucker et al. 2000). $K_V1.3$

deletion in mice subjected to high-fat diet results in lower body weight but normal basal activity. Since the channel is expressed in the hypothalamus, a region of the brain regulated by insulin that control adaptive thermogenesis, a role of $K_V1.3$ in thermogenesis has been postulated (Xu, Koni et al. 2003).

Besides its localization at the cell membrane, $K_V1.3$ has also been localized at the mitochondrial membrane, where it plays an important role in the regulation of the mitochondrial membrane potential $\Delta\Psi m$. Inhibition of the channel through membrane-permeable specific blockers (Psora-4, PAP-1, correolide compound C) or through binding to Bcl-2-associated X protein (Bax) leads to hyperpolarisation of the membrane with subsequent radical oxygen species (ROS) production, cytochrome c release and finally apoptosis (Gulbins, Sassi et al. 2010, Leanza, Henry et al. 2012). Hence, $K_V1.3$ channel has been identified as a target for anti-tumour therapies (Leanza, Venturini et al. 2015).

1.6. The Ca^{2+}-gated K^+ channel $K_{Ca}3.1$

Ca^{2+}-gated K^+ channels (K_{Ca}) are a family of K^+ channels activated by a rise in intracellular Ca^{2+} concentrations ($i[Ca^{2+}]$). Their activation leads to K^+ efflux and to repolarization or even hyperpolarization of the membrane. There are three subfamilies of Ca^{2+}-gated K^+ channels: big conductance $K_{Ca}1.1$ channel, also known as BK_{Ca}, intermediate conductance $K_{Ca}3.1$ channel (or IK_{Ca}), and small conductance SK_{Ca} channels $K_{Ca}2.1$, $K_{Ca}2.2$ and $K_{Ca}2.3$.

The intermediate conductance $K_{Ca}3.1$ channel is expressed in both excitable and non-excitable cells.

1.6.1. Structure and gating of $K_{Ca}3.1$

$K_{Ca}3.1$ is composed out of four α-subunits rearranged into a central pore. Each α-subunits is a transmembrane protein with six transmembrane domains (**Fig 1.5**). The selectivity filter and the central pore are formed by the extracellular loop between the fifth and sixth transmembrane domains. Both the NH_2- and COOH-termini are intracellular. Gating of the channel is induced by a rise in $i[Ca^{2+}]$, which is sensed by the binding of Calmodulin (CaM) to the Calmodulin binding domain (CaMBD) at the COOH-terminus of the channel. The COOH-terminus localizes just after the channel pore and it interacts with CaM even in the absence of Ca^{2+}. The Ca^{2+}-dependent binding of CaM to the channel involves the CaMBD2A and CaMBD2B (Morales, Garneau et al. 2013). Each α-subunit must interact with CaM to get activated (Gueguinou, Chantome et al. 2014).

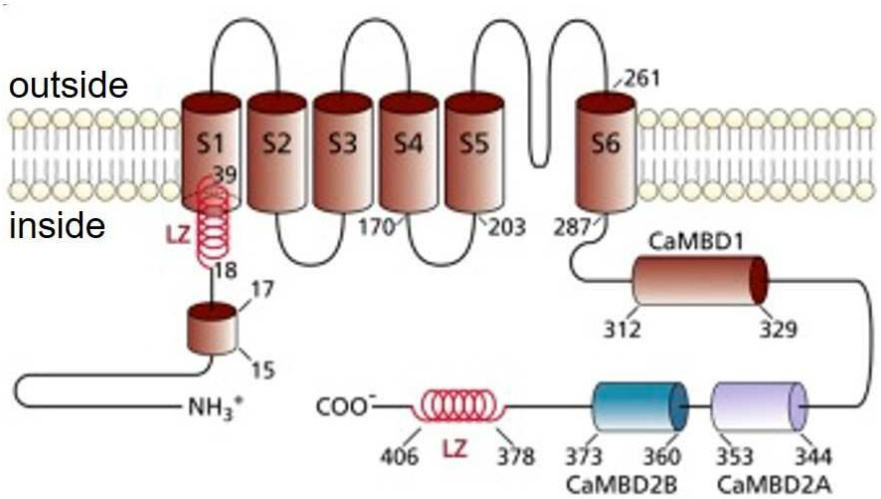

Figure 1.5: Structure of the Ca^{2+}-gated K^+ channel $K_{Ca}3.1$

Cartoon of the $K_{Ca}3.1$ α-subunit, organized in six transmembrane segments (S1-S6) plus a pore region between S5 and S6. The channel Ca^{2+} sensitivity is conferred by Calmodulin (CaM), with the CaM C-lobe constitutively bound to the CaM binding domain 1 (CaMBD1). The Ca^{2+}-dependent binding of CaM to the channel also involves the CaMBD2A and CaMBD2B. Modified from (Morales, Garneau et al. 2013).

The exact molecular mechanism of $K_{Ca}3.1$ gating through Ca^{2+}-CaM is not well known and there is no high-resolution 3D-structure crystallized for $K_{Ca}3.1$ yet. However, structural information from the crystallization of the rat $K_{Ca}2.2$–CaMBD in the presence of Ca^{2+} led to a proposed model where Ca^{2+} binding to CaM induces its conformational change that drives the interaction of the NH_2-terminus of a subunit with the COOH-terminus of an adjacent channel subunit. This, in turn, induces a conformational change in the S6 transmembrane segments leading finally to the opening of the channel pore (**Fig 1.6**) (Morales, Garneau et al. 2013).

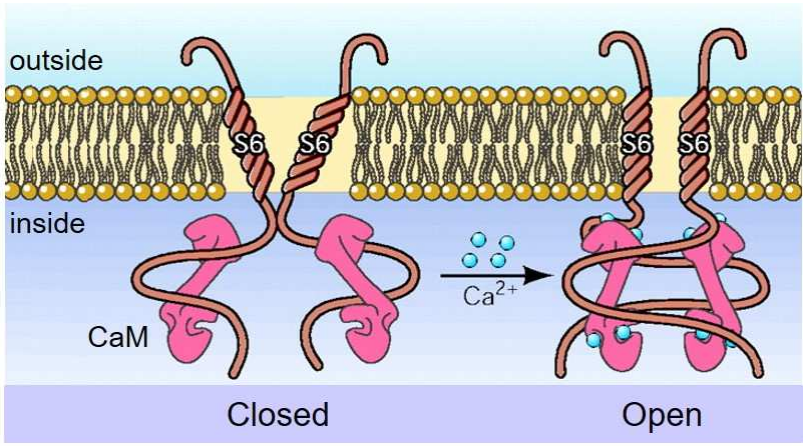

Figure 1.6: Model of $K_{Ca}3.1$ channel gating

CaM-binding to the COOH-terminus confers channel sensitivity to Ca^{2+}. Ca^{2+}-binding to CaM induces a conformational change in the S6 segment leading to the opening of the pore. Adapted from (Ledoux, Werner et al. 2006)

1.6.2. Functions of $K_{Ca}3.1$ channel

As well as $K_V1.3$, $K_{Ca}3.1$ has been involved in induction of cell proliferation not only in SMCs (Kohler, Wulff et al. 2003, Shepherd, Duffy et al. 2007, Tharp, Wamhoff et al. 2008, Su, Wang et al. 2011, Bi, Toyama et al. 2013) but also in ECs, playing a role in angiogenesis (Grgic, Eichler et al. 2005, Yang, Li et al. 2013), in T cells (Ghanshani, Wulff et al. 2000), in cancer cells (Wang, Shen et al. 2007, Lallet-Daher, Roudbaraki et al. 2009, Yang, Liu et al. 2013) and in fibroblasts (Grgic, Kiss et al. 2009).

Besides its effect on cell proliferation, $K_{Ca}3.1$ plays an important role in endothelium-derived hyperpolarization factor (EDHF)-mediated vasodilation. As already mentioned, the endothelium regulates vascular tone by releasing vasodilator factors or transmitting electrical signals that induce the relaxation of the SMCs underneath. EDHF-mediated vasodilation is characterized by a hyperpolarization of the SMC membrane preceding relaxation. It is well accepted that EDHF depends to a large extent on the activation of the endothelial $K_{Ca}2.3$ and $K_{Ca}3.1$ K^+ channels (Eichler, Wibawa et al. 2003, Feletou 2011). Even though both channels play a role in the process, their function cannot be substituted by each other. Indeed, $K_{Ca}3.1$ deficient mice have impaired EDHF-mediated vasodilation and increased blood pressure compare to wild type mice (Si, Heyken et al. 2006). The different subcellular localization could explain their specific functions. While $K_{Ca}2.3$ is confined in endothelial gap junctions, $K_{Ca}3.1$ localizes in endothelial projections towards the IEL, often associated with myoendothelial junctions (MEJ) (Feletou 2011). Following $K_{Ca}3.1$ activation, the accumulation of K^+ ions in the intercellular space between ECs and SMCs could drive the activation of the K^+-sensitive $K_{ir}2.1$ channels and the Na^+/K^+ ATPase on the SMC membrane, leading to its hyperpolarization. Another explanation sustains that $K_{Ca}3.1$-mediated endothelial hyperpolarization is directly propagated to the SMC membrane through MEJ. This goes with the fact that both MEJ and EDHF-mediated vasodilation increase as the vessel size decreases (Feletou 2011).

1.7. Aim of the project

SMCs play an important role in arteriogenic vascular remodelling. Besides proliferating and contributing to the enlargement and lengthening of collateral arteries, they secrete matrix degradation enzymes achieving place for migrating and new proliferating cells. Finally, they contribute to the synthesis of the new extracellular matrix and by differentiating into contractile cells to functional mature collateral arteries. Due to their pleiotropic functions, SMCs are an interesting target for therapeutic arteriogenesis.

Several K^+ channels have been involved in phenotypic modulation and proliferation of SMCs. The voltage-gated K^+ channel $K_V1.3$ and the Ca^{2+}-gated K^+ channel $K_{Ca}3.1$ are upregulated in cultured SMCs and in proliferating SMCs in *in vivo* models of neointima hyperplasia. However, their role in arteriogenesis has not been investigated so far. On the other hand, while several mechanisms have been described for K^+ channel-mediated cell proliferation, it remains unclear how these channels orchestrate their mitogenic function.

This study aimed to shed light on the role of $K_V1.3$ and $K_{Ca}3.1$ in arteriogenic SMC proliferation focusing on the following points:

- Characterization of $K_V1.3$ and $K_{Ca}3.1$ expression and localization patterns in the FAL model of arteriogenesis
- Effects of pharmacological $K_V1.3$ and $K_{Ca}3.1$ channel blockade on arteriogenic SMCs proliferation in the FAL model
- Role of the channels in the regulation of the RTK signalling pathway in arteriogenesis and in cultured MArSMCs

Materials and methods

2. Materials and methods

2.1. Materials

Table 2.1. Consumables

Consumable		Company
Reaction tubes	200 µl PCR tubes	Eppendorf AG, Hamburg, Germany
	1.5 ml and 2 ml	Eppendorf AG, Hamburg, Germany
	15 ml FALCON tubes	Greiner Bio-One GmbH, Kremsmünster, Austria
	50 ml FALCON tubes	Corning Inc., Corning, New York, USA
	Nunc CryoTube^{Tm} 1.8 ml vials	Nunc^{Tm}, Roskilde, Denmark
	innuSPEED lysis tubes P	Analytik Jena AG, Jena, Germany
Tips	0.1-10 µl epT.I.P.S.® LoRetention filter tips	Eppendorf AG, Hamburg, Germany
	0.1-10, 2-30, 10-100, 2-200 and 100-1000 µl Diamond® filter tips	Gilson Inc., Middleton, USA
	10, 100, 200, 1000 µl tips	Eppendorf AG, Hamburg, Germany
	Combitips Advanced®	Eppendorf AG, Hamburg, Germany
Syringes	1 ml syringe Plastipak	BD Biosciences, California, USA
	2 ml and 5 ml syringe, Discardit II	BD Biosciences, California, USA
	10 ml Injekt syringes	Braun, Melsungen, Germany
Needles	24G and 30G Microlance 3	BD Biosciences, California, USA
Slides and coverslips	Thermo Scientific Superfrost plus slides	Gerhard Menzel GmbH, Braunschweig, Germany
	Coverslips	Medite Medizintechnik, Burgdorf, Germany
Embedding cassettes	Histosette I, Embedding Cassettes with LID, blue	Simport, Beloeil, Quebec, Canada
	Cryomold® Standard 25 x 20 x 5 mm	Sakura Finetek., Tokyo, Japan
Flasks	25, 75 and 175 cm^2 Corning® TC-treated surface treatment with vent cap	Corning Inc., New York, USA

Well plates	Costar® 12-, 24-, 96-well cell culture plates flat bottom with lid, tissue culture treated	Corning Inc., New York, USA
	Costar® EIA/ RIA 96 well plate flat bottom, non-treated	Corning Inc., New York, USA
	96 well Semi-Skirted qPCR Plates	4titude® Ltd., Wotton, UK
Serological pipettes	2 ml, 5 ml, 10 ml and 25 ml costar STRIPETTE	Corning Inc., New York, USA
PAGE gels	PAGE 4-20 % gels (43230.01)	SERVA Electrophoresis GmbH, Heidelberg, Germany
	Filter paper and	Whatman GmbH, Dassel, Germany
	Nitrocellulose membrane (WB)	Whatman GmbH, Dassel, Germany
Aortic catheteri-zation	Venofix Safety 25G	Braun, Melsungen, Germany
	ETHICON 4-0	Johnson&Johnson, New Jersey, USA
	VICRYL 6-0	Johnson&Johnson, New Jersey, USA
	Silk Braided Suture 7/0	Peasalls Sutures, Somerset, England

Table 2.2. Devices

Device	Model	Company
Centrifuges	Mikro 200R Rotina 420R	Andreas Hettich GmbH & Co.KG, Tuttlingen, Germany
Cryotome	Leica CM3050 S Research Cryostat	Leica Biosystems, Wetzlar, Germany
Dispenser	Isoflurane Vapor 19.3	Abbott, Wiesbaden, Germany
Embedding machine	Tissue-Tek TEC 5	Sakura Finetek., Tokyo, Japan
Hemocytometer	Neubauer improved	Laboroptik Ltd, Lancing, United Kingdom
Homogenizer	SpeedMill PLUS	Analytik Jena AG, Jena, Germany
Incubators	CO2 Brutschrank C150	BINDER GmbH, Tuttlingen, Germany
	Heating cabinet	Heraeus, Hanau, Germany
Laser Doppler Imaging	moorLDI2-IR	Moor Instruments Ltd., Millwey, Axminster, Devon, England

Microscopes	Axioskop 40 and Axiocam 105 color camera	Carl Zeiss AG, Feldbach, Switzerland
	LEICA M60 and LEICA MC120 HD camera	Leica Biosystems, Wetzlar, Germany
	Zeiss Axio Examiner.Z1	Carl Zeiss AG, Feldbach, Switzerland
	Axio Imager 2 and Axiocam ICc 5	Carl Zeiss AG, Feldbach, Switzerland
Microtome	Rotationsmikrotom 2030	Reichert-Jung, Heidelberg, Germany
Microwave		Siemens AG, Munich Germany
pH-Meter	inoLab pH 720	WTW GmbH, Weilheim, Deutschland
Pipetboy	Pipetboy comfort	INTEGRA Biosciences Corp., Hudson, New Hampshire, USA
Pipettes	0.1-10 µl Eppendorf Xplorer® plus	Eppendorf AG, Hamburg, Germany
	1-10, 10-100, 20-200, 100-1000 µl Eppendorf Research	Eppendorf AG, Hamburg, Germany
	1-10, 10-100, 20-200, 100-1000 µl Pipetman	Gilson Inc., Middleton, USA
	Multipette Plus	Eppendorf AG, Hamburg, Germany
Power supply	ECO-Power-Supply 300 V / 700 mA	Kisker Biotech GmbH, Steinfurt, Germany
Shaker	GFL 3005	GFL Gesellschaft für Labortechnik mbH, Burgwedel, Germany
Spectrophotometers	ELISA reader Infinite F200	Tecan Group Ltd., Männedorf, Switzerland
	NanoDrop 2000c	Thermo Fischer Scientific, Waltham, Massachusetts, USA
Sterile bank	LaminAir HBB 2448	Heraeus Holding GmbH, Hanau, Germany
Surgical instruments	Adson Forceps Medical	Fine Science Tools, Heidelberg, Germany
	Dumont #5, #7, #5/45 Forceps Inox	
	Vannas Spring Scissor - Straight	

	Iris Scissors - Straight 11.5 cm Olsen-Hegar Needle Holder 12 cm	
Thermocyclers	Thermal Cycler 2720 StepOnePlus™ Real-Time PCR System	Life Technologies, Carlsbad, California, USA
Thermomixer	Thermomixer Compact	Eppendorf AG, Hamburg, Germany
Tissue processor	Shandon Citadel 1000	Thermo Fischer Scientific, Waltham, Massachusetts, USA
Vortexer	IKA MS2 Minishaker Vortexer	IKA®-Werke GmbH & Co. KG, Staufen, Germany
Weighing machine	CPA225D	Sartorius AG, Göttingen, Germany

Table 2.3. Buffers, cell culture media and solutions

	Name	**Company**
Buffers	Dulbecco's phosphate buffered saline (DPBS)	PAN BIOTECH, Aidenbach, Germany
	TRIzol Reagent	Thermo Fisher Scientific Inc, Waltham, USA
	Laemmli Buffer 10x, for SDS-PAGE	SERVA Electrophoresis GmbH, Heidelberg, Germany
	Roti®-Load 1 protein loading buffer (4x)	Carl Roth GmbH, Karlsruhe, Germany
Media	Dulbecco's modified Eagle's medium (DMEM)	Thermo Fisher Scientific Inc, Waltham, USA
	Smooth muscle cell growth medium (SMCGM)	Cell Biologics, Chicago, USA
Solutions	Acetic acid	Sigma-Aldrich Chemie GmbH, Steinheim, Germany
	Aqua ad iniectabilia	Braun, Melsungen, Germany
	Chloroform	Sigma-Aldrich Chemie GmbH, Steinheim, Germany
	70 %, 96 % and 99.8 % EtOH	SAV Liquid Production GmbH, Flintsbach, Germany
	EtOH BioUltra, for molecular biology, ≥99.8%	Sigma-Aldrich Chemie GmbH, Steinheim, Germany
	Eukitt quick-hardening mounting medium	Sigma-Aldrich Chemie GmbH, Steinheim, Germany

	Gelatine, 2 % in PBS	PAN BIOTECH, Aidenbach, Germany
	Giemsa - Solution for microscopy	AppliChem, Darmstadt, Germany
	Isopropanol	Sigma-Aldrich Chemie GmbH, Steinheim, Germany
	Mayer's Hämalaun	AppliChem, Darmstadt, Germany
	Methanol	AppliChem, Darmstadt, Germany
	Mythramycin A	Santa Cruz Biotechnology, California, USA
	PageRulerTM Prestained Protein	Thermo Fisher Scientific Inc, Waltham, USA
	Penicillin (10 000 units/ml)/ Streptomycin (10 mg/ml) solution	PAN BIOTECH, Aidenbach, Germany
	Ponceau S solution	Sigma-Aldrich Chemie GmbH, Steinheim, Germany
	Super Signal West Femto Maximum Sensitivity Substrate	Thermo Fisher Scientific Inc, Waltham, USA
	Tissue-Tek® O.C.T.™ Compound	Sakura Finetek., Tokyo, Japan
	Trypan blue solution	Sigma-Aldrich Chemie GmbH, Steinheim, Germany
	Trypsin	PAN BIOTECH, Aidenbach, Germany
	Xylene	AppliChem, Darmstadt, Germany
Others	Foetal calf serum (FCS)	PAN BIOTECH, Aidenbach, Germany
	Industrial Latex	Chicago Latex Products, Crystal Lake, Illinois, USA

Table 2.4. Chemicals

Name	**Company**
Adenosine	Sigma-Aldrich Chemie GmbH, Steinheim, Germany
Agarose LE, analytical grade	Promega GmbH, Mannheim, Germany
Albumin from bovine serum	Sigma-Aldrich, Steinheim, Germany
Blotting Grade Blocker non Fat Dry Milk	Bio-Rad Laboratories GmbH München, Germany
5-Bromo-2'-deoxyuridine	Sigma-Aldrich Chemie GmbH, Steinheim, Germany

cOmplete ULTRA Tablets, Mini, EDTA-free EASYpack, protease inhibitor cocktail tablets	Roche Diagnostics GmbH, Mannheim, Germany
1,4-diamino-2,3-dicyano-1,4-bis[2-aminophenylthio] butadiene (UO126)	Cell Signaling Technology, Inc., Cambridge, USA
4',6-diamidino-2-phenylindole (DAPI)	Sigma Aldrich Chemie GmbH, Steinheim, Germany
Ethylenediaminetetraacetate	AppliChem GmbH, Darmstadt, Germany
Glycine	AppliChem, Darmstadt, Germany
Hypo chloride acid	Merck KGaA, Darmstadt, Germany
Paraformaldehyde	Merck KGaA, Darmstadt, Germany
Paraplast Plus Tissue Embedding Medium	Leica, Solms, Germany
Phosphate	Sigma Aldrich Chemie GmbH, Steinheim, Germany
PhosphoStop, phosphataseInhibitor tablets	Roche Diagnostics GmbH, Mannheim, Germany
Potassium chloride	Merck KGaA, Darmstadt, Germany
Potassium Hydrogen phosphate	Merck KGaA, Darmstadt, Germany
Phenylmethylsulphonyl fluoride (PMSF)	Calbiochem, La Jolla CA, USA
Sodium chloride	AppliChem, Darmstadt, Germany
Sodium deoxycholate	Sigma Aldrich GmbH, Seelze, Germany
Sodium dodecyl sulfate	Merck KGaA, Darmstadt, Germany
Sodium hydrogen phosphate	Merck KGaA, Darmstadt, Germany
Sodium orthovanadate	Sigma Aldrich Chemie GmbH, Steinheim, Germany
Sucrose	Sigma Aldrich Chemie GmbH, Munich, Germany
Tris base	AppliChem, Darmstadt, Germany
Triton-X-100	Sigma Aldrich Chemie GmbH, Steinheim, Germany
Tween 20	AppliChem GmbH, Darmstadt, Germany

Table 2.5. Drugs and substances administered to the mice

Application	Brand name	Active ingredient	Company
Analgesic	Temgesic®	Buprenorphine	Reckitt Benckiser Healthcare (UK) Ltd., Slough, England

Anesthesia	Dorbene®	Medetomidine hydrochloride	Pfizer GmbH, Berlin, Deutschland
	Fentanyl-Curamed®	Fentanyl	CuraMED Pharma, Karlsruhe, Germany
	Forene®	Isoflurane	Dräger Medical, Lübeck, Germany
	Midazolam-Ratiopharm®	Midazolam	Ratiopharm GmbH, Ulm, Germany
Antidote	Flumazenil Inresa	Flumazenil	Inresa Arzneimittel GmbH, Freiburg, Germany
	Naloxon Inresa	Naloxone hydrochloride	Inresa Arzneimittel GmbH, Freiburg, Germany
	Revertor®	Atipamezole hydrochloride	cp-pharma, Burgdorf, Germany
Cell proliferation marker	BrdU	Bromodeoxyuridine	Sigma-Aldrich, Steinheim, Germany
Eye protection	Bepanthen® eye ointment	Dexpanthenol	Bayer Vital GmbH, Leverkusen, Germany
K_V1.3 blockade	PAP-1	5-(4-Phenoxybutoxy)psoralen	Sigma-Aldrich Chemie, Taufkirchen, Germany
K_{Ca}3.1 blockade	TRAM-34	1-[(2-Chlorophenyl) diphenylmethyl]-1H-pyrazole	Alomone labs, Jerusalem, Israel
Skin disinfection	Bode Cutasept® F spray	Propan-2-ol	Bode Chemie GmbH, Hamburg, Germany

Table 2.6. Antibodies

	Antigen	Host		Conjugation	Clone	Company
IHC/ ICC	$K_V1.3$	rabbit	pAb	no	APC-101	Alomone labs, Jerusalem, Israel
	$K_{Ca}3.1$	rabbit	pAb	no	APC-064	Alomone labs, Jerusalem, Israel
	α-SMA	mouse	mAb	Cy3	1A4	Sigma-Aldrich, Steinheim, Germany
	CD31	rat	mAb	Alexa fluor 647	MEC13.3	BioLegend, San Diego, CA, USA
	Rabbit IgG	goat	pAb	Alexa fluor 488	711-545-152	Jackson ImmunoResearch Labotatories Inc., CA, USA
WB	p44/42 MAPK (ERK-1/2)	rabbit	mAb	no	137F5	Cell Signaling Technology, Inc., Cambridge, USA
	Phospho-p44/42 MAPK (ERK-1/2)	rabbit	mAb	no	D13.14.4E	Cell Signaling Technology, Inc., Cambridge, USA
	Rabbit IgG	goat	pAb	Horseradish peroxidase (HRP)	sc-2030	Santa Cruz Biotechnology, California, USA

Table 2.7. Primers

Gene name	Accession no.	Primer sequence	anT (°C)	Length (bp)	E
rRNA 18S (*18S*)	NR_003278	for: GGACAGGATTGACAGATTGATAG rev: CTCGTTCGTTATCGGAATTAAC	64	108	1.91
Alpha-smooth muscle actin (*αSma*)	NM_007392.3	for: GAGCATCCGACACTGCTG rev: GTACGTCCAGAGGCATAG	58	146	1.88
Early growth response 1 (*Egr1*)	NM_007913.5	for: CGAACAACCCTATGAGCACCTG rev: CAGAGGAAGACGATGAAGCAGC	64	270	1.77
Fibroblast growth factor receptor 1 (*Fgfr1*)	NM_001079908.2	for: CTTGCCGTATGTCCAGATCC rev: TCCGTAGATGAAGCACCTCC	63	77	1.89
Voltage-activated K^+ channel 1.3 (*Kcna3*)	NM_008418.2	for: TGAGTAAGTCGGAGTATATGGTGAT rev: GCAAGTGGCTGTGGAGTTG	60	98	2
Platelet-derived growth factor beta (*Pdgfrb*)	NM_001146268.1	for: AGGACAACCGTACCTTGGGTGACT rev: CAGTTCTGACACGTACCGGGTCTC	63	89	1.77
Transcription factor Sp1 (*Sp1*)	NM_013672.2	for: ACAGGGTGCCAATGGCTGGC rev: GCCCACCAGAGACTGTGCGG	60	124	1.91

Table 2.8. Kits

Name	Application	Company
BrdU In-situ detection kit	Staining of proliferative cells	BD Pharmingen, CA, USA
BrdU proliferation assay	Cell proliferation	Roche Diagnostics GmbH, Germany
Pierce™ BCA protein assay kit	Protein quantification	Thermo Fischer Scientific, Waltham, USA
Power Sybr green	Real time PCR	Life technologies

QuantiTect reverse transcription kit	cDNA synthesis	Qiagen, Hilden, Germany
Rneasy Kit	RNA isolation	Qiagen, Hilden, Germany
RQ1 RNase-Free DNase	DNase digestion of RNA	Promega, Mannheim, Germany

Table 2.9. Software, programs and websites

Name	**Company**
AxioVision 4.8.2.0	Carl Zeiss AG, Feldbach, Switzerland
AxioVision SE64 Rel. 4.9.1	Carl Zeiss AG, Feldbach, Switzerland
Endnote® X4.01	Thomson Reuters, New York, USA
GraphPad prism 6	GraphPad Software, California, USA
i-control I.9	Tecan Group Ltd., Männedorf, Switzerland
MatInspector	Genomatix GmbH, Munich, Germany
Microsoft Excel, Power point, Word 2007	Microsoft Corporation, Redmond, USA
moorLDI Version 5.3	Moor Instruments Ltd., Axminster, Devon, England
Photoshop	Microsoft Corporation, Redmond, USA
StepOne Software v2.2.2	Life Technologies, Carlsbad, California, USA
Wasabi software	Hamamatsu PHOTONICS GmbH, Herrsching, Germany
ZEN Blue	Carl Zeiss AG, Feldbach, Switzerland

2.2. Murine model of femoral artery ligation

2.2.1. Animals

C57BL/6J mice were purchased from Charles River and kept under 12 hours light/ night cycle with water and food *ad libitum*. Experiments were performed with 7 to 10 weeks old male mice.

2.2.2. Drugs and channel blockers administration

2.2.2.1 Anaesthesia, antidote and analgesia

Before the surgical procedure, mice were anesthetized with a mixture of 5 mg/kg Midazolam, 0.5 mg/kg Medetomidine and 0.05 mg/kg Fentanyl (MMF) injected subcutaneously. Just after the surgical procedure, anaesthesia effects were antagonized with an antidote consisting of a combination of 0.5 mg/kg Flumazenil, 1.2 mg/kg Naloxone and 2.5 mg/kg Atipamezole (FNA), injected subcutaneously.

To avoid pain, 1.2 mg/kg of Buprenorphine was injected subcutaneously immediately after surgery and 12 hours later.

2.2.2.2 Channel blockers

For channel blockade experiments *in vivo*, the $K_V1.3$ channel blocker 5-(4-Phenoxybutoxy)psoralen (PAP-1) (Sigma) and the $K_{Ca}3.1$ channel blocker TRAM-34 (Alomone labs) were dissolved in peanut oil and administered intraperitoneally at 40 mg/kg and 120 mg/kg per day, respectively. To maintain PAP-1 and TRAM-34 levels in blood as constant as possible, the doses were administered in two injections, one in the morning and another in the afternoon. Treatment started 4 hours before the surgical procedure and finished on day 6.

2.2.3. Surgical procedure

Once anaesthetized with MMF, mice were placed over a heated bench cover to control body temperature for the whole surgery. A veterinary ointment (Bepanthen®) was applied over the eyes to avoid desiccation. The skin of the upper thigh was first disinfected with Cutasept® and then shaved with a scalpel. A small skin incision on the right thigh was performed over the epigastric artery (**Fig 2.1, A**). A few millimetres downstream the epigastric artery, the femoral artery was dissected from the nerve, vein, fat and connective tissues (**Fig 2.1, B**). A thread was introduced surrounding the artery and tied off (**Fig 2.1, C**

and D). A contra-lateral sham operation on the left leg was performed as described above, except that the thread was let untied (**Fig 2.1, E**). Finally, the wound was closed with a surgical suture (**Fig 2.1, F**). To avoid pain, the analgesic Buprenorphine was injected subcutaneously immediately after surgery. 15 min after the first Buprenorphine injection, mice were waked up with the antidote, (FNA) injected subcutaneously.

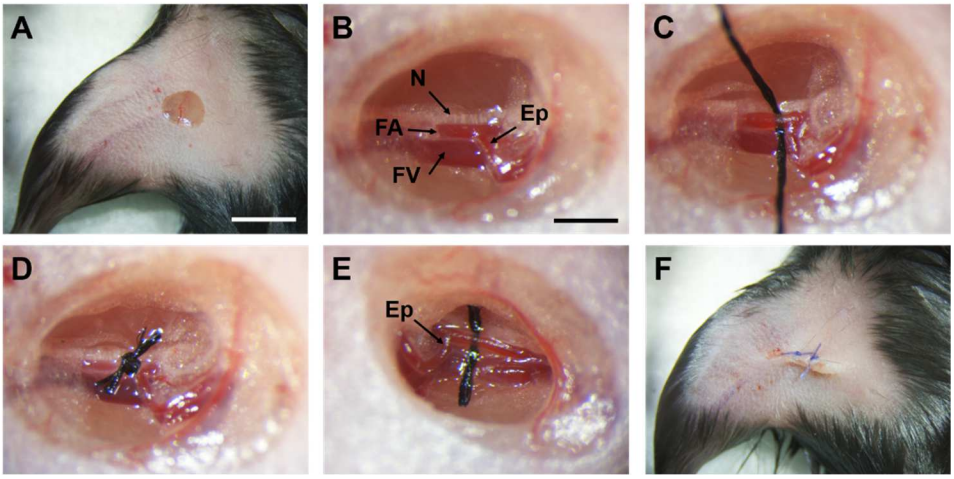

Figure 2.1: Surgical procedure of femoral artery ligation

A. Upper right thigh of the mouse. Small skin incision over the bifurcation of the femoral artery and the epigastric artery. **B**. Ligation site proximal to the epigastric bifurcation free of fat and connective tissues. **C**. Silk surrounding the femoral artery. In **D**, silk tied off (occluded) and **E** let untied (sham). **F**. Skin incision is sutured. N: nerve, FA: femoral artery, FV: femoral vein, Ep: Epigastric artery. White scale bar: 5 mm, dark scale bar: 1 mm.

2.2.4. Laser Doppler Imaging

While ligation of the femoral artery on the right leg impairs perfusion of the hind-limb, in the sham-operated left leg, the perfusion remains intact. Hind-limb perfusion was established before surgery, immediately thereafter as well as three and seven days after FAL with a laser Doppler moorLDI2-IR (Moor Instruments Ltd). Results were expressed as the perfusion ratio of the occluded hind-limb relative to the sham-operated one. Basal measurements were performed as control, since no differences should be observed in the perfusion of both feet before surgery. Just after ligation, the occluded-to-sham hind-limb-perfusion ratio was lower than 10 %. Mice showing higher perfusion ratios were discarded.

Mice were either anaesthetized with MMF as described for surgery or were sedated by inhalation of 5 % isoflurane for 5 seconds following 1.5 % mixed with oxygen flowing at ~ 2.5 l/min connected to a warm chamber (37 °C). Mice were led in a supine position and hind-limbs were fixed with double-band adhesive for an acclimatisation period of 10 min. Between the minutes 10 and 21, a measurement was performed each 3 minutes. During this period, occluded-to-sham ratios reach a maximum and then decrease. The maximal ratio

was selected for analysis. The setup parameters were the following: distance from Laser Doppler to warm plate: 20 cm, image dimension: 3.6x2.3 cm, Gain: DC 2, FLUX 0, CONC 2; Background Threshold BK 65. For analysis, a region of interest of 0.55 mm^2 was delimited per hand around the paws and perfusion was assessed with the moorLDI Version 5.3 software (Moor Instruments Ltd.).

2.2.5. Mouse tissue harvesting

2.2.5.1 Aortic catheterization and perfusion

Before collecting thigh muscles for histology, mice were perfused with vasodilation and fixation buffers via an aortic catheterization, to allow maximal vasodilation of collateral arteries and tissue fixation. Likewise, for gene expression analysis, the perfusion per hand of 0.5 ml of latex facilitated the dissection of thigh collateral arteries.

Mice were first anaesthetized with MMF. Skin was removed from the abdomen up to the thoracic cavity. Abdominal cavity was opened downstream the xiphoid process. To control bleeding, aorta and vena cava were clamped upstream the kidneys with a vascular clamp (**Fig 2.2, A**). Downstream to the kidney, the abdominal aorta was dissected from connective tissue and vena cava and was surrounded by a suture silk (**Fig 2.2, B**). A small cut was performed in the aorta and the point of a butterfly needle was introduced and fixed with the silk (**Fig 2.2, C** and **D**). The butterfly needle was first connected to an open syringe located at 1 meter over the bench and solution was let perfused to eliminate air bubbles before catheterization. Finally, solutions were let flow through the aorta by constant pressure after cutting the cava vein.

For histology, 20 ml of vasodilation buffer, 0.1 % (w/v) adenosine and 0.5 % (w/v) bovine serum albumin (BSA) in phosphate-buffered saline (PBS), were perfused to allow maximal vasodilation of the collateral vessels. To fix the tissue for paraffin wax conservation, 20 ml of 4 % (w/v) paraformaldehyde (PFA) in PBS were perfused afterwards. For cryoconservation, tissue was fixed with 3 % PFA in PBS. All three buffers were freshly prepared and gently prewarmed to 37 °C.

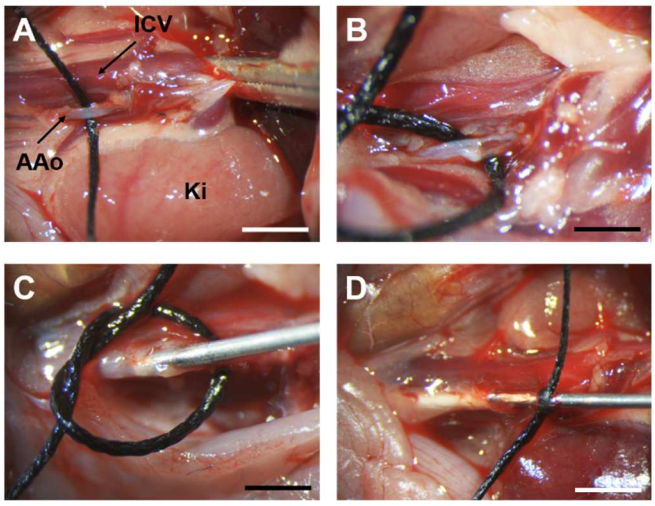

Figure 2.2: Aortic catheterization for perfusion fixation and latex perfusion

A. Open abdomen of the mouse showing the abdominal aorta (AAo), the inferior cava vein (ICV) and left kidney (Ki). Upstream of the kidney, AAo and ICV are clamped with a vascular clamp. **B**. Suture silk is placed surrounding the AAo and a small incision in AAo is realized. **C**. Introduction of a butterfly needle in the aorta through the aortic incision and fixation with silk. **D**. Perfusion, in this case with latex, used to make visible the vascular system like the collateral arteries subject of study. White scale bar: 5 mm, dark scale bar: 1 mm.

2.2.5.2 Processing of adductor samples for paraffin- and cryoconservation

For paraffin conservation, thigh samples were collected immediately after perfusion fixation and placed in fixation solution allowing to fix for 12 h more at 4 °C. Samples were then washed with tap H_2O for 30 min and immersed in 70 % ethanol for few hours to several days. Following dehydration in increasing concentrations of ethanol and xylene, samples were finally embedded in paraffin wax in a carousel-type tissue processor (see **table 2.10**). Adductors were then cut in the middle, crossing muscle fibres and collateral arteries, and embedded in paraffin wax with the cut face laying down. Samples were stored at room temperature (RT).

Before cutting, thigh samples were cooled down by incubating them in a freezer to -20 °C. 2 µm thick sections were placed over glass slides and let dry 24 h to 48 h at 37 °C in a warm chamber. Slides were then stored at RT or stained immediately.

Table 2.10. Dehydration and paraffin embedding protocol

Step	**1-2**	**3-5**	**6-8**	**9-10**	**11-12**
Solution	70 % EtOH	96 % EtOH	99.8 % EtOH	Xylene	Paraffin wax
Time	2 x 60 min	3 x 60 min	3 x 60 min	2 x 90 min	2 x 90 min

For cryoconservation, following perfusion fixation, adductor samples were immersed first in 15 % sucrose (w/v) in PBS for 4 h at RT and then in 30 % sucrose (w/v) in PBS overnight at 4 °C. Sucrose should avoid the formation of crystals and protect cellular structure and tissue morphology during freezing. Adductor were cut in the middle as for paraffin conservation and embedded in OCT compound over cryomolds placed on dry ice and let freeze slowly. Samples were stored at -80 °C.

Thigh samples were cut with a cryotome in 6 µm thick sections, that were placed over glass slides and stored at -80 °C.

2.2.5.3 Collateral arteries sampling for gene expression studies

To avoid RNA degradation by endogenous ribonucleases, catheterization and sampling was performed as quick as possible. After latex perfusion, the skin of the upper tight was sprayed with Cutasept® to avoid the dispersion of hairs and then cut carefully. Using clean scissors, the two superficial collateral arteries were dissected from the Profunda artery to the femoral artery, collected in 1.5 ml RNases-free reaction tubes and quick-frozen on dry ice. Samples were immediately stored at -80 °C.

2.3. Histology

2.3.1. Giemsa staining and morphometric analysis

Morphometric analysis was performed on collateral artery cross-sections stained with Giemsa's solution. Giemsa's solution is composed of a mixture of eosin, methylene blue and Azure B. Eosin is an acidic dye which binds to basic structures such as cytoplasm, proteins and collagen. Methylene blue and Azure B are basic dyes that bind to acidic structures such as nucleic acids. Paraffin sections stained with Giemsa's solution in an acidic pH display blue nuclei and pink collagen fibres making possible the delimitation of the arterial wall.

Sections were stained following the protocol described in **table 2.11**. Finally, sections were mounted over coverslips using Eukitt® quick-hardening mounting medium, let dry and stored at RT. Images of the collateral arteries were taken with a 40x oil immersion objective of an Axioskop 40 microscope equipped with an Axiocam 105 colour camera (Zeiss) and analysed with the AxioVision 4.8.2.0 software.

Table 2.11. Giemsa staining protocol of paraffin sections

Step	Time	Temperature
Immerse in xylene	20 min	RT
Hydrate in abs EtOH, 96 % EtOH, 70% EtOH	5 min each	
Immerse in Giemsa's solution	1 h	60 °C
Wash with tap H_20		RT
Immerse in 1 % acetic acid	3 s	
Dehydrate in 96 % EtOH and abs EtOH	15 s each	
Immerse in xylene	2x 5 min	
Cover with Eukitt® quick-hardening mounting medium and glass coverslips		

The inner and outer luminal circumferences were assessed as these two parameters are constant, independent on the vessel shape (Limbourg, Korff et al. 2009). The circumferences were then used to calculate the luminal diameter and the medial wall thickness. For this, collateral sections were assumed to be perfect circles. The following equations were used:

$$Co = D \times \pi,$$

where Co is outer circumference and D diameter, and

$$A = \pi \times r^2,$$

where A is vessel area and r the radius of the circumference.

Medial thickness area was calculated then subtracting inner from outer vessel area, and wall thickness subtracting inner radius from outer radius.

2.3.2. BrdU staining in paraffin sections

Due to their distinct localization and morphology, ECs and SMCs can be very well identified in collateral artery cross-sections and their proliferation quantified in histological sections. ECs in growing collateral arteries have big round nuclei projected to the intraluminal space. SMCs are big cells immersed in the vessel media layer with round nuclei and can be easily differentiated from fibroblasts, localized in the adventitia layer. Compared to other cell proliferation markers expressed only during cell replication, bromodeoxyuridine (BrdU), a thymine analogue, is introduced into the deoxyribonucleic acid (DNA) during genome replication and remains in the genome after several cell divisions. This way, cells that have

replicated in the past will be BrdU positive too, increasing the sensitivity of the method respect to other cell proliferation markers. Together with the corresponding channel blocker, mice were given 50 mg/kg BrdU for five days starting just before surgery. BrdU (Sigma-Aldrich) was dissolved in PBS à 12.5 mg/ml and sterile filtrated.

Staining was performed using the BrdU detection kit (BD Pharmingen), based on exposition of BrdU antigen via antigen retrieval and further detection with an anti-BrdU antibody conjugated indirectly to a peroxidase enzyme. Oxidation of the chromogen 3,3'-diaminobenzidine (DAB) by the peroxidase enzyme in the presence of hydrogen peroxide results in a brown alcohol soluble precipitate. See **table 2.12.** for a detailed protocol.

Images were taken with a 40x oil immersion objective of an Axioskop 40 microscope equipped with an Axiocam 105 colour camera (Zeiss) and analysed with the AxioVision 4.8.2.0 software. For the analysis of $BrdU^+$ SMCs-to-total SMCs ratios, 50 SMCs were counted per mouse. For analysis of $BrdU^+$ ECs-to-total ECs ratio, 150 ECs were counted per mouse. The average of $BrdU^+$ cells-to-total cells of 3 mice was calculated and used as parameter for comparison between groups.

Table 2.12. BrdU staining protocol of paraffin sections

Step	Time	Temperature
Immersion in xylene	2x 20 min	RT
Hydration in abs EtOH, 96 % EtOH, 70% EtOH	5 min each	
Destillated water	5 min	
7.5 % H_2O_2	5 min	
Destillated water	5 min	
Antigen retrieval buffer (ARB)	15 min	800 watts microwave
ARB refilled	15 min	
Cool down slowly in open jars	30-45 min	RT
Washing step with PBS	2x 5 min	
Incubation biotin conjugated- BrdU antibody	90 min	
Washing step with PBS	2x 5 min	
Peroxidase conjugated-streptavidin	30 min	
Washing step with PBS	2x 5 min	
Drop of DAB	3-4 min	
Washing step with tap water	10 min	
Counterstaining with Hämalaun solution	45 s	

Washing step with tap water	5 min
Dehydration in 96 % EtOH and abs EtOH	5 min each
Immersion in xylene	5 min
Cover with Eukitt® quick-hardening mounting medium and glass coverslips	

2.3.3. Fluorescence immunohistochemistry

For fluorescence immunohistochemistry of collateral artery cross-sections, adductors were cryoconserved and cut as described above. Sections were let dry at RT for 15 min and then fixed in 2 % PFA for 3 min. After washing twice with PBS for 5 min, sections were permeabilized with 1 % tween 20 in PBS (PBST) for 20 min. Sections were then incubated with 1:100 rabbit anti-K_V1.3 or rabbit anti-K_{Ca}3.1 antibodies (Alomone) in PBST overnight at 4 °C. After three washing steps with PBS, sections were incubated with 1:100 goat Alexa Fluor 488-conjugated anti-rabbit antibody, together with 1:100 Cy3-conjugated mouse anti-α-SMA (Sigma) and 1:100 Alexa Fluor 647-conjugated rat anti-CD31 (cluster of differentiation 31) antibody in PBST for 1 h at RT. Sections were then washed three times for 5 to 10 min in PBS and imaging was performed immediately. Images were taken with a Zeiss Axio Examiner.Z1 microscope using a 60x water objective, equipped with a Colibri.2 illumination system.

Analysis of K_V1.3 or K_{Ca}3.1 expression in α-SMA positive SMCs and CD31 positive ECs was performed with the ZEN Blue software (Zeiss). Briefly, the collateral artery section was delimited from the rest of the tissue. Positive α-SMA or CD31 areas were selected to create a mask of the SMC layer or endothelium respectively. Areas smaller than 10 μm^2 were not considered for calculations. Fluorescence intensity means for Alexa Fluor 488 (K_V1.3 and K_{Ca}3.1) in the selected masks were calculated and used as parameter for relative protein quantification.

2.3.4. Fluorescence immunocytochemistry

MArSMCs were stained for K_V1.3 and K_{Ca}3.1 channels as well as for the SMC marker α-SMA together with the nuclear dye 4',6-diamidino-2-phenylindole (DAPI).

Cells were seeded à 5 $x10^4$/ per well of a 24 well plate over sterile and with 1 % collagen pre-coated coverslips. After let them growing for 2 more days in SMCGM, cells were washed with PBS and fixed with 2 % PFA in PBS for 3 min. Following two wash steps with PBS, cells were permeabilized with PBST for 20 min at RT. Cells were then incubated with 1:100 diluted rabbit anti-K_V1.3 or anti-K_{Ca}3.1 antibody in PBST overnight at 4 °C. After

washing three times with PBS, cells were incubated for 1 h at RT with a combination of Alexa Fluor 488-conjugated anti-rabbit secondary antibody and Cy3-conjugated anti α-SMA antibody, both diluted 1:100 in PBST. After three washing steps, cells were incubated with the nuclear dye DAPI à 500 nmol/l for 20 min at RT and washed again with PBST. Finally, coverslips were washed with PBS and mounted with ProLong anti fade mounting medium (Invitrogen).

Images were taken with a 40x objective of a Axio Imager 2 fluorescence microscope equipped with a fluorescence Axiocam ICc 5 camera and Axiocam ICc 5 software.

2.4. Cell culture

2.4.1. MArSMCs culture

Cell isolation from mouse tissues often results in a mixture of cell populations. SMCs isolated from aorta and arteries are usually contaminated by fibroblasts, which grow faster and better than SMCs, overwhelming them after several passages. For this reason and to assure high quality standard and reproducible data, primary SMCs were purchased from Cell Biologics. Furthermore, since SMCs from different beds can have different phenotypes, special attention was done in choosing SMCs isolated from arteries and not from the aorta. In addition, cells were used in lower passages to avoid cell dedifferentiation.

MArSMCs were cultured with SMC growth medium (SMCGM) (Cell Biologics) containing 20 % foetal calf serum (FCS), Insulin and the growth factors FGF-2 (10 ng/µl) and EGF (5 ng/µl). Cells were grown in collagen-coated flasks and medium was changed every other day.

When cells reached 80 % confluence, they were splitted and used for experiments. Briefly, cells were washed with prewarmed Ca^{2+}- and Mg^{2+}-free PBS and loosed from the bottom of the flask with trypsin/ Ethylenediaminetetraacetic acid (EDTA) (1 ml in 25 cm^2 flask, 2 ml in 75 cm^2 flask) for several minutes in a reaction controlled under the microscope. Reaction was stopped with 1:4 ml 10 % FCS Dulbecco's modified Eagle's medium (DMEM). After centrifugation à 2800 rpm (Rotina 420R) at RT for 5 min, cells were resuspended in SMCGM and either used for experiments or cultured further in coated flasks (1:4).

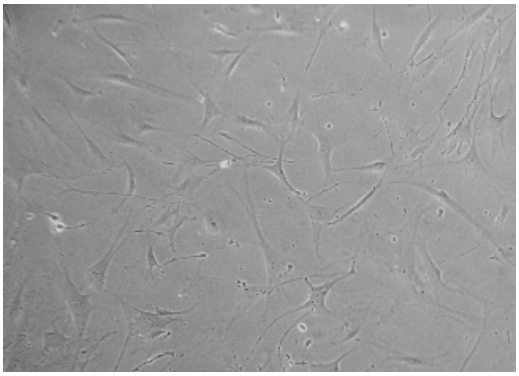

Figure 2.3: Light microscope image of MArSMCs after 2 passages

2.4.2. MArSMCs counting and trypan blue exclusion

Cell concentration of cell suspensions was determined with a Neubauer improved hemocytometer (Laboroptik) through staining with trypan blue solution (Sigma) allowing exclusion of dead cells (blue).

2.4.3. BrdU proliferation assay

To assess the effects of channel blockade on MArSMCs proliferation, the BrdU proliferation assay kit (ROCHE) was used, following manufacturer's instructions. Briefly, MArSMCs were seeded in a 96 well plate à 1 x 10^4 cells/well in 100 µl SMCGM overnight. The next day, medium was replaced for starvation medium, DMEM containing 1 % FCS for 24 h. Cells were then stimulated with 10 % FCS in DMEM with or without the channel inhibitors PAP-1 or TRAM-34 together with 10 µM BrdU supplied by the kit. PAP-1 was diluted to 0.1, 1 and 5 µM while TRAM-34 was diluted to 10, 100 and 500 nM end concentrations. Negative control cells were stimulated with 2 % FCS medium. Cells were let grow for 3 days and then were fixed with 200 µl/well FixDenat buffer. After 30 min at RT, the solution was removed by flicking off and tapping. Then, 100 µl/well of anti-BrdU-POD solution was added and incubated for 90 min at RT. The antibody conjugate was removed, and cells were washed 3 times with 200-300 µl Washing Solution. After removing the washing solution, 100 µl/well Substrate Solution was added and incubated for 5 to 30 min at RT. Then reaction was stopped with 25 µl of 1 n/l H_2SO_4 for 1 min on a shaker at 30 rpm. Finally, the absorbance at 450 nm was measured within 5 min after adding stop solution with an Infinite F200 ELISA reader (Tecan). The reference wavelength was set to 620 nm.

2.4.4. MArSMCs samples collection for gene expression studies

MArSMCs were seeded in a 12 well plate precoated with 1 % gelatine à 0.5 -1 x 10^6 cells/well in 0.5 ml SMCGM overnight. For gene expression experiments with channel inhibitors, cells were serum starved for 24 h in DMEM containing 2 % FCS. Cells were then stimulated with 0.5 ml SMCGM/well with or without 1 µmol/l PAP-1 or 100 nmol/l TRAM-34 for 6 h in a cell incubator at 37 °C and 5 % CO_2. PAP-1 was first dissolved in Dimethyl sulfoxide (DMSO) à 1 mmol/l and TRAM-34 à 10 mmol/l. Both solutions were sterile filtrated with a 0.22 µm filter, aliquoted and stored à -20 °C. Stock solutions were fresh pre-diluted in DMEM. DMSO end concentrations were lower than 0.1 %. Finally, cells were washed twice with ice cold PBS and lysed with 100 µl Trizol for RNA extraction. Sample were either stored at -20 °C or continued processing for RNA isolation.

For gene expression studies with the Sp1-blocker Mithramycin A (MTM), MArSMCs were serum starved for 3 days in DMEM 0.5 % FCS. Cells were then stimulated with SMCGM with or without 200 nmol/l MTM for 6 h in a cell incubator. Finally, cells were washed twice with ice cold PBS and lysed with 100 µl TRIzol for RNA extraction. MTM was first dissolved in DMSO à 10 mM and was sterile filtrated with a 0.22 µm filter. Stock aliquots were stored at -20 °C.

2.4.5. MArSMCs samples collection for western blot

For western blot analysis, MArSMCs were seeded in 12 well plate precoated with 1 % gelatine à 0.8-1x10^6 cells/well in 1 ml SMCGM/well for several days, with daily medium changing. When confluence was reached, medium was changed to DMEM with 0.5 % FCS (starvation medium) for 3 days. Two hours before stimulation with SMCGM, MArSMCs were incubated with 10 µmol/l UO126, a Mitogen-activated protein kinase kinase 1/2 (MEK1/2) inhibitor in starvation medium. UO126 was first resuspended in DMSO at a concentration of 10 mM and stock aliquots were stored at -20 °C. 30 min before stimulation, MArSMCs were incubated with the $K_V1.3$ inhibitors PAP-1 and Margatoxin (MgTX) à 1 µM and 100 nM respectively in starvation medium. MArSMCs were then stimulated with SMCGM for 5 min with or without UO126 and the channel inhibitors PAP-1 and Margatoxin. After two washing steps with ice cold PBS, cells were lysed with the corresponding lysis buffer.

2.5. Protein biochemistry

2.5.1. Preparation of protein lysates

After cell stimulation, cells were washed twice with ice cold PBS and lysed by scraping with 100 µl/well radio-immunoprecipitation assay (RIPA) buffer containing fresh added protease and phosphatase inhibitors (see **Table 2.13.**). Cell lysates were transferred to 1.5 ml reaction tubes, incubated on ice for 30 min and vortexed each 10 min. Cell lysates were then centrifuged for 5 min à 10 000 g at 4 °C. Supernatants were transferred to new reaction tubes and pellets were discarded.

Table 2.13. Composition of cell lysis buffer (RIPA)

Component	**Concentration**
Tris/ HCl (pH 7.4)	50 mM
NaCl	150 mM
EDTA	1 mM
Triton-X-100	1 % (v/v)
Sodiumdeoxycholate	1 % (w/v)
SDS (10 %)	0.1 % (v/v)
Freshly added:	
Protease inhibitor cocktail (Roche)	1 tablet /10 ml buffer
PhosphoStop (Roche)	1 tablet /10 ml buffer
Sodium orthovanadate	1 mM
PMSF	0.5 mM

2.5.1. Protein quantification

Protein concentration of cell lysates was determined with the Pierce™ bicinchoninic acid BCA protein assay kit with a standard curve ranging 0.125 mg/ml to 2 mg/ml bovine serum albumin supplied with the kit. 1:5 diluted samples and standards were pipetted in duplicates in a 96 well plate. Reaction buffer was freshly prepared by mixing 50 parts BCA Reagent A with 1 part BCA Reagent B. After 30 min of incubation à 37 °C, colorimetry was measured with the Infinite F200 ELISA reader (Tecan) à 562 nm.

2.5.2. Immunoblotting

Changes in protein concentration as well as post-translational modifications in MArSMC lysates were assessed by western blot.10 µg cell lysates aliquots were reduced and denatured by adding Roti®-Load protein loading buffer (4x) (Carl Roth) and incubating à 95 °C for 5 min. Samples were then chilled on ice for 5 min and stored at -80 °C until western blot was performed.

MArSMCs lysates, containing 10 µg protein were thawed on ice, centrifuged, mixed by pipetting and loaded in a 4-20 % gradient Sodium dodecyl sulfate- polyacrylamide gel electrophoresis (SDS-PAGE) gel (Serva). Gel was placed before in an electrophorese chamber and covered with Laemmli running buffer (Serva) (see **Table 2.14** for buffer composition). For future control of the size of the proteins of interest, the prestained protein marker PageRuler^{TM} Prestained Protein (Thermo Fischer Scientific) with a band pattern of 10 to 180 kDa was loaded in the first lane. Electrophorese chamber was then connected to a power supply and a current of 10 mA was first elicited for 10 min and then increased to 20 mA for 1 h.

From the gel, proteins were transferred to a nitrocellulose membrane to allow detection with specific antibodies. Briefly, filter paper and nitrocellulose membrane were first equilibrated in transfer buffer for 5 min (see **Table 2.14** for buffer composition). In a blotting chamber, filter paper, membrane and gel were placed in the following order, from cathode to anode: filter paper, membrane, gel, filter paper. The presence of SDS in sample loading buffer charged the proteins negatively so that they move from the cathode to the anode in the presence of a current. A current of 44 mA was applied for 1 h.

To control that transfer occurred successfully, the membrane was then stained with Ponceau solution for 30 s and washed with Tris-buffered saline containing 0.1 % Tween20 wash buffer (TBST). Additionally, the Ponceau stained membrane was scanned and used as evidence of equal loading. Before incubation with specific antibodies, the membrane was blocked for 1 h with 5 % dry milk in TBST in a shaker à 200 rpm. The membrane was then incubated overnight, either with the rabbit mAb anti-phospho-p44/42 MAPK (ERK-1/2) à 1:2000 or with the rabbit mAb anti-p44/42 MAPK à 1:1000 in TBST with 5 % BSA at 4 °C with gentle shaking. After several washing steps under shaking, membrane was incubated with horseradish peroxidase (HRP)-conjugated goat anti-rabbit mAb, à 1:10000 in TBST with 5 % dry milk for 1 h at RT. Finally, HRP was detected with the luminol-based enhanced chemiluminescent substrate SuperSignal West Femto Substrate (Thermofischer) incubating

for 3-5 minutes and visualized in an ORCA system (Hamamatsu) and the Wasabi software (Hamamatsu).

Table 2.14. Composition of running, transfer and wash buffers for western blot

Running buffer:		**Transfer buffer:**		**Wash buffer (TBST)**	
Component	**Conc.**	**Component**	**Conc.**	**Component**	**Conc.**
Tris	250 mM	Tris		Tris	
Glycin	1.92 M	Glycin		NaCl	
SDS	1 %	SDS		HCl	
pH 8.4-8.9		Methanol		Tween20	0.1 %
		pH 8.3		pH 7.5	

2.6. Real time Polymerase Chain Reaction

2.6.1. RNA isolation

RNA isolation was performed with TRIzol, a monophasic solution of phenol and guanidine isothiocyanate which maintains integrity of RNA while disrupting cells. MArSMCs were detached and lysed with 100 µl TRIzol reagent while collateral samples, around 15 mg tissue, were homogenised with 300 µl TRIzol in lysis tubes containing beads in a SpeedMill PLUS homogenizer (Analytic Jena). Addition of chloroform (1/5 volume of TRIzol) followed by centrifugation at 12.000 g for 15 min at 4 °C allowed the separation of the sample into an upper aqueous phase and an organic phase. The RNA-rich aqueous phase was then mixed with cold isopropanol (1/2 of TRIzol volume) and centrifuged at 12.000 g for 30 min at 4 °C to finally precipitate the RNA.

To eliminate any rest of genomic DNA, RNA was digested with 1 unit of RQ1 RNase-Free DNase enzyme (Promega)/µg RNA at 37 °C for 30 min. RNA samples were then cleaned up from DNase and DNase buffer with the RNeasy MinElute Cleanup kit® from Qiagen following manual's instructions. Briefly, samples were first mixed with buffer RLT, then with 100 % ethanol and transferred to spin columns (supplied by the kit). Spin columns were centrifuged to 14.000 g for 30 s at RT, washed twice with RPE buffer followed by 80 % ethanol. Spin columns were let dry by centrifugation at full speed and RNA was finally eluted with 15-20 µl H_2O.

RNA concentration was measured at a UV wavelength of 260 with a NanoDrop® spectrophotometer and calculated with the Beer-Lambert equation (solved for concentration):

$$C = A/(\mathrm{Ɛ} \times b),$$

where C is RNA concentration in molarity (n/L), A is UV absorbance in absorbance units (AU), Ɛ is extinction coefficient (liter/mol-cm) and b pathlength in cm.

RNA purity was assessed analysing the ratios 260/230 and 260/280. While low 260/230 ratios indicate contamination with guanidinium isothiocyanate, phenol and other buffer components, low 260/280 ratios reflect protein contamination. Samples were considered pure when the ratios 260/230 and 260/280 ranged from 1.8- to 2 and 2 to 2.2, respectively. RNA integrity was analysed in 1 % agarose gels. RNA samples were used when the 28s and 18s ribosomal RNAs bands were visible and the upper 28s band was thicker than the 18s band.

2.6.2. cDNA synthesis

RNA samples were reverse transcribed to complementary DNA (cDNA) with the QuantiTect® Reverse Transcription kit from Qiagen, following manufacturer's instructions. Briefly, 250 ng RNA was incubated with Wipeout buffer at 42 °C for 4 min to eliminate any rest of genomic DNA and chilled on ice for 5 min. Samples were mixed with reverse-transcription master mix containing RT primer mix, a mixture of random and poly dT primers and reverse transcriptase and incubated for 30 min to 42 °C. Finally, reverse transcriptase was inactivated by incubating the samples at 95 °C for 3 min. Samples were diluted 1:5 and stored at -20 °C.

2.6.3. Real time PCR

Real time PCR was performed with the StepOne Plus PCR machine (Life technologies) and data were analysed with the ΔΔCt method, described elsewhere (Pfaffl 2001).

Usually 2 µl of 1:5 diluted cDNA was amplified per well using the Power Sybr green kit (Life technologies). Forward and reverse primers (Eurofins GmbH) were mixed in a master mix à 5 µM each and used to a final concentration of 250-500 µM. Samples were run in triplicates and mean values were used for calculations. See **Table 2.15.** for running protocol.

Table 2.15. Real time PCR running protocol

Step	Polymerase activation	PCR		Melt curve		
		Cycle (40x)		Step and hold		
	Hold	Den at.	Ann./ Ext.			
Temp	95 °C	95 °C	58-64 °C *	95 °C	64 °C	+ 0.7 °C/min until 95 °C
Time	10 min	15 s	1 min	15 s	1 min	

* Annealing temperature is primer-dependent.

2.7. Statistics

Results were analysed with the statistical software GraphPad Prism 6 (GraphPad Software, California, USA). For statistical comparison of two groups, data was first tested for normality. For normally distributed data, groups were compared with Student's t test and for data not distributed normally by Rank Sum test. For the comparison of multiple groups, 1-way or 2-way analysis of variance (ANOVA) followed by a Holm-Sidak Post Hoc test was carried out. The corresponding tests are indicated in the figure legends. All experimental values are displayed as mean ± standard error of the mean (SEM). Results were considered significant with a p-value < 0.05.

Results

3. Results

3.1. $K_V1.3$ and $K_{Ca}3.1$ localization and abundance pattern during arteriogenesis

In order to investigate the role of the potassium channels $K_V1.3$ and $K_{Ca}3.1$ in arteriogenesis, at first, their localization and expression patterns were characterized in collateral arteries, employing the murine model of FAL. Three different time points of collateral artery growth were analyzed: at baseline (sham), two days after FAL (2d), and seven days after FAL (7d). Two days after FAL, collateral arteries are characterized by a strong cellular proliferation rate while seven days after FAL they have already reached a low-proliferative state. $K_v1.3$ and $K_{Ca}3.1$ specific localization in SMCs and in ECs was assessed by immunofluorescence imaging through multi-staining with the SMC marker α-SMA and the EC marker CD31. Furthermore, fluorescence intensity measurements of the channels in SMCs and ECs allowed a relative quantification between time points.

3.1.1. $K_V1.3$ localization and abundance in collateral arteries

Immunofluorescence imaging revealed $K_V1.3$ expression in SMCs and ECs of collateral arteries at all time points analyzed, as demonstrated by co-localization with α-SMA and CD31 respectively (**Fig 3.1, A**). Other vascular cells such as adventitial fibroblasts and perivascular inflammatory cells as well as skeletal muscle fibers were $K_V1.3^+$ too. However, as displayed in **Figure 3.1, B**, no changes in $K_V1.3$ fluorescence intensity between the different time points analyzed were evident in neither SMCs nor ECs, indicating a constant protein abundance in these cells during arteriogenesis. Interestingly, $K_V1.3$ staining intensities were stronger in ECs than in SMCs.

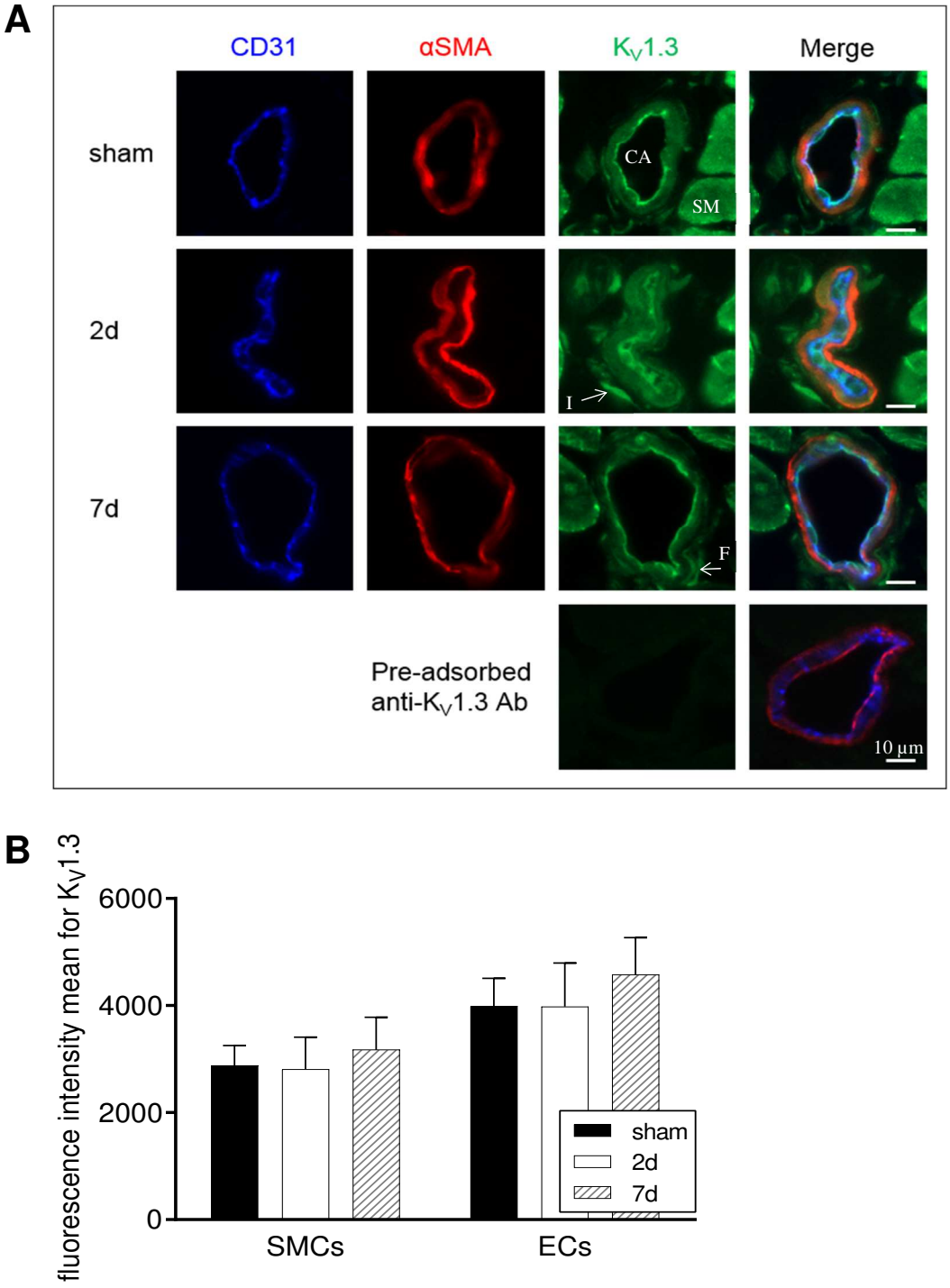

Figure 3.1: K_V1.3 localization and abundance pattern in collateral arteries of wild type mice during arteriogenesis

A. Immunofluorescence staining against K_V1.3 (green) together with the SMC marker α-SMA (red) and the EC marker CD31 (blue) in cross-sections of collateral arteries in sham-operated hind-limb (sham) and collateral arteries 2 (2d) and 7 days (7d) after FAL. Lower line, negative control staining performed with anti-K_V1.3 antibody (Ab) pre-adsorbed with K_V1.3 antigenic peptide. CA: collateral artery, SM: skeletal muscle, F: fibroblast, I: inflammatory cell. Scale bar 10 µm. **B**. Quantitative analysis of the fluorescence intensity mean values for K_V1.3 in SMCs and ECs. Mean ± SEM, 1-way ANOVA and Holm-Sidak Post Hoc test: * $p<0.05$, n=3 mice per group, 4-12 sections/ mouse.

3.1.2. $K_{Ca}3.1$ localization and abundance in collateral arteries

$K_{Ca}3.1$ expression was more evident in collateral SMCs and ECs 2 days after FAL (**Fig 3.2, A**). Like $K_V1.3$, $K_{Ca}3.1$ staining was also positive in fibroblasts, perivascular inflammatory cells and skeletal muscle. A comparison of $K_{Ca}3.1$-staining fluorescence intensities in SMCs, revealed a strong but still insignificant induction of $K_{Ca}3.1$ expression 2 days after FAL compared to resting collateral arteries (2407.53 ± 157.50 2d vs 1693.74 ± 251.07 sham) (**Fig 3.2, B**). Interestingly, at day 7, $K_{Ca}3.1$ expression was significantly downregulated compared to 2 days after FAL (1238.51 ± 172.89 7d vs 2407.53 ± 157.50 2d), reaching even lower levels than in resting collateral arteries (1238.51 ± 172.89 7d vs 1693.74 ± 251.07 sham). In ECs, as in SMCs, $K_{Ca}3.1$ staining reached a peak 2 day after FAL (2433.64 ± 109.26 2d vs 1768.34 ± 270.43) and its expression was significantly downregulated again 7 days after FAL (1300.53 ± 202.36). $K_{Ca}3.1$ expression increased albeit not significantly during the proliferative phase of arteriogenesis in both SMCs and ECs.

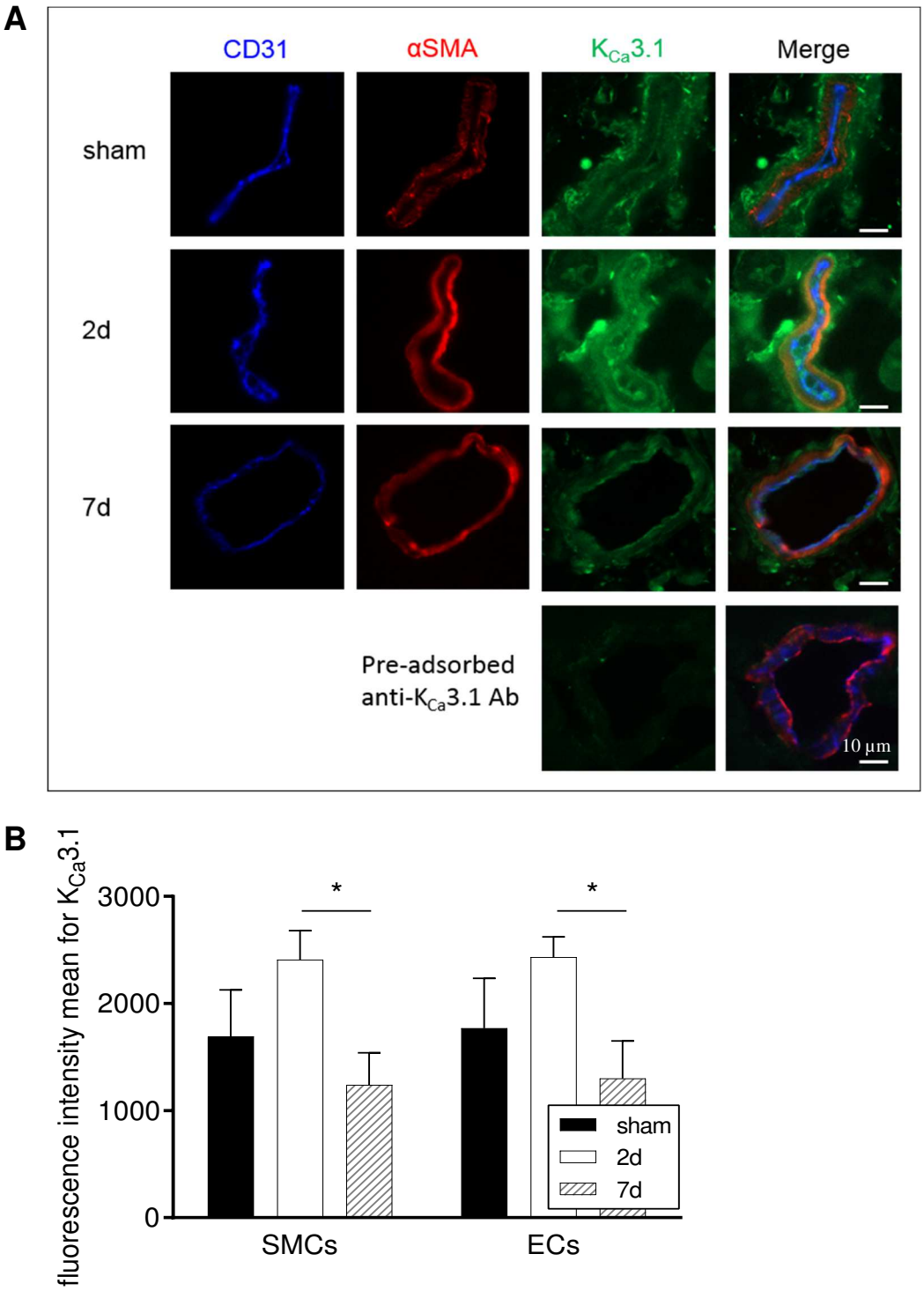

Figure 3.2: $K_{Ca}3.1$ localization and abundance pattern in collateral arteries of wild type mice during arteriogenesis

A. Immunofluorescence staining against $K_{Ca}3.1$ (green) together with the SMC marker α-SMA (red) and the EC marker CD31 (blue) in cross-sections of collateral arteries of sham-operated hind-limb and collateral arteries 2 (2d) and 7 days (7d) after FAL. Lower line, negative control staining performed with anti-$K_{Ca}3.1$ Ab pre-adsorbed with the $K_{Ca}3.1$ antigenic peptide. Scale bar 10 µm. **B.** Quantitative analysis of the fluorescence intensity mean values for $K_{Ca}3.1$ in SMCs and ECs. Mean ± SEM, 1-way ANOVA and Holm-Sidak Post Hoc test: * $p<0.05$, n=3 mice per group, 5-12 sections/mouse.

3.2. Effects of $K_V1.3$ and $K_{Ca}3.1$ blockade on arteriogenesis

To elucidate the role of $K_V1.3$ and $K_{Ca}3.1$ in arteriogenesis, mice were treated with the $K_V1.3$ channel blocker PAP-1 (40 mg/kg per day) or with the $K_{Ca}3.1$ channel blocker TRAM-34 (120 mg/kg per day), while control mice received vehicle only. Mice were subjected to femoral artery ligation and the effect of channel blockade on hind-limb perfusion recovery and collateral artery remodeling were assessed.

3.2.1. Hind-limb perfusion recovery after FAL

Blood perfusion of the hind-limb was monitored via laser Doppler imaging (LDI) and hind-limb perfusion recovery was calculated as the ratio of perfusion of the occluded hind-limb to the perfusion of the sham-operated hind-limb.

As displayed in **Figure 3.3**, treatment with the channel blockers had no effects on perfusion ratios at the baseline, showing values around 100 % in the 3 groups. Immediately after FAL, values decreased to less than 10 %, again independent on the treatment. At day 3, hind-limb perfusion ratio in control mice reached 42.5 ± 1.67 % and at day 7 already 89.17 ± 1.49 % (**Fig 3.3**). While 3 days after FAL both treated groups displayed only an attenuated perfusion recovery respect to controls (33.33 ± 2.19 TRAM-34 and 33.50 ± 3.45 PAP-1), this reduction, however, became significant at day 7 (67.5 ± 4.67 % TRAM-34 and 75.5 ± 3.02 PAP-1).

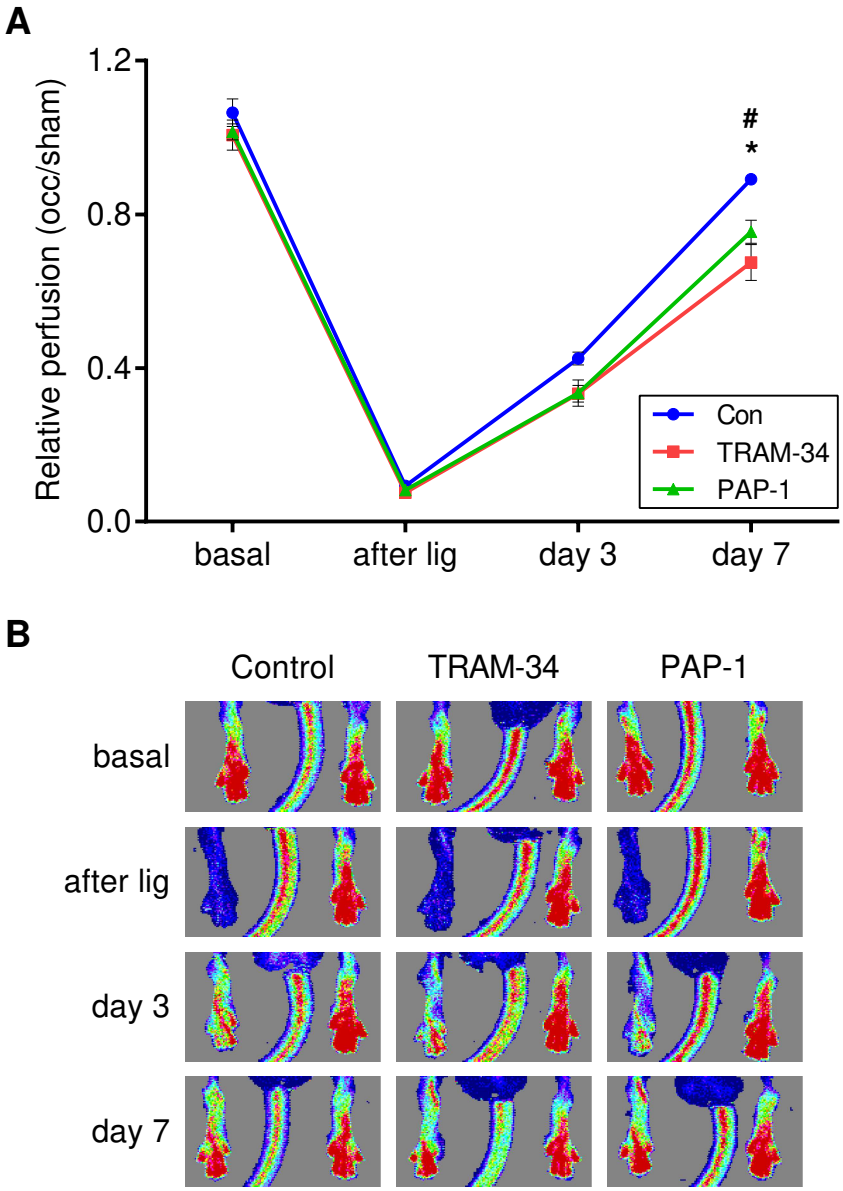

Figure 3.3: Hind-limb perfusion recovery after femoral artery ligation

A. Line plot displaying the ratio perfusion in occluded (occ) versus perfusion in sham hind-limb (occ/sham) of control, TRAM-34-treated and PAP-1-treated mice, before (basal), just after (after lig) and 3 and 7 days after FAL. **B.** Representative flux images. Mean ± SEM, 2-way ANOVA and Holm-Sidak Post Hoc test, n=6 per group, * PAP-1 vs Con, # TRAM-34 vs Con.

3.2.2. Morphometric analysis of collateral arteries

To contrast the results on hind-limb perfusion recovery, the effects of channel blockade on collateral artery growth were investigated directly on collateral artery cross-sections seven days after FAL. The luminal and external perimeters of collateral arteries were measured in Giemsa stained cross-sections. Luminal diameter, medial area and medial thickness were then calculated using perfect circle formulas.

As noticed in the representative images of **Figure 3.4**, femoral artery ligation induced a strong collateral artery growth compared to resting collateral arteries of the sham-operated hind-limb in all three groups. Unexpectedly, while sections of collateral arteries of mice treated with the channel blockers compared to control collateral arteries suggested thinner collateral arteries, arterial lumen respect to resting collaterals appears as large as in control mice.

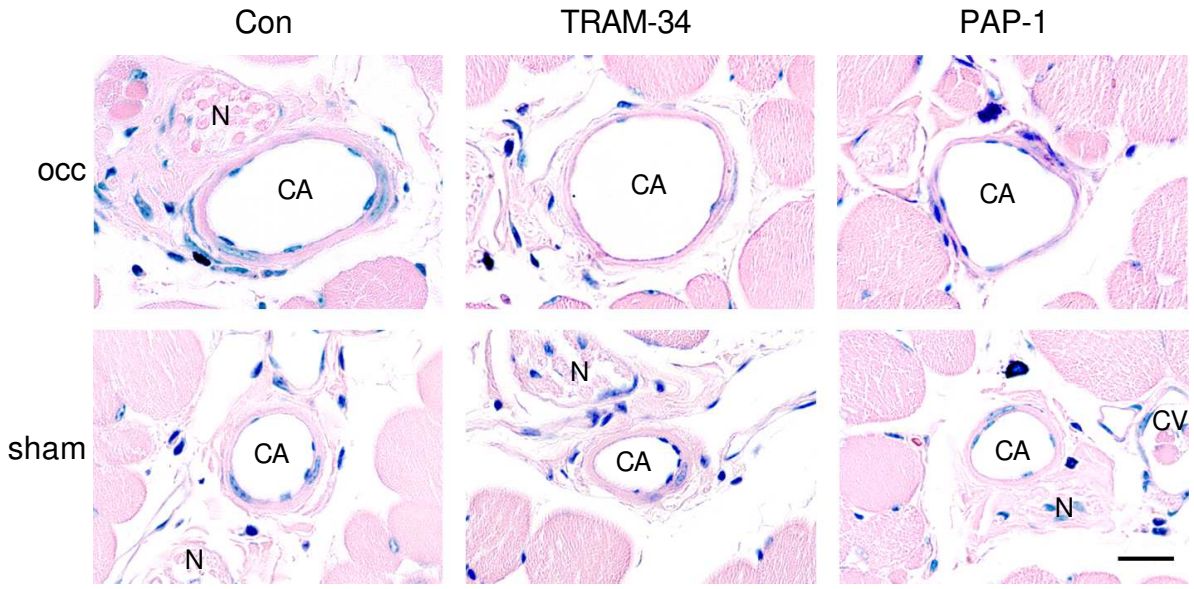

Figure 3.4: Representative images of thigh muscle cross-sections seven days after femoral artery ligation

Sections of thigh muscle in the occluded hind-limb (occ) and sham-operated hind-limb (sham) of control, TRAM-34-treated and PAP-1-treated mice were stained with Giemsa. Inner and outer arteriole circumference were measured to determine luminal diameter, medial thickness and medial area. CA: collateral artery, CV: collateral vein, N: nerve. Scale bar: 20 µm

As expected, the luminal diameter of collateral arteries in occluded hind-limb of control mice increased significantly 1.61-fold with respect to those of collateral arteries in sham-operated hind-limb (44.33 ± 4.62 µm occ vs 27.54 ± 1.34 µm sham) (**Fig 3.5, A**). However, and in contrast to that what one would expect from the perfusion recovery data, the luminal diameter of collateral arteries of TRAM-34-treated and PAP-1-treated mice were significantly increased too with respect to their relatives in sham-operated hind-limb. In TRAM-34 treated mice, the increase in luminal diameter was found to be slightly larger than in control mice, reaching 2-fold values respect to the contralateral collaterals (53.84 ±.2.92 µm occ vs 25.76 ± 2.19 µm sham). However, the raise in luminal diameter in TRAM-34 collateral arteries was not significant with respect to control arteries as shown after normalization of values to those in the respective sham-operated hind-limb (**Fig 3.5, A, right**). The enlargement in luminal diameter of collateral arteries in PAP-1-treated mice was similar to controls, with a 1.79-fold increase (49.92 ± 3.90 µm occ vs 27.92 ± 1.99 µm sham).

Parallel to the results on luminal diameter, collateral artery medial area in the occluded hind-limb of control mice experienced a significant 1.48-fold increase respect to their contralateral counterparts (27.43 ± 1.50 μm^2 occ vs 18.50 ± 0.43 μm^2 sham) (**Fig 3.5, B**). Interestingly, this increase was attenuated under treatment with TRAM-34 in collateral arteries of occluded hind-limb and, with 1.2-fold increase, no more significant with respect to those in sham-operated hind-limb (23.40 ± 2.10 μm^2 occ vs 19.14 ± 0.71 μm^2 sham). However, this increase was almost inexistent in PAP-1-treated mice (21.77 ± 0.77 μm^2 occ vs 20.35 ± 1.40 μm^2 sham). Normalization of collateral medial area in occluded hind-limb with those in the sham-operated hind-limb revealed a significant reduction in PAP-1 treated mice respect to control mice.

Analogous to arterial medial area, medial thickness of collateral arteries in the occluded hind-limb of control mice significantly increased 1.52-fold when compared to those in sham-operated hind-limb (4.46 ± 0.65 µm occ vs 2.94 ± 0.14 µm sham) (**Fig 3.5, C**). Again, media thickening under treatment with TRAM-34 was attenuated increasing only 1.24-fold (3.67 ± 0.78 µm occ vs 2.96 ± 0.12 µm sham), while treatment with the $K_V1.3$ blocker PAP-1 abolished media thickening in collateral arteries of occluded hind-limb versus their contralateral counterparts (3.41 ± 0.33 µm occ vs 3.24 ± 0.55 µm sham). Again, normalization with respect to medial thickness values in sham-operated hind-limb revealed a significant reduction in PAP-1-treated mice compared to controls.

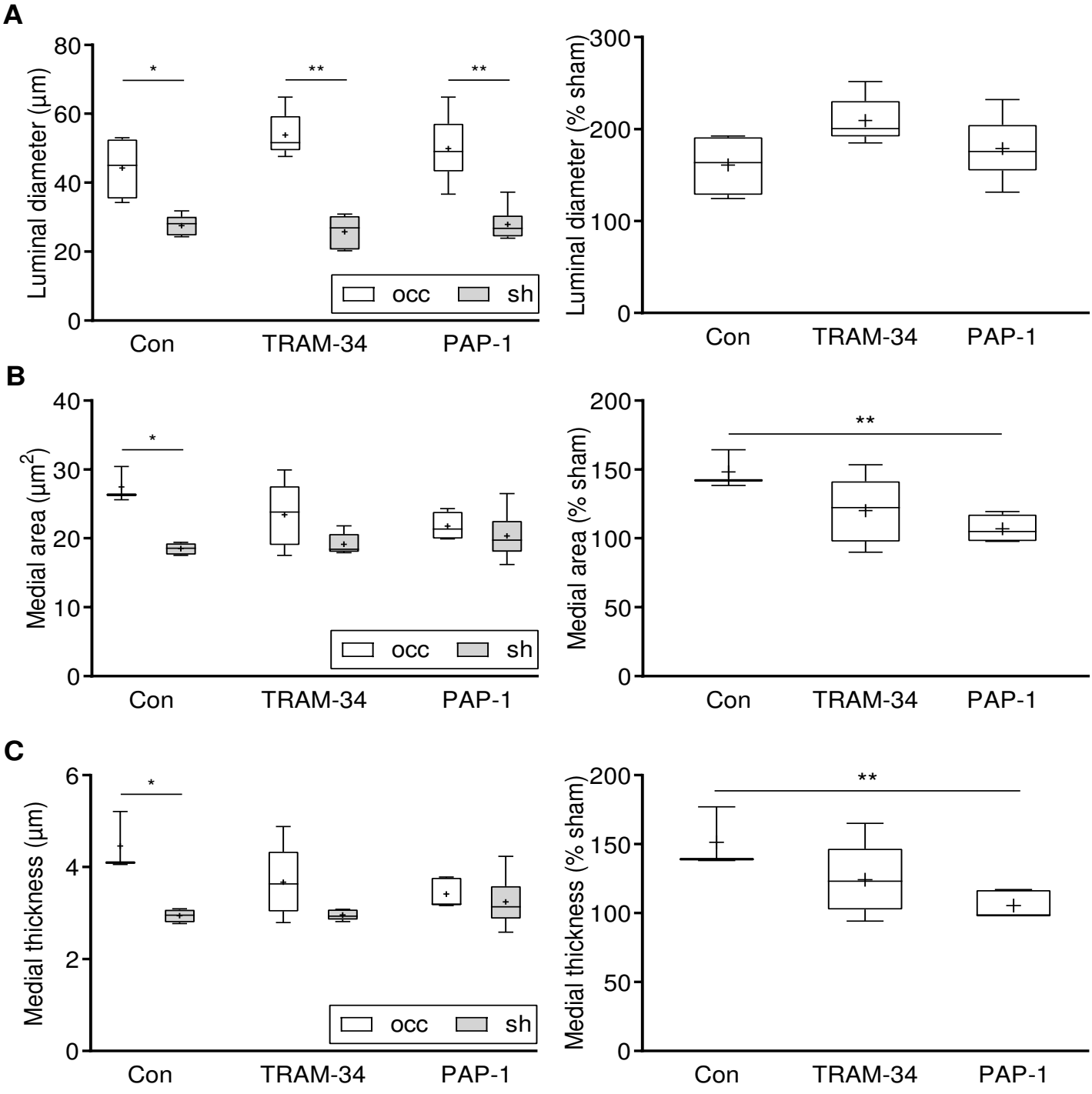

Figure 3.5: Morphometric analysis of collateral arteries seven days after femoral artery ligation

A. On the left, box-and-whiskers graph representing the luminal diameter of collateral arteries in occluded and sham-operated hind-limb. On the right, after normalization to sham values and measured as percentages. **B.** Quantitative analysis of the collateral medial area of collateral arteries in occluded- and sham-operated hind-limb, before (left) and after normalization to values in sham-operated hind-limb (right). **C.** Quantitative analysis of the collateral medial thickness before (left) and after normalization to values in sham-operated hind-limb (right). One-way ANOVA and Holm-Sidak Post Hoc test, *p<0.05, ** p<0.01, n=3-6 mice per group.

3.3. Effects of $K_V1.3$ and $K_{Ca}3.1$ blockade on SMC proliferation in arteriogenesis

The data on wall thickening alluded to an inhibition of SMC proliferation during arteriogenesis under channel blockade, particularly under $K_V1.3$ blockade. In this chapter, the effects of channel blockade on SMC proliferation *in vivo* were investigated more specifically. Mice were treated with the proliferation cell marker BrdU and seven days after ligation, BrdU positive cells were quantified in collateral artery cross-sections. Additionally, these data were complemented with gene expression analysis of α-SMA, a SMC effector protein whose expression is strongly downregulated in proliferative SMCs.

3.3.1. Analysis of collateral SMC and EC proliferation via BrdU staining

To quantify SMC and EC proliferation in collateral arteries, immunohistochemical analysis of the proliferation marker BrdU was performed 7 days after FAL. Collateral artery transversal sections were stained against BrdU, followed by Haemalaun to counterstain tissue morphology. As exhibited in **Figure 3.6, A**, localization and distinctive morphology of SMCs and ECs at the vessel wall allowed an easy identification and quantification of both cell types, without cell specific staining. Since SMCs of collateral arteries in sham-operated hind-limb don't proliferate, only collateral arteries in occluded hind-limb were examined and compared between groups. Results were calculated as the ratio of $BrdU^+$ cell numbers to total cell numbers, normalized to control values and expressed as percentages.

Quantification of $BrdU^+$ SMCs in collateral arteries of TRAM-34-treated mice, seven days after occlusion, revealed that $K_{Ca}3.1$ blockade with TRAM-34 did not influence the number of $BrdU^+$ SMCs with respect to the control group (**Fig 3.6, B**). On the contrary, $K_V1.3$ blockade with PAP-1 resulted in a strong reduction of SMC proliferation, with 54.2 % decrease respect to control arteries (**Fig 3.6, C**).

Interestingly, although statistically insignificant, both treatments slightly increased the numbers of $BrdU^+$ ECs, with an increase of 38.78 % in the TRAM-34 group and 34.13 % in the PAP-1 group above control values (**Fig 3.6**). The tendency to higher EC numbers under channel blockade supports morphometric analysis by which luminal diameters of collateral arteries were found to be as in controls in PAP-1 or even slightly higher in TRAM-34 collateral arteries on

occluded hind-limbs, seven days after ligation. However, both analysis contrast with perfusion data, by which PAP-1- and TRAM-34-treated mice recovered worse than control mice.

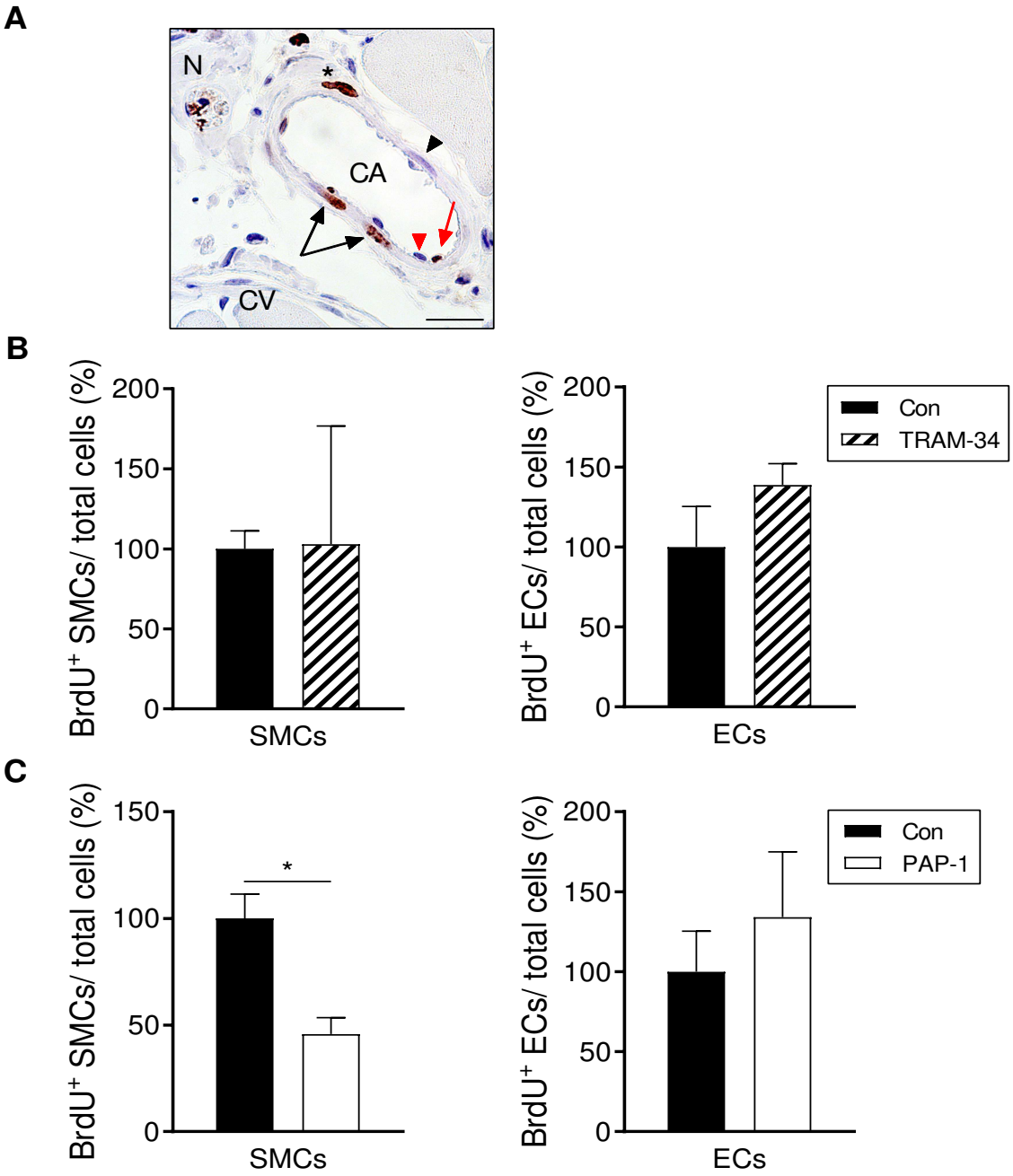

Figure 3.6: Quantitative analysis of SMC and EC proliferation in collateral arteries seven days after femoral artery ligation via BrdU incorporation

A. Representative image of BrdU immunohistochemical staining counterstained with Haemalaun. CA: collateral artery, CV: collateral vein, N: nerve. Black arrows: $BrdU^+$ SMCs and black arrow's head $BrdU^-$ SMC, red arrow: $BrdU^+$ EC, red arrow's head: $BrdU^-$ EC, asterisk: $BrdU^+$ adventitial fibroblast. Scale bar: 20 µm. **B.** Bar plots representing the ratio $BrdU^+$ SMCs-to-total SMC (left panel) and the ratio $BrdU^+$ EC-to-total ECs (right panel) in TRAM-34-treated versus control mice. **C.** Bar plots representing the ratio $BrdU^+$ SMCs-to-total SMCs (left panel) and the ratio $BrdU^+$ ECs-to-total ECs (right panel) in PAP-1-treated versus control mice. Student's *t*-test, $p<0.05$, n=3 mice/group.

3.3.2. Analysis of *aSma* expression in collateral arteries

Alpha smooth muscle actin (α-SMA) is a characteristic SMC effector protein and its expression is strongly repressed during SMC phenotypic modulation (PM) and in proliferative SMCs. To assess when SMC PM is induced following FAL, *aSma* expression was analyzed over time in collateral arteries of wild type mice via real time PCR. Results are expressed as the ratio between messenger RNA (mRNA) levels normalized to 18S rRNA in collateral arteries of occluded hind-limb and the mRNA levels in collateral arteries of sham-operated hind-limb.

As displayed in **Figure 3.7,** *aSma* expression reached a depression point 12h after FAL, recovered 24h after ligation and from 36h on was even upregulated. Repression of *aSma* expression 12h after FAL indicated that at this time point phenotypic modulation towards proliferative SMCs probably occur.

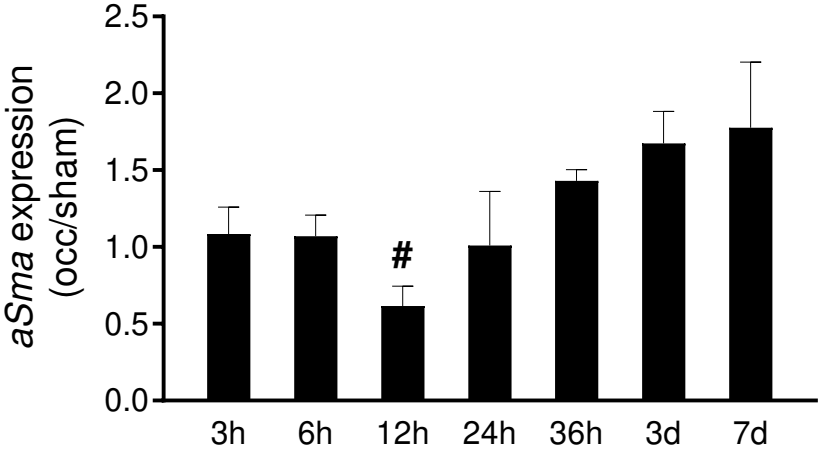

Figure 3.7: *aSma* expression profiling during arteriogenesis in wild type mice

Bar graph displaying *aSma* expression pattern represented as the ratios of mRNA levels measured by real time PCR normalized to 18S rRNA in collateral arteries of occluded to collateral arteries of sham-operated hind-limb of wild type mice at several time points after FAL. One-way ANOVA and Holm-Sidak Post Hoc test, n=3-5. # $p<0.05$ refers to 12h occ vs 12h sham.

To analyze the role of $K_V1.3$ and $K_{Ca}3.1$ in phenotypic modulation induction, mice were treated with the corresponding blockers and the expression of *aSma* was assessed 12h after FAL. Again, *aSma* mRNA levels in control mice were downregulated in collateral arteries 12h after ligation respect to their contralateral counterparts. The same downregulation was evident under treatment with the $K_{Ca}3.1$ blocker TRAM-34 (0.867 ± 0.06 TRAM-34 vs 0.886 ± 0.04 Con) (**Fig 3.8, B**). However, $K_V1.3$ blockade with PAP-1 resulted in an upregulation of *aSma* expression in collateral arteries of occluded hind-limb compared to those of the sham-operated hind-limb. Compared to controls this upregulation was statistically significant (1.366 ± 0.03 PAP-1 vs 0.886 ± 0.04 Con).

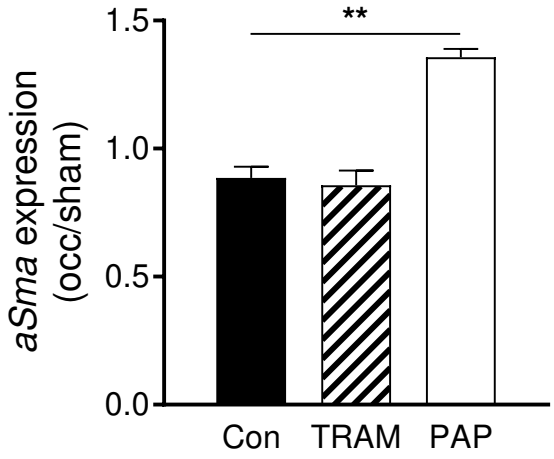

Figure 3.8: *aSma* expression in collateral arteries 12h after femoral artery ligation

Bar graph representing *aSma* expression in TRAM-34-treated, PAP-1-treated and control mice collateral arteries 12h after FAL. One-way ANOVA and Holm-Sidak Post Hoc test, ** $p<0.01$, n=3 per group.

3.4. Effects of $K_V1.3$ and $K_{Ca}3.1$ blockade on MArSMCs proliferation *in vitro*

The role of $K_V1.3$ and $K_{Ca}3.1$ K^+ channels on SMC proliferation was investigated further on primary mouse artery SMCs (MArSMCs) *in vitro*.

3.4.1. $K_V1.3$ and $K_{Ca}3.1$ subcellular localization in MArSMCs

First, a qualitative analysis of $K_V1.3$ and $K_{Ca}3.1$ expression in MArSMCs with special attention on their cellular localization was performed via immunofluorescence imaging.

As exposed in **Figure 3.9**, MArSMCs cultured *in vitro* with SMC growth medium (SMCGM) expressed both $K_V1.3$ and $K_{Ca}3.1$ channels. Interestingly, immunofluorescence staining revealed a strong localization of both channels around and in the nuclei of MArSMCs together with a much weaker localization in the cytoplasm and at the cytoplasmic membrane.

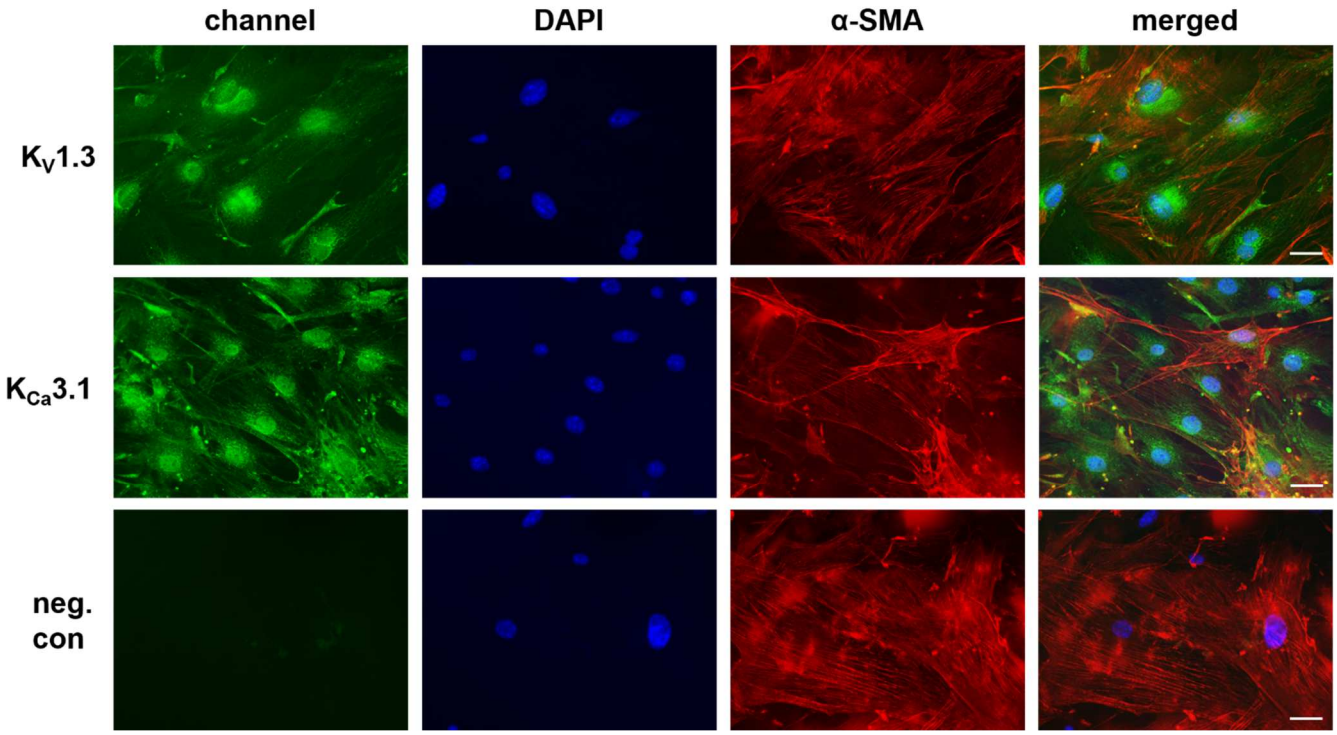

Figure 3.9: K_V1.3 and K_{Ca}3.1 subcellular localization in MArSMCs

MArSMCs were immunostained against K_V1.3 (upper line) and K_{Ca}3.1 (middle line) (green), together with the SMC marker α-SMA (red). Nuclei were stained with DAPI (blue). **C**. Negative control (lower line) staining performed without primary antibody. Scale bar 40 µm.

3.4.2. Analysis of MArSMCs proliferation via BrdU assay

To investigate the effects of K_V1.3 and K_{Ca}3.1 blockade on MArSMCs proliferation, cells were cultured under increasing doses of TRAM-34 (10, 100, 500 nM) and PAP-1 (0.1, 1 and 5 µM) and cell proliferation was quantified via a BrdU incorporation assay.

MArSMC proliferation was indeed inhibited in the presence of both channel blockers TRAM-34 and PAP-1 (**Fig 3.10**). 100 nM TRAM-34 significantly reduced MArSMC proliferation 0.26-fold compared to control cells (73.70 ± 10.23 100 nM TRAM-34 vs 100 ± 17.13 pos Con). Moreover, PAP-1 inhibition of MArSMC proliferation was found to be dose-dependent and significant at 1 µM PAP-1, with a 0.27-fold reduction compared to control cells stimulated with 10 % FCS only (73.33± 8.24 1 µM PAP-1). Furthermore, cells treated with 1 µM PAP-1 or with 100 nM TRAM-34 displayed similar proliferation rates as negative control cells maintained in starvation medium with 0.27-fold reduction (73.06 ± 16.73 2% FCS), reflecting decreased proliferation but not cell death. Furthermore, toxicity and cell viability were assessed with a trypan blue staining (data not shown).

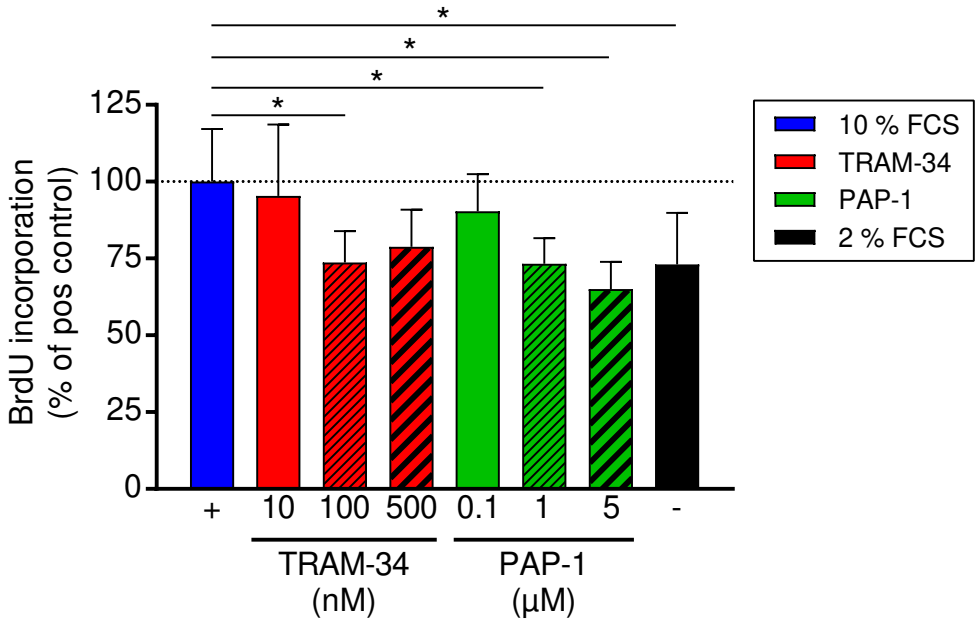

Figure 3.10: Assessment of MArSMC proliferation via BrdU incorporation

Bar graph displaying BrdU incorporation values expressed as percentage to positive control: MArSMCs stimulated with 10 % FCS. Together with 10 % FCS stimulation, MArSMCs were cultured under increasing doses of TRAM-34: 10 to 500 nM or PAP-1: 100 nM to 5 µM. Negative control: MArSMCs cultured in 2 % FCS. One-way ANOVA and Holm-Sidak Post Hoc test, *p<0.05, n=3.

3.5. Effects of $K_V1.3$ and $K_{Ca}3.1$ blockade on *Fgfr1* and *Pdgfrb* expression

3.5.1. *Fgfr1* and *Pdgfrb* expression in MArSMCs under TRAM-34 and PAP-1

RTK signalling plays an important role in SMC proliferation, activating the cell division machinery. Furthermore, FGFR-1 and PDGFR-ß signalling are important stimulators of arteriogenic SMC proliferation. To investigate the role of $K_V1.3$ on *Fgfr1* and *Pdgfrb* expression regulation in SMCs, experiments were performed in cultured MArSMCs. Cells were stimulated with SMCGM containing 2 RTK ligands: FGF-2 and EGF after 24h serum-starvation.

Stimulation with SMCGM did not induce *Fgfr1* and *Pdgfrb* expression in cultured MArSMCs (*Fgfr1*: 0.892 ± 0.074 SMCGM vs 1.065 ± 0.065 neg Con, *Pdgfrb*: 0.890 ± 0.067 SMCGM vs 1.008 ± 0.008 neg Con). Parallelly, treatment with the $K_{Ca}3.1$ channel blocker TRAM-34 had no significant effects on *Fgfr1* and *Pdgfrb* expression compared to cells stimulated with SMCGM alone (*Fgfr1*: 0.892 ± 0.074 SMCGM vs 0.783 ± 0.034 TRAM-34, *Pdgfrb*: 0.890 ± 0.067 SMCGM vs 0.823 ± 0.061 TRAM-34). However, the presence of the $K_V1.3$ channel

blocker PAP-1 significantly repressed both, *Fgfr1* 0.62-fold as well as *Pdgfrb* with 0.58-fold compared to cells stimulated with SMCGM only (*Fgfr1*: 0.892 ± 0.074 SMCGM vs 0.557 ± 0.035 PAP-1; *Pdgfrb*: 0.890 ± 0.067 SMCGM vs 0.520 ± 0.014 PAP-1) (**Fig 3.11**).

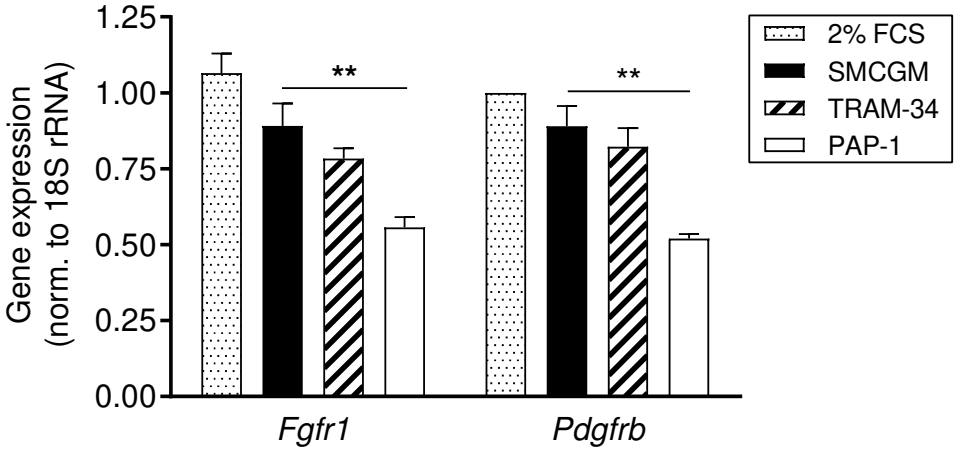

Figure 3.11: *Fgfr1* and *Pdgfrb* expression in MArSMCs under RTK stimulation

Bar graph representing *Fgfr1* and *Pdgfrb* expression values normalized to 18S rRNA, assessed by real time PCR. After serum starvation in 2 % FCS for 24h, cells were stimulated with SMCGM containing FGF-2 and EGF only or together with 100 nM TRAM-34 or 1 µM PAP-1 for 6h. One-way ANOVA and Holm-Sidak Post Hoc test, **p<0.01, n=3.

3.5.2. *Fgfr1* and *Pdgfrb* expression in collateral arteries

Since $K_V1.3$ blockade altered *Fgfr1* and *Pdgfrb* expression in MArSMCs, the effects of channel blockade on the expression of both RTK 12h after FAL was investigated next.

In control mice *Fgfr1* and *Pdgfrb* were not differentially expressed, with occ-to-sham ratios of 1.117 ± 0.103 for *Fgfr1* and 1.036 ± 0.019 for *Pdgfrb* (**Fig 3.12**). In mice treated with the $K_{Ca}3.1$ blocker TRAM-34, both genes were slightly depressed. However, this downregulation was not significant respect to controls for neither of the 2 genes (*Fgfr1*: 0.843 ± 0.175 vs 1.117 ± 0.103 con, *Pdgfrb*: 0.744 ± 0.120 vs 1.036 ± 0.019). A much stronger and significant downregulation was evident under $K_V1.3$ blockade with PAP-1 for both genes, *Fgfr1*: 0.608 ± 0.051 PAP-1 vs 1.117 ± 0.103 Con and *Pdgfrb*: 0.644 ± 0.019 PAP-1 vs 1.036 ± 0.019 con, respect to the control group.

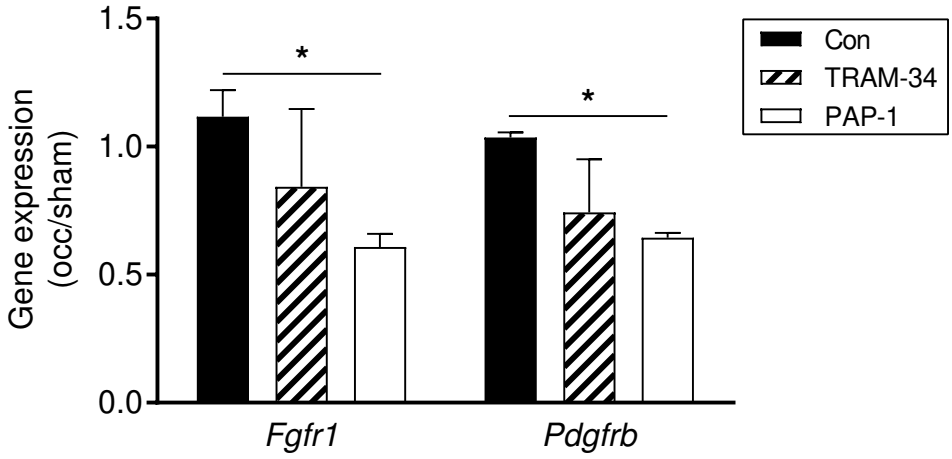

Figure 3.12: *Fgfr1* and *Pdgfrb* expression in collateral arteries 12h after femoral artery ligation

Bar plot representing *Fgfr1* and *Pdgfrb* gene expression as the ratio occ-to-sham collateral arteries in control, TRAM-34-treated and PAP-1-treated mice. One-way ANOVA and Holm-Sidak Post Hoc test, *p<0.05, n=3.

3.6. Role of K_V1.3 in receptor tyrosine kinase signalling

So far, the data pointed to an important role of K_V1.3 in SMC proliferation during arteriogenesis by regulating the expression of two important receptor tyrosine kinases involved in SMC proliferation: FGFR1 and PDGFR-ß. In this chapter, the role of K_V1.3 in RTK signalling was investigated further.

3.6.1. Effect of K_V1.3 blockade on *Egr1* expression *in vitro* and *in vivo*

RTK activation signals among others through the MAPK/ ERK pathway. In arteriogenesis, MAPK/ ERK activation plays an important role in SMC proliferation by inducing the expression of the transcription factor EGR-1. Hence, *Egr1* expression is upregulated 12h after FAL and in growing collaterals and EGR-1 controls SMC proliferation by regulating proteins involved in cell division as well as SMC phenotypic modulation (Pagel, Ziegelhoeffer et al. 2012).

To investigate the role of K_V1.3 in RTK signalling, the expression of *Egr1* in cultured MArSMCs under stimulation with RTK ligands as well as in collateral arteries 12h after FAL were assessed in the presence of the K_V1.3 blocker PAP-1.

MArSMCs stimulated with SMCGM containing FGF-2 and EGF slightly upregulated *Egr1* expression compared to cells cultured further in starvation medium (negative control) (0.501 ± 0.008 SMCGM vs 0.436 ± 0.006 neg Con) (**Fig 3.13, A**). Interestingly, in the presence of 1 µM

PAP-1, *Egr1* expression was significantly downregulated 0.72-fold with respect to MArSMCs stimulated with SMCGM (0.359 ± 0.024 PAP-1 vs 0.501 ± 0.008 SMCGM), reaching values even lower than in negative control cells.

As expected, 12h after FAL, a strong 1.879-fold upregulation of *Egr1* expression in control mice was observed in collateral arteries of occluded hind-limb compared to their contralateral counterparts (1.162 ± 0.237 occ vs 0.646 ± 0.190 sham) (**Fig 3.13, B**). Analogous to *in vitro* data, $K_V1.3$ blockade significantly repressed *Egr1* expression 0.46-fold with respect to controls (0.860 ± 0.063 PAP-1 vs 1.879 ± 0.292 Con). Interestingly, this upregulation was not only truncated in mice treated with PAP-1 but was even slightly downregulated (0.906 ± 0.381 occ vs 1.109 ± 0.587 sham).

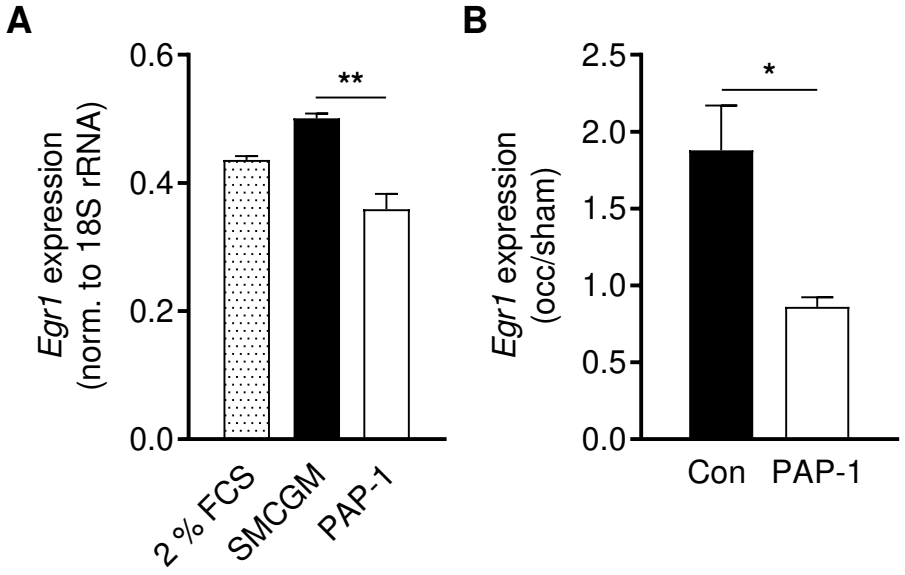

Figure 3.13: *Egr1* expression in cultured MArSMCs under RTK stimulation and in collateral arteries 12h after femoral artery ligation

A. *Egr1* expression values normalized to 18S rRNA in MArSMCs maintained in starvation medium and in MArSMCs stimulated with SMCGM containing FGF-2 and EGF for 6h, with or without 1 µM PAP-1. One-way ANOVA and Holm-Sidak Post Hoc test. **B.** *Egr1* expression 12h after FAL in collateral arteries of PAP-1-treated versus control mice, represented as ratio occluded- to sham-operated hind-limb. Student's *t*-test, *p<0.05, **p<0.01, n=3.

3.6.2. Effect of K_V1.3 blockade on ERK1/2 phosphorylation under RTK stimulation in MArSMCs

K_V1.3 channel blockade resulted in downregulation of *Egr1* expression. Since K_V1.3 localizes at the cytoplasmic membrane and at the nuclear envelope, K_V1.3-mediated *Egr1* expression regulation could be effectuated at one of these two cellular levels.

To investigate if K_V1.3 channel blockade inhibits RTK activation at the cytoplasmic membrane, downstream phosphorylation of ERK by MEK was assessed via western blot in MArSMCs under treatment with two different K_V1.3 channel blockers: PAP-1 and the membrane impermeable Margatoxin (MgTX). As a negative control for ERK phosphorylation, MArSMCs were treated with the specific MEK inhibitor UO126.

In MArSMCs, ERK phosphorylation was strongly induced after stimulation with SMCGM containing FGF-2 and EGF for 5 min compared to MArSMCs cultured further in starvation medium (**Fig 3.14**). This increase was not due to higher ERK protein levels since ERK signals displayed similar intensities in both groups. As expected, addition of the MEK inhibitor UO126 resulted in a reduced ERK phosphorylation, again without affecting ERK levels. In this setting, the presence of the K_V1.3 channel blockers PAP-1 (1 µM) or MgTX (10 nM) did not influence ERK phosphorylation compared to MArSMCs stimulated with SMCGM alone. Total ERK levels were not affected neither.

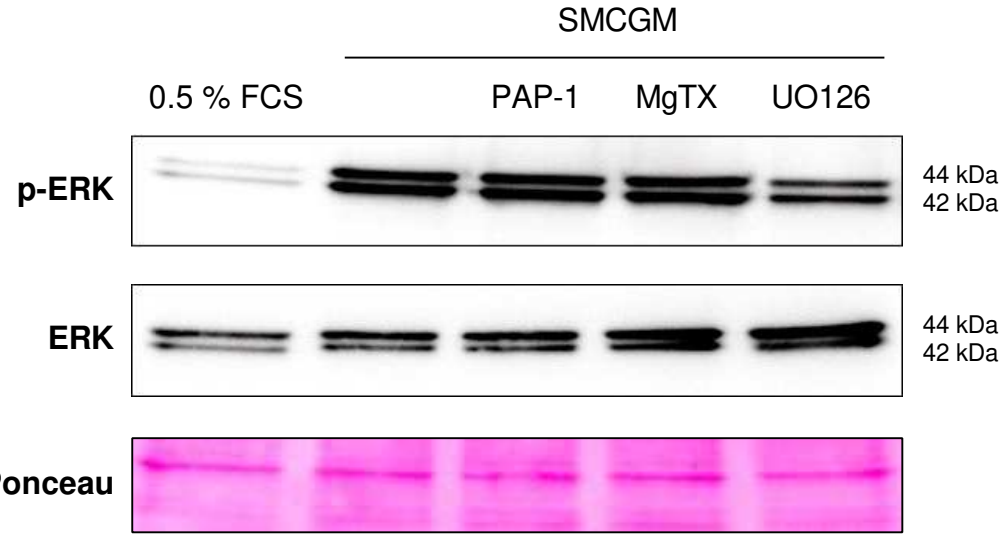

Figure 3.14: Analysis of ERK phosphorylation after RTK stimulation in MArSMCs

Western blot with MArSMC lysates plotted against p-ERK and ERK, upper and middle panel respectively. Lower panel, Ponceau staining confirming equal loading. MArSMCs were stimulated with SMCGM containing FGF-2 and EGF for 5 min in the presence of 1 µM PAP-1 or 100 nM MgTX after a starvation period of 3 days in 0.5 % FCS. As a negative control, MArSMCs were incubated with the MEK inhibitor UO126 (10 µM).

3.7. Role of Sp1 in K_V1.3-mediated *Fgfr1*, *Pdgfrb* and *Egr1* expression regulation

Fgfr1, *Pdgfrb* and *Egr1* expression were downregulated under K_V1.3 channel blockade both in MArSMCs cultured *in vitro* under RTK stimulation and during arteriogenesis. A literature research and an *in silico* analysis of transcription factor binding sites in the promoter sequences, revealed Specificity protein-1 (Sp1) as a common transcription factor for all three genes. In this section, its role in the expression regulation of the three genes was specifically assessed in MArSMCs. Furthermore, the effect of K_V1.3 blockade on Sp1 expression was investigated in MArSMCs and in collateral arteries 12h after FAL.

3.7.1. *In silico* analysis of Sp1 binding sites on *Fgfr1*, *Pdgfrb* and *Egr1* promoters

The presence of Sp1 binding sites in *Egr1* promoter has been reported elsewhere (Sakamoto, Bardeleben et al. 1991, Schwachtgen, Campbell et al. 2000). Moreover, Cao et al, demonstrated that Sp1 activates *Egr1* expression in fibroblast in *in vitro* transfection studies (Cao, Mahendran et al. 1993). On the other hand, an Sp1-dependent regulation of *Fgfr1* expression has been reported in myoblasts, chicken skeletal muscle and cardiomyocytes (Saito, Kouhara et al. 1992, Patel and DiMario 2001, Parakati and DiMario 2002, Seyed and Dimario 2007, Parakati and DiMario 2013). *Pdgfrb* expression regulation through Sp1 has also been reported *in vitro* in neuroblastoma cells (Molander, Hackzell et al. 2001, Kaneko, Yang et al. 2006).

MatInspector software revealed two binding sites for Sp1 on *Egr1* promoter, six binding sites on *Fgfr1* promoter and two binding sites on *Pdgfrb* promoter (**Table 3.1**).

Table 3.1. Sp1 binding sites on *Egr1*, *Fgfr1* and *Pdgfrb* promoters

Gene	Accession no.	Nr. BS	Opt	Start	End	Strand	Sequence	Core sim.	Matrix sim.
Egr1	GXP_3614163	1	0.91	211	227	+	ggttgGGGCgggggcaa	1.000	0.979
		2	0.91	578	594	-	ggctgGGGCaggggccg	1.000	0.917
Fgfr1	GXP_270509	1	0.88	284	300	-	gggagGGGCgggtgcct	1.000	0.959
		2	0.91	580	596	+	gctgcGGGCggcgcgga	1.000	0.921
		3	0.85	922	938	+	accccGGGCggcggacc	1.000	0.854
		4	0.88	938	954	-	cggggGGGAgggctcgg	0.807	0.891
		5	0.88	946	962	-	aggcgGGGCgggggga	1.000	0.997
		6	0.91	986	1002	-	agcccGGGCgggaacaa	1.000	0.932
Pdgfrb	GXP_423602	1	0.85	470	486	-	cctgtGGGCggagttat	1.000	0.947
		2	0.88	483	499	-	gttagGGGCgggccctg	1.000	0.969

In silico analysis of Sp1 binding sites in *Egr1*, *Fgfr1* and *Pdgfrb* promoters performed with the MatInspector software. BS: binding sites, Opt: optimized, Core sim.: core similarity, Matrix sim.: matrix similarity.

3.7.2. Effects of Sp1 DNA-binding blockade on *Fgfr1*, *Pdgfrb* and *Egr1* expression in MArSMCs

In order to investigate the specific role of Sp1 in the regulation of *Fgfr1*, *Pdgfrb* and *Egr1* in SMCs specifically, their expressions were analyzed in MArSMCs in the presence of the Sp1-specific blocker Mithramycin A.

In MArSMCs, following three days in starvation medium, stimulation with SMCGM containing FGF-2 and EGF strongly induced *Egr1* expression 4.65-fold (5.175 ± 0.159 SMCGM vs 1.112 ± 0.063 2 % FCS) (**Fig 3.15**). Addition of the Sp1 blocker Mithramycin A (MTM) resulted in a significant decrease of 0.84-fold in *Egr1* mRNA levels compared to cells stimulated with SMCGM alone (5.175 ± 0.159 SMCGM vs 4.338 ± 0.195 MTM) (**Fig 3.15, A**). The same effect was observable on *Fgfr1* expression. Stimulation with SMCGM resulted in an upregulation of *Fgfr1* expression of 2.44-fold (0.562 ± 0.033 SMCGM vs 0.230 ± 0.013 2 % FCS) while treatment with MTM significantly repressed this upregulation 0.80-fold (0.448 ± 0.011 MTM vs 0.562 ± 0.033 SMCGM) (**Fig 3.15, B**). On the contrary, *Pdgfrb* was strongly downregulated 1.80-fold after stimulation with SMCGM compared to starved MArSMCs (0.610 ± 0.054 SMCGM vs 1.096 ± 0.048 2 % FCS). Treatment with MTM did not affect its expression compared to SMCGM stimulation alone (0.610 ± 0.054 SMCGM vs 0.577 ± 0.062 MTM).

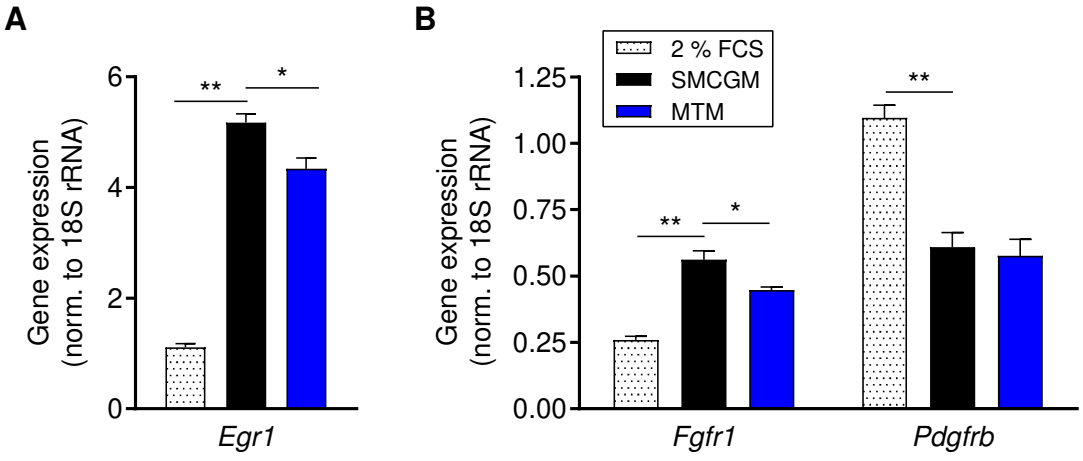

Figure 3.15: Effects of Sp1 binding blockade on *Egr1*, *Fgfr1* and *Pdgfrb* expression in MArSMCs under RTK stimulation

MArSMCs were stimulated with SMCGM containing FGF-2 and EGF for 6h after a starvation period of 3 days with 2 % FCS in the presence or not of the Sp1 blocker Mithramycin A (MTM) (20 µM). Expression of *Egr1* (**A**) and the RTKs *Fgfr1* and *Pdgfrb* (**B**) was analyzed by real time PCR. One-way ANOVA and Holm-Sidak Post Hoc test, *p<0.05, **p<0.01, n=3.

3.7.3. Effects of $K_V1.3$ blockade on *Sp1* gene expression in MArSMCs and collateral arteries

Since Sp1 regulates *Egr1* and *Fgfr1* expression in MArSMCs, a possible role of $K_V1.3$ in Sp1 transcription activity was investigated too. It has been reported that Sp1 transcription activity can be modulated not only through post-transcriptional modifications but also by protein abundance (Tapias, Ciudad et al. 2008). Therefore, *Sp1* expression was assessed first in MArSMCs in the presence or not of the $K_V1.3$ blocker PAP-1 following stimulation with SMCGM. Parallelly, *Sp1* expression was determined in collateral arteries 12h after FAL of control and PAP-1-treated mice.

In vitro stimulation of MArSMCs with SMCGM did not affect *Sp1* mRNA levels compared to cells cultured in 2 % FCS (0.875 ± 0.052 SMCGM vs 0.894 ± 0.095 neg Con). However, MArSMCs stimulated with SMCGM in the presence of PAP-1 significantly downregulated *Sp1* expression 0.69-fold (0.605 ± 0.049 PAP-1 vs 0.875 ± 0.052 SMCGM) (**Fig 3.16, A**). Contrastingly, in collateral arteries 12h after FAL, treatment with the $K_V1.3$ blocker PAP-1 did not influence *Sp1* expression compared to control mice treated with vehicle only (1.192 ± 0.132 Con vs 1.112 ± 0.165 PAP-1) (**Fig 3.16, B**).

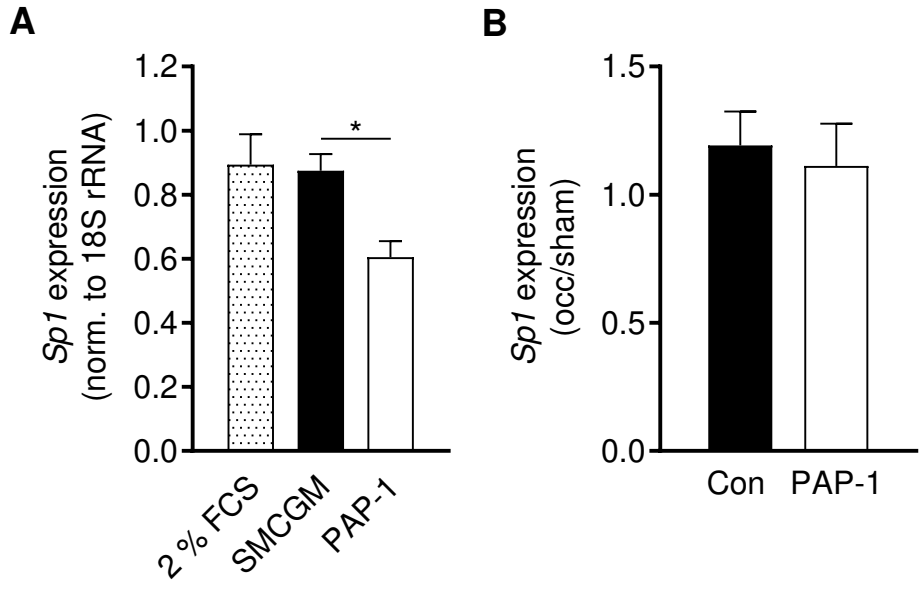

Figure 3.16: Sp1 gene expression in MArSMCs under RTK stimulation and in collateral arteries 12h after femoral artery ligation

A. *Sp1* gene expression analysis represented as Sp1 values normalized to 18S in MArSMCs stimulated with SMCGM containing FGF-2 and EGF following a FCS-starvation period, in the presence or not of 1 µM PAP-1. One-way ANOVA and Holm-Sidak Post Hoc test. **B**. *Sp1* expression expressed as the ratio of collateral arteries in occluded- to collateral arteries in sham-operated hind-limbs of control and PAP-1-treated mice, 12h after FAL. Student's *t*-test *p<0.05, n=3.

3.8. Effects of Sp1 DNA-binding blockade on *Kcna3* expression

Sp1 has been involved in *Kcna3* (K_V1.3 gene) expression regulation in carcinoma cells (Jang, Byun et al. 2015). To contrast these data in primary MArSMCs, cells were stimulated with RTK ligands in the presence of the Sp1-specific blocker MTM. Interestingly, *Kcna3* expression was strongly induced in MArSMCs stimulated with SMCGM containing FGF-2 and EGF almost 2-fold (1.886 ± 0.446 neg Con vs 3.756 ± 0.257 SMCGM) (**Fig 3.17**). However, K_V1.3 mRNA levels were not affected with the addition of MTM under RTK stimulation (3.609 ± 0.625 MTM vs 3.756 ± 0.257 SMCGM).

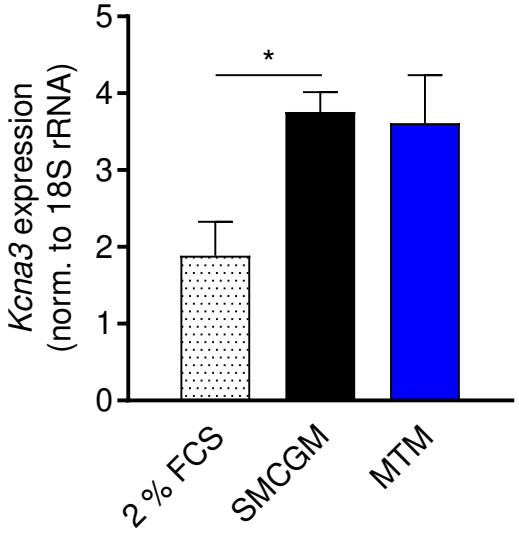

Figure 3.17: K_V1.3 gene expression in MArSMCs under RTK stimulation and Sp1-DNA binding blockade

K_V1.3 gene (*Kcna3*) expression values normalized to 18S in MArSMCs stimulated with SMCGM containing FGF-2 and EGF for 6h were assessed with or without the Sp1-specific blocker MTM by real time PCR. Negative control, MArSMCs maintained in 2 % FCS. One-way ANOVA and Holm-Sidak Post Hoc test, $p<0.05$, n=3

Discussion

4. Discussion

4.1. Channel blockade versus channel-knockout mice

To investigate the role of channels *in vivo*, two different strategies can be followed: the analysis of channel-specific knockout (KO) or the treatment of wild type mice with channel specific blockers (loss of function) or openers (gain of function).

$K_V1.3$ and $K_{Ca}3.1$ KO mice have been reported so far (Fadool, Tucker et al. 2004, Si, Heyken et al. 2006). However, both are constitutive KO mice, that is, gene expression is missing from the whole embryonic development and is deleted in all the tissues where the gene is expressed. In these mice, collaterogenesis, the formation of collateral arteries during embryogenesis, could be affected and influence the parameters used to evaluate arteriogenesis in adulthood. Moreover, it is well known that constitutive KO mice can develop compensation mechanisms by which the gene's function is undertaken usually by high-conserved genes, unmasking any function (Sprossmann, Pankert et al. 2009). Hence, compensatory mechanisms have been detected in thymocytes of $K_V1.3$-KO mice, by which a lack of voltage-gated K^+ current is compensated by an increase in chloride currents (Koni, Khanna et al. 2003). On the other hand, while $K_{Ca}3.1$-KO exhibit a normal phenotype, a mild 7 mmHg increase in mean arterial blood pressure has been detected, probably due to interference with its EDHF function and other developmental compensations (Wulff and Castle 2010). To study the role of $K_V1.3$ and $K_{Ca}3.1$ channels in SMCs specifically, the best strategy would be the use of inducible SMC-specific KO mice. In these mice expression of the channel would be controlled temporally and spatially by using SMC-specific marker gene promoter (Kuhbandner, Brummer et al. 2000). The generation of these mouse models is however time-consuming and very expensive.

Chemical inhibition with channel specific blockers neither affects embryonic development nor give place to compensation mechanisms, since the treatment starts shortly before the surgical procedure. Furthermore, treatment with channel blockers is quick, flexible and cheap. For all these reasons, the use of specific channel blockers was considered the best strategy in this study. However, chemical inhibition of channels presents some disadvantages to consider. As well as constitutive KO mice, the treatment with channel blockers is not cell type-specific: all cells expressing the channel will be affected. Furthermore, channel blockers must be tested for toxicity as any other drug and the dose used must be specific. Since family channels have highly conserved members, high concentrations of the channel blocker could act non-specifically over highly related-channels (Schmitz, Sankaranarayanan et al. 2005).

4.1.1. K_V1.3 channel blocker PAP-1

5-(4-Phenoxybutoxy)psoralen (PAP-1) is a membrane-permeable specific K_V1.3-channel blocker, that is 23-fold selective over K_V1.5 and 33- to 125-fold selective over other K_V1-family channels (Schmitz, Sankaranarayanan et al. 2005). Furthermore, PAP-1 has been used in several *in vivo* studies in mice, rats and monkeys without toxic effects (Schmitz, Sankaranarayanan et al. 2005, Azam, Sankaranarayanan et al. 2007, Pereira, Villinger et al. 2007, Straub, Perez et al. 2011, Cidad, Novensa et al. 2014). In this study, the dose and administration route used, 40 mg/kg/day i.p., is based on a rat study performed by Chen et al (Chen, Lam et al. 2013). To maintain a relative constant concentration of the blocker, the daily dose was administered in two injections with 10-12 h interval. In addition, special attention was paid to any manifestation of toxicity or any disease symptom. Since drugs were injected i.p., any signs of infection or inner organs damage were checked out during organ sampling or perfusion fixation. In PAP-1-treated mice, drinking and eating behaviors, weight, feces and fur were as usual.

4.1.2. K_{Ca}3.1 channel blocker TRAM-34

TRAM-34 (1-[(2-chlorophenyl)diphenylmethyl]-1H-pyrazole) is a membrane-permeable K_{Ca}3.1-specific blocker that has also been used in *in vivo* experiments with mice, rats and swine showing no toxicity so far (Kohler, Wulff et al. 2003, Tharp, Wamhoff et al. 2008). The dose and frequency used in this study, 120 mg/kg/d i.p., in two different injections with 10-12h interval were already reported in mice (Toyama, Wulff et al. 2008, Hua, Deuse et al. 2013) and rats (Kohler, Wulff et al. 2003, Grgic, Wulff et al. 2009).

As in PAP-1-treated mice, treatment with TRAM-34 did not affect drinking and eating behaviors, weight, feces or fur. No symptoms were observed during the whole study.

4.2. The role of K_V1.3 in arteriogenesis and SMC proliferation

4.2.1. K_V1.3 is constantly expressed in collateral SMCs and ECs

First, K_V1.3 expression in collateral arteries of wild type mice undergoing FAL was confirmed through immunofluorescence histology. To further examine its expression regulation during collateral artery growth, immunofluorescence intensities were quantified in resting, two and seven day growing collateral arteries, corresponding to a highly proliferative and to a quiescent phase, respectively. Co-localization of K_V1.3 with the SMC marker α-SMA and the EC marker CD31 revealed the expression of the channel in both cell types. Interestingly, quantification of

Kv1.3 immunofluorescence intensities in all time points investigated reflected no changes in K_V1.3 protein levels, neither in SMCs nor in ECs.

In contrast to this finding, two studies report an upregulation of the channel in proliferative versus contractile SMCs, albeit in models of neointima hyperplasia, such as the murine femoral artery balloon injury model (Cidad, Moreno-Dominguez et al. 2010) or in human saphenous vein segments cultured *ex vivo* following endothelial damage (Cheong, Li et al. 2011). However, even if both arteriogenesis and neointima hyperplasia share a strong SMC proliferation, in neointima hyperplasia is characteristic an endothelial dysfunction occasioned by endothelium damage. During arteriogenesis, however, SMC proliferation induction follows a FSS-driven endothelial activation without endothelial damage or dysfunction (Hui 2008, Patel, Waltham et al. 2010). It is well known that the endothelium regulates SMC proliferation through several mechanisms. The endothelium acts as a barrier from continuous contact to GFs present in the vessel lumen and secrete products that directly inhibit SMCs proliferation, like nitric oxide (Feletou 2011, Napoli, Paolisso et al. 2013). Indeed, re-endothelization after vascular injury results in less neointima hyperplasia (Nugent, Rogers et al. 1999, Patel, Waltham et al. 2010, Adamo, Fishbein et al. 2016). Hence, the course of SMC proliferation during arteriogenesis may proceed to a different manner as the one in the pathological situation of neointima hyperplasia and explain the different K_V1.3 expression regulation in proliferative SMCs in both models.

Besides the regulation of protein abundance, channel function can also be modulated at the level of channel activity as well as subcellular localization. While K_V1.3 channel gating occurs through membrane depolarization, mechanisms regulating channel gating have been reported such as post-translational modifications or modulation by auxiliary subunits (Cook and Fadool 2002). The auxiliary subunit KCNE4 for example, strongly inhibits K_V1.3 activation and increases its rate and extent of cumulative inactivation (Grunnet, Rasmussen et al. 2003, Sole, Roura-Ferrer et al. 2009). Auxiliary subunits also mediate channel sorting and trafficking. Hence, interaction with KCNE4 or the prodomain of the metalloproteinase 23 impair K_V1.3 targeting to the cell membrane and retains it in the endoplasmic reticulum (ER) (Sole, Roura-Ferrer et al. 2009, Nguyen, Galea et al. 2013), while co-expression of Kv1.3 with the ß subunits K_Vß1 or K_Vß2 in oocytes results in increase channel localization and K^+ currents at the cell membrane, without affecting its activation kinetic (McCormack, McCormack et al. 1999). K_V1.3 has been found in different subcellular localizations such as nuclei and nuclear envelope as well as the mitochondrial membrane. Hence, as discussed in the next chapter, it may be

subject to recycling from the cell membrane to the nucleus (Gulbins, Sassi et al. 2010, Jang, Byun et al. 2015).

In summary, $K_V1.3$ might be regulated during arteriogenesis through channel activity and/or subcellular localization instead of protein abundance. Further investigations on channel subcellular localization, expression analysis of auxiliary subunits or $K_V1.3$ post-translational modifications in collateral SMCs following FAL specifically will complement our knowledge on $K_V1.3$ regulation in arteriogenesis.

Along with its localization in SMCs, $K_V1.3$ was strongly and constantly expressed in ECs. Interestingly, the fluorescence signal in ECs was stronger than in SMCs, reflecting higher $K_V1.3$ levels in ECs than in SMCs. A stronger expression of $K_V1.3$ in ECs versus SMCs was also reported at the mRNA level by Fountain et al in mouse mesenteric arteries (Fountain, Cheong et al. 2004). The role of endothelial $K_V1.3$, however, has not been investigated extensively. $K_V1.3$ may mediate endothelial proliferation, since $K_V1.3$ blockade with Margatoxin inhibited human umbilical vein ECs (HUVECs) proliferation *in vitro*, by interfering with VEGF-mediated hyperpolarization and NO production, a well-known endothelial mitogenic factor (Erdogan, Schaefer et al. 2005).

Based on cell morphology and localization, perivascular inflammatory cells and adventitial fibroblasts, in addition to skeletal muscle were also stained for $K_V1.3$. Macrophages and T cells are recruited to collateral arteries where they foster collateral artery growth (Arras, Ito et al. 1998, Scholz, Ito et al. 2000, Stabile, Kinnaird et al. 2006). In macrophages, $K_V1.3$ plays a role in proliferation and migration (Vicente, Escalada et al. 2003, Kan, Gao et al. 2016). In T cells, $K_V1.3$ is involved in T cell receptor-mediated activation and proliferation (Azam, Sankaranarayanan et al. 2007). While in fibroblasts, $K_V1.3$ expression has not been described so far, in skeletal muscle $K_V1.3$ has been involved in glucose uptake (Li, Wang et al. 2006). Due to the broad expression of $K_V1.3$ in collateral arteries, results on the effects of channel blockade on SMC proliferation *in vivo* were analysed carefully and contrasted with *in vitro* experiments effectuated with primary MArSMCs.

4.2.2. PAP-1 impaired arteriogenesis by inhibiting SMC PM and proliferation

The expression of $K_V1.3$ in resting and growing collateral SMCs, prompted us to investigate the impact of $K_V1.3$ channel blockade on arteriogenesis and specially on SMC proliferation. Moreover, a first seven day follow up of the perfusion recovery of the hind-limb after femoral

artery ligation revealed an attenuation of the perfusion recovery on day three after FAL that became significant on day seven under $K_V1.3$ channel blockade. To contrast LDI data, a more specific and detailed analysis of arterial morphometry was performed in collaterals of adductor samples of control and PAP-1-treated mice. Adductors were collected after maximal vasodilation and perfusion fixation with paraformaldehyde, seven days after ligation of the femoral artery. Histological cross-sections of the middle region were stained with Giemsa solution to delimitate vascular wall, and collaterals were compared between occluded- and sham-operated hind-limb and between groups. As expected, a strong increase in diameter and in medial thickness was detected in control mice between collaterals of the occluded hind-limb and their sham-operated counterpart. While collateral arteries in occluded hind-limb of PAP-1-treated mice depicted similar diameters compared to control ones, a significant decrease was observed in collateral medial thickness and medial area. These results pointed to an inhibition of SMC proliferation by $K_V1.3$ blockade with PAP-1 while EC proliferation remained unaffected. In order to verify this hypothesis, a quantitative analysis of proliferative SMCs and ECs was carried out in collateral cross-sections of occluded hind-limb of mice treated with the thymine substitute BrdU, seven days after occlusion of the femoral artery. Indeed, while $BrdU^+$ ECs-to-total ECs ratios were similar in control versus PAP-1-treated mice, a strong reduction was observed in the $BrdU^+$ SMCs-to-total SMCs ratio in collateral arteries under PAP-1 treatment. Interestingly, an *in vivo* inhibition of SMC proliferation by PAP-1 has also been reported though in a murine model of hypertension-mediated neointima hyperplasia (Cidad, Novensa et al. 2014).

Considering that collaterals luminal diameters in both PAP-1-treated and control mice were similar, it is at first glance surprising that channel blockade impaired blood perfusion recovery. However, as assessed by collateral morphometry and $BrdU^+$ SMC counting in seven days growing collateral arteries, PAP-1 significantly decreased SMC numbers. Since SMCs play a crucial role in vascular tone regulation, collateral arteries of PAP-1-treated mice could be affected in their vasodilation function. Hence, during LDI measurement the mouse is placed in a warm chamber to induce a physiological vasodilation that could be hindered in the thinner collateral arteries of PAP-1-treated mice. In contrast, for collateral morphometry analysis, collaterals are externally vasodilated by perfusion fixation before sample collection, so that the same vasodilation is reached in all groups.

In addition, an involvement of $K_V1.3$ in vascular tone regulation cannot be excluded neither. Even though a direct role of $K_V1.3$ in vascular tone regulation has not been reported yet, studies with isolated and endothelium-denuded mesenteric arteries have associated the highly-related

K^+ channels $K_V1.2$, $K_V1.4$, $K_V1.5$ and $K_V1.6$ with tone regulation in terminal arterioles by employing K_V1 inhibitors (Yuan, Wang et al. 1998, Cheong, Dedman et al. 2001, Plane, Johnson et al. 2005). Hence, $K_V1.3$ blockade with PAP-1 could increase vascular tone and blood pressure, preventing so optimal vasodilation in the warm chamber during LDI measurements and giving misleading results. For instance, a similar situation was observed in endothelial nitric oxide synthase knockout mice (eNOS-KO). eNOS produces nitric oxide (NO) that diffuses towards the SMC layer inducing SMC relaxation and subsequent vasodilation. While eNOS-KO mice have a very bad perfusion recovery measured with LDI compared to their wild type littermates, their collateral arteries have surprisingly normal diameters and wall thicknesses. The restoration to a normal perfusion recovery in eNOS-KO mice after injection of the NO-donor S-Nitroso-N-Acetyl-D,L-Penicillamine (SNAP) just before LDI measurement, indicated that the low perfusion observed was due to an interference in the vasodilation induced in the warm chamber during LDI measurement and not to poorer collateral growth (Schaper and Schaper 2004).

Unfortunately, no measurements of blood pressure in PAP-1-treated and control mice were performed in this study and reports characterizing $K_V1.3$-KO mice did not assessed explicitly alterations in blood pressure and vascular tone neither (Xu, Koni et al. 2003, Fadool, Tucker et al. 2004). Therefore, it remains an open question if bad recovery in feet perfusion under $K_V1.3$ blockade was due to dysfunctional collateral arteries as a result of less SMC numbers and/or to a role of the channel in vascular tone regulation.

In several studies, $K_V1.3$ has been correlated with *in vitro* SMC proliferation too. To contrast our *in vivo* findings and the reported data, the inhibitory effects of PAP-1 on SMC mitogenesis were assessed in MArSMCs through a BrdU-based proliferation ELISA test.

Indeed, MArSMCs proliferation was proportionally inhibited with increasing concentrations of PAP-1. This inhibition was already significant with 1 µM PAP-1, a dose reported to be non-toxic in Jurkat T cells and in mouse erythroleukemia (MEL) cells treated for 48h and no mutagenic for *Salmonella typhimurium* in an Ames test (Schmitz, Sankaranarayanan et al. 2005). PAP-1 has also been reported to inhibit SMCs as well as HEK-293 cell proliferation transfected with a $K_V1.3$ plasmid *in vitro* (Cidad, Moreno-Dominguez et al. 2010, Cidad, Jimenez-Perez et al. 2012).

Since PAP-1 is a membrane-permeable $K_V1.3$ channel blocker, its effects on SMC proliferation, both *in vitro* and in *in vivo*, could be consequence of the blockade in both nuclear and cell membrane $K_V1.3$ channels

According to the presence of $K_V1.3$ in SMCs of resting collateral arteries and the inhibitory effect that $K_V1.3$ channel blockade exerted on SMC proliferation, we raised the question if $K_V1.3$ could mediate SMC PM soon after arteriogenesis induction. Since SMCs undergoing PM strongly downregulate the expression of the contractile marker α-SMA (Mack 2011), its expression was assessed in collateral arteries of mice treated with the channel blocker. A previous analysis of *αSma* expression at several time points after ligation of the femoral artery revealed a depression point 12h after FAL, while the expression recovered 24h after and was even upregulated from 36h on. This reflected a first SMC proliferation wave 12h after arteriogenesis induction. After proliferation, SMC differentiate again giving rise to a mixture of SMC populations in collateral arteries and explain the upregulation of α-SMA from 36h on. Supporting this finding, Pagel et al also detected a downregulation of *aSma* 12h after FAL (Pagel, Ziegelhoeffer et al. 2012). Interestingly, *aSma* was no more repressed when $K_V1.3$ was blocked with PAP-1 compared to control mice treated with vehicle only.

Despite the strong expression of $K_V1.3$ in collateral ECs observed by immunofluorescence staining, the regular arterial diameters and $BrdU^+$ ECs ratios of collateral arteries in occluded hind-limb of PAP-1 treated mice, made assume that in arteriogenesis endothelial $K_V1.3$ probably does not play a role in EC proliferation in contrast to what reported by Erdogan et al. in HUVECs (Erdogan, Schaefer et al. 2005).

Altogether, *in vivo* findings point to a role of the Kv1.3 channel in the regulation of SMC proliferation during arteriogenesis and probably in the mediation of SMC PM soon after arteriogenesis induction. However, since the channel is also expressed in ECs and perivascular cells, known to foster collateral growth, blockade of the channel in these cells could influence SMC phenotype and proliferation too. To verify that the effects seen on SMC proliferation under PAP-1 treatment were indeed consequence of channel blockade on SMC themselves, *in vitro* experiments were performed in parallel with MArSMCs.

4.2.3. $K_V1.3$ localizes in the nucleus and could regulate gene expression

The *in vivo* findings on $K_V1.3$ expression in collateral SMCs and on SMC proliferation under channel blockade were contrasted with *in vitro* experiments performed with primary MArSMCs. Cells cultured in SMCGM containing the GFs EGF and FGF-2 were characterized by immunofluorescence cytochemistry. $K_V1.3$ staining not only confirmed the expression of the channel but, moreover, it revealed an unexpected localization at the nucleus and ER, together with a much weaker signal in cytoplasm and cell membrane. Interestingly, the nuclear

localization of $K_V1.3$ has been reported in several cancer cells, human brain tissue and Jurkat cells (Jang, Byun et al. 2015) but not in SMCs yet (Cidad, Moreno-Dominguez et al. 2010).

How $K_V1.3$ is transported to the nuclear envelope (NE) and/or into the nuclei and moreover, through which stimulus, is not well known. Nuclear proteins are transported to the nucleus usually through the recognition of a nuclear localization signal (NLS). Then, they cross the nuclear pore complexes (NPC) that connect the outer nuclear membrane (ONM) with the inner nuclear membrane (INM) together. However, $K_V1.3$ protein has no conventional NLS in its sequence, and even if an atypical NLS cannot be discarded, its nuclear localization can be explained by other mechanisms (Jang, Byun et al. 2015). As other transmembrane proteins, $K_V1.3$ channel may diffuse from the ER where it folders to the outer nuclear membrane (ONM), since both membranes are continuous. The channel, if located at the INM, could then be translocated from the ONM to the INM or to the nucleus through vesicular fusion or through peripheral channels present between the NPC core and the membrane (Zuleger, Korfali et al. 2008, Ungricht and Kutay 2015). Interestingly, the voltage-gated K^+ channel $K_V10.1$ has been detected in the cell membrane but also in the INM of neurons, tumor cells and several cell lines (Chen, Sanchez et al. 2011). Even though $K_V10.1$ contains a NLS, its translocation to the INM seems to precede channel recycling from the cell membrane via endocytosis and lysosomes sorting representing an alternative pathway to the NE, the so called retrograde pathway (Kohl, Lorinczi et al. 2011). Intriguingly, a recent publication reported the endocytosis of $K_V1.3$ following EGF-EGFR signalling in HEK-293 cells, targeting the channel to endosomes together with the EGFR, in an ERK1/2-dependent process (Martínez-Mármol, Comes et al. 2016). Even if the authors found $K_V1.3$ in lysosomes and concluded that the channel is finally degraded, a possible route from endosomes to the nucleus via the retrograde pathway, as described for $K_V1.10$, cannot be excluded neither. Hence, the translocation from endosomes to the nucleus has also been described for EGFR itself, together with other RTKs such as FGFR-1 (Wang, Yamaguchi et al. 2010). Moreover, since EGF is one of the GF present in the growth medium used in this study to culture MArSMCs, EGFR engagement might explain the different $K_V1.3$ localization pattern observed in SMCs respect to other reports (Cidad, Moreno-Dominguez et al. 2010).

The NE is a permeable barrier to ions. The perinuclear space (NE lumen) acts as a Ca^{2+} store, with high $[Ca^{2+}]$ inside compared to cytoplasm and nucleoplasm. Inversely, $[K^+]$ in the perinuclear space is lower than outside (Garner 2002). The presence of intranuclear electrical charges (negatively charged DNA and positively charged histones) and the diffusion of ions across the NE through ion channels and along the NPCs generate a nuclear membrane electrical

potential difference (nmΔΨ). Thus, changes in the nuclear K^+ channels activity alters K^+ flux across the NE and affects nmΔΨ. Subsequently, changes in perinuclear [Ca^{2+}] activates Ca^{2+}-regulated gene expression (Checchetto, Teardo et al. 2016). Hence, the blockade of the nuclear channels ATP-sensitive potassium channel (K_{ATP}) and $K_{Ca}1.1$ or activation of the nuclear inositol triphosphate receptor ($InsP_3R$) trigger nuclear Ca^{2+} transients able to activate the transcription of the Ca^{2+}-activated TF cAMP response element-binding (CREB) (Quesada, Rovira et al. 2002, Cardenas, Liberona et al. 2005, Li, Jie et al. 2014).

Interestingly, Jang et al reported an increased phosphorylation and activation of CREB and an increased c-fos abundance under PAP-1 channel blockade and thus suggested a role for $K_V1.3$ in the regulation of gene expression. Accordingly, since Margatoxin induced hyperpolarization of the NE in isolated nuclei, this regulation may be permeation-dependent and Ca^{2+}-mediated (Jang, Byun et al. 2015). Moreover, Klemm et al correlated high CREB levels with a lower SMC proliferation both *in vivo* and *in vitro* (Klemm, Watson et al. 2001).

In addition, Jang et al demonstrated a direct interaction between $K_V1.3$ and the TF Upstream binding transcription factor 1 (UBTF1), a TF that controls RNA polymerase I, responsible for the transcription of rRNA (Jang, Byun et al. 2015). rRNAs assemble with ribosomal proteins to form ribosomes, that in the cytoplasm, control mRNA translation to proteins. Both rRNA and the subsequent protein synthesis take place before mitosis and are crucial for successful cell proliferation. rRNA synthesis increases during the G1 phase and reach a maximum in G2 phase (Hernandez-Verdun 2011). Interestingly, $K_V1.3$ silencing in A549 lung adenocarcinoma cells resulted in anti-proliferative effects by affecting the G1 to S transition (Jang, Choi et al. 2011).

Furthermore, nuclear K^+ ions can directly influence the physical structure of heterochromatin, regulating so transcription efficiency and splicing. K^+ ions increase the stability of G-quadruplex structures, inter or intramolecular non-Watson-Crick pairs in guanine-rich area, which can act as transcriptional repressor elements (Siddiqui-Jain, Grand et al. 2002). Chen et al postulated that $K_V10.1$ could bind to heterochromatin since its localization correlated with the absence of Lamin A/C, compatible with heterochromatin (Chen, Sanchez et al. 2011). Interestingly, immunofluorescence staining of MArSMCs revealed $K_V1.3$ signal surrounding pericentric heterochromatin stained with DAPI.

In summary, the nuclear localization of $K_V1.3$ in MArSMCs may be explained by recycling from the cell membrane following EGFR engagement and MAPK activation (**Fig 4.1**). In the nuclei or NE, $K_V1.3$ may then influence gene transcription and subsequent SMC proliferation

through almost three different mechanisms: the regulation of TF activity/ abundance, rRNA synthesis and subsequent protein translation and/or by modifying heterochromatin structure and accessibility.

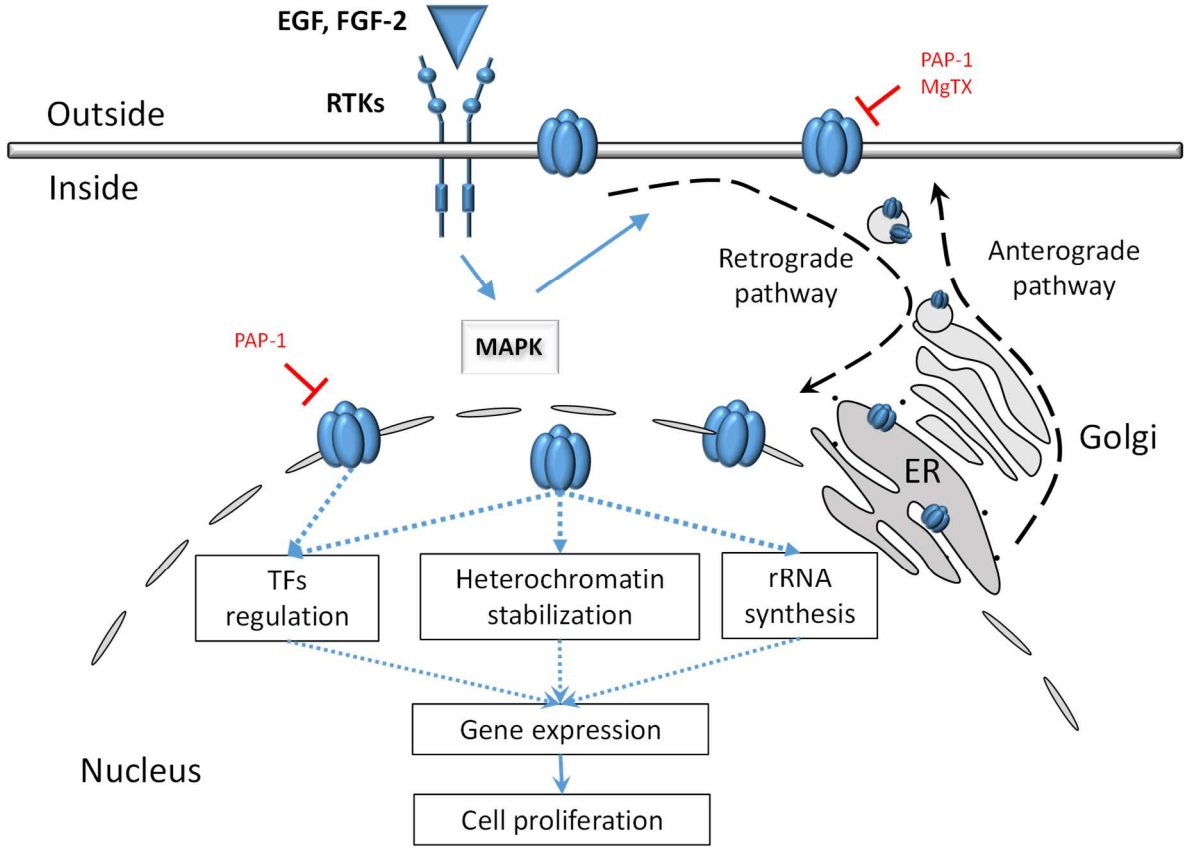

Figure 4.1: Proposed model of nuclear K_V1.3-mediated gene expression regulation

EGFR engagement and MAPK activation leads to K_V1.3 endocytosis from the cell membrane together with the EGFR (Martínez-Mármol, Comes et al. 2016). As described for K_V10.1 and the EGFR itself, K_V1.3 could be then recycled to the nucleus through the retrograde pathway (Wang, Yamaguchi et al. 2010, Kohl, Lorinczi et al. 2011). In the nucleus, Kv1.3 might regulate gene expression by several mechanisms such as TF regulation, rRNA synthesis or heterochromatin stabilization (Siddiqui-Jain, Grand et al. 2002, Jang, Byun et al. 2015).

4.2.4. Role of K_V1.3 in RTK signalling

GF signalling through RTK and downstream MAPK is a strong inducer of SMC proliferation (Mack 2011). In SMCs, engagement of FGFR-1, PDGFR-ß and other RTK leads to the activation of the MAPK kinase (MEK) that in turn phosphorylates ERK. ERK translocates to the nucleus and phosphorylates among others the transcription activator Elk-1. Finally, Elk-1 binds to the TF SRF inducing the expression of early growth genes, such as the TF EGR-1 (Santiago, Lowe et al. 1999, Hjoberg, Le et al. 2004, Vogel, Kubin et al. 2006).

Hence, the influence of K_V1.3 blockade on RTK and MAPK signalling was investigated next. First, the effect of channel blockade on the expression of the SMC mitogenic FGFR-1 and

PDGFR-ß receptors was analysed both in MArSMCs and in collateral arteries. Furthermore, we investigated the expression of the RTK downstream target EGR-1. Additionally, to elucidate if $K_V1.3$ participates in RTK signalling at the cell membrane upstream ERK, ERK phosphorylation following RTK stimulation, was examined by western-blot in MArSMCs.

PAP-1 repressed Fgfr1 and Pdgfrb expression in MArSMCs and in arteriogenesis

Since FGFR-1 and PDGFR-ß gene expression is induced by FGF-2, MArSMCs were stimulated for 6h with SMCGM containing FGF-2 and EGF after a starvation period of 24h (Kano, Morishita et al. 2005). Compared to negative control cells cultured further in starvation medium, no significant up-regulation of *Fgfr1* and *Pdgfrb* mRNA levels were observed under SMCGM stimulation. The absence of upregulation of the RTKs could be explained by the short starvation period (24h) in which SMCs could not have reached total quiescence and still express high amounts of RTKs. Nevertheless, an intriguing significant repression of *Fgfr1* and *Pdgfrb* expression was manifested when MArSMCs were stimulated with SMCGM under $K_V1.3$ blockade.

Likewise, gene expression analysis in collateral arteries 12h after FAL revealed a strong downregulation of *Fgfr1* and *Pdgfrb* in mice treated with PAP-1. Since 12h after FAL is a very early time point and SMC proliferation reaches a peak three day after FAL, the lower levels of *Fgfr1* and *Pdgfrb* detected under PAP-1 rather point to an involvement of $K_V1.3$ in RTK signalling or *Fgfr1* and *Pdgfrb* expression regulation directly and not to lower SMC numbers. In control mice, *Fgfr1* and *Pdgfrb* were not differentially upregulated, presumably due to its earlier upregulation (Deindl, Hoefer et al. 2003).

The relevance of FGFR-1 in arteriogenesis has been reported by Deindl et al. who not only detected an upregulation of the receptor in collateral arteries as early as 3h after FAL with a peak after 6h in the rabbit, but also a poor collateral growth under blockade of the binding of the receptor to its ligand with polyanetholesulfonic acid (PAS) (Deindl, Hoefer et al. 2003). FGF-2 in collateral arteries is secreted by recruited monocytes and tissue macrophages as well as mast cells (Arras, Ito et al. 1998, Scholz, Ito et al. 2000, Chillo, Kleinert et al. 2016). Likewise, tissue macrophages and mast cells release PDGF-BB in growing collaterals (Takeda, Costa et al. 2011, Chillo, Kleinert et al. 2016). The PDGF-BB-PDGFR-ß axis is well known for its mediation in SMC proliferation and migration also in arteriogenesis (Heldin and Westermark 1999, de Paula, Flores-Nascimento et al. 2009).

Considering the important role of the RTK FGFR-1 and PDGFR-ß on SMC proliferation, it may well be that their soon downregulation under $K_V1.3$ channel blockade observed *in vivo*, is

responsible, at least partially, for the reduced SMC proliferation detected in collateral arteries of mice treated with the $K_V1.3$ channel blocker PAP-1.

PAP-1 repressed the expression of the downstream transcription factor EGR-1 in MArSMCs and in arteriogenesis

To induce *Egr1* expression *in vitro*, MArSMCs were stimulated with SMCGM after 24h serum starvation. *Egr1* was slightly upregulated after SMCGM stimulation compared to starved control cells, while, intriguingly, its expression was strongly downregulated when cells were given PAP-1 together with SMCGM.

In vivo, analysis of *Egr1* mRNA levels in collaterals of occluded- versus sham-operated hind-limbs of control mice confirmed its already reported upregulation 12h after FAL (Pagel, Ziegelhoeffer et al. 2012). Moreover, and correlating with *in vitro* findings, *Egr1* upregulation was significantly truncated in mice treated with the $K_V1.3$ channel blocker.

Besides *Egr1* upregulation in collateral arteries 12h after FAL, Pagel et al also reported the involvement of EGR-1 in SMCs PM. Egr1-KO mice expressed higher α-SMA and splicing factor 1 (SF-1) levels compared to wild type mice, hallmarks of the SMC contractile phenotype. Moreover, the lack of *Egr1* decreased the collateral expression of the proliferation marker Ki67 and cyclin D, a cell cycle regulatory protein (Pagel, Ziegelhoeffer et al. 2012).

Together with the expression repression of the RTK receptors FGFR-1 and PDGFR-ß, truncation of *Egr1* upregulation may be responsible for the low SMC proliferation detected in growing collaterals of PAP-1 treated mice. *Egr1* repression under $K_V1.3$ channel blockade might be consequence of the downregulation of the upstream receptors FGFR-1 and PDGFR-ß themselves, but also to a role of $K_V1.3$ in *Egr1* expression regulation as postulated above.

$K_V1.3$ acts downstream ERK phosphorylation in MArSMCs

$K_V1.3$ channel current at the cell membrane is inhibited following EGFR engagement, in part through tyrosine phosphorylation by v-src tyrosine kinase (Holmes, Fadool et al. 1996, Bowlby, Fadool et al. 1997). Interestingly, v-src-mediated tyrosine phosphorylation of $K_V1.3$ and current inhibition is reverted by the adaptor protein growth factor receptor-bound protein 10 (Grb10), a positive adaptor protein of RTK downstream signalling (Wang, Dai et al. 1999, Cook and Fadool 2002, Cailliau, Le Marcis et al. 2003).

Hence, we asked if $K_V1.3$ blockade at the cell membrane could inhibit downstream FGFR-1 and EGFR signalling in MArSMCs. For this, ERK phosphorylation was assessed under

stimulation with SMCGM containing FGF-2 and EGF in the presence of two K_V1.3 channel blockers, Margatoxin and PAP-1. As a negative control, cells were stimulated with SMCGM in the presence of the MEK inhibitor UO126. After five minutes stimulation with SMCGM, ERK phosphorylation by MEK was induced compared to cells maintained in starvation medium. Furthermore, treatment with UO126, strongly blocked ERK phosphorylation without affecting total ERK protein levels. However, neither Margatoxin nor PAP-1 could revert ERK phosphorylation, questioning a role of the channel upstream ERK.

Interestingly, Jimenez-Perez et al. recently reported that K_V1.3 conformational change following membrane depolarization leads to the exposure of a segment at the C-terminus of the channel that is subsequently phosphorylated by p-ERK increasing K_V1.3 mitogenic effects (Jimenez-Perez, Cidad et al. 2016). In addition, EGF-mediated K_V1.3 endocytosis from the cell membrane following EGFR engagement is also ERK1/2-dependent (Martínez-Mármol, Comes et al. 2016). Contrastingly, Kan et al. reported that K_V1.3 downregulation via siRNA in cultured macrophages reduced ERK-phosphorylation and ERK-mediated migration, while UO126 inhibited migration and increased ERK-phosphorylation induced by K_V1.3 overexpression (Kan, Gao et al. 2016).

This *in vitro* finding and the recent literature demonstrating a role of ERK in K_V1.3 regulation and trafficking following RTK engagement point to a role of K_V1.3 in RTK signalling downstream ERK. Furthermore, in view of the strong localization of the channel at the nuclei and nuclear envelope of MArSMCs cultured in SMCGM, a role of the nuclear K_V1.3 in cell proliferation cannot been discarded neither. However, as reported for Kv1.3-mediated migration in macrophages, it cannot be excluded that K_V1.3 also signals upstream ERK in other signalling pathways and functions such as migration.

4.2.5. Sp1 could be involved in K_V1.3-mediated gene regulation

Considering the strong localization of K_V1.3 in MArSMCs nuclei, we endeavored to define the role of the nuclear K_V1.3 in RTK signalling. An intriguing role for K_V1.3 in the activation of the TFs CREB and c-fos abundance in cancer cells has been reported, involving the channel in gene expression regulation (Jang, Byun et al. 2015). The authors detected an increased phosphorylation of CREB under PAP-1 treatment in lung adenocarcinoma cells. Interestingly, a correlation of increased CREB levels with downregulation of GFs and RTKs such as PDGFR-α and Endothelin-1 receptor has been reported in SMCs (Klemm, Watson et al. 2001). One may hypothesize that the downregulation of *Fgfr1*, *Pdgfrb* and *Egr1* observed under PAP-1 treatment in MArSMCs and in collateral arteries could be mediated by an increased

phosphorylation of CREB. However, there is until now no evidence of a CREB-mediated downregulation of these genes following phosphorylation. Quite the contrary, a study in gonadotrophs described the binding of p-CREB to the *Egr1* promoter and increased expression while a dominant negative mutant of CREB resulted in less *Egr1* expression (Mayer, Willars et al. 2008). Hence, other TFs must be involved in the regulation of *Fgfr1*, *Pdgfrb* and *Egr1* by $K_V1.3$. Interestingly, a recent publication reported c-fos-dependent *Fgfr1* transcription in osteosarcoma cells (Weekes, Kashima et al. 2016). Moreover, in arteriogenesis, activator protein-1 (AP-1), the heterodimer composed of c-fos and c-Jun, is activated 24h after FAL and regulates the transcription of MCP-1 in SMCs (Demicheva, Hecker et al. 2008). Since c-fos transcription is induced by MAPK signalling activation, it might also be involved in $K_V1.3$-mediated gene expression regulation of *Fgfr1* (Karin 1995).

Interestingly, Specificity protein 1 (Sp1), a member of the specificity protein/Krüppel-like factor (Sp/KLF) zinc finger family of transcription factors, regulates SMC PM and SMC proliferation (Andres, Urena et al. 2001, Deaton, Gan et al. 2009, Tang, Yu et al. 2017) and has been involved in the transcription of *Fgfr1*, *Pdgfrb* and *Egr1* in different cell types, albeit not in SMCs specifically (Cao, Mahendran et al. 1993, Patel and DiMario 2001, Kaneko, Yang et al. 2006).

Sp1-DNA binding blockade inhibits the expression of Fgfr1 and Egr1 in MArSMCs under RTK stimulation

Since Sp1 transcription of *Fgfr1*, *Pdgfrb* and *Egr1* has not been assessed in SMCs specifically, the effects of the Sp1-DNA binding blocker Mithramycin A (MTM) were investigated in MArSMCs via real time PCR. To induce Sp1 activation and transcription activity, MArSMCs were stimulated with SMCGM containing FGF-2 and EGF, as these GFs induce ERK-1/2-dependent Sp1 phosphorylation and transcription activity in SMCs (Merchant, Du et al. 1999, Bonello and Khachigian 2004).

After three days in starvation medium, MArSMCs stimulated with SMCGM for six hours significantly upregulated *Fgfr1* and *Egr1* expression. Addition of MTM significantly repressed this upregulation, even though both genes were still upregulated compared to negative controls. In contrast, *Pdgfrb* expression was strongly downregulated in MArSMCs following RTK stimulation independent on MTM treatment compared to cells in starvation medium.

The partial repression of *Fgfr1* and *Egr1* upregulation indicated additional Sp1-independent transcription regulation mechanisms. Indeed, *Fgfr1* gene expression is regulated by c-Fos/ AP-1, the pRB/E2F pathway and by AP-2 in different cell types (Tashiro, Maruki et al. 2003,

Mitchell and DiMario 2010, Weekes, Kashima et al. 2016). Regarding *Egr1*, its expression is activated by Elk-1 following RTK engagement through binding with SRF among others (Gregg and Fraizer 2011). Regarding *Pdgfrb* regulation, a negative feedback loop in *Pdgfrb* expression has been reported in fibroblasts and in SMCs stimulated with FCS for a long period of time (Vaziri and Faller 1995, Kaplan-Albuquerque, Van Putten et al. 2005). Hence, 5 minutes stimulation with PDGF-BB resulted in a strong *Pdgfrb* upregulation and PDGFR-ß phosphorylation in SMCs, while six hours stimulation strongly repressed its expression (Kaplan-Albuquerque, Van Putten et al. 2005). In our setting, the strong downregulation observed under SMCGM stimulation could well be due to this negative feedback response.

From these findings, it can be affirmed that indeed, Sp1 regulates the transcription of *Fgfr1* and *Egr1* under engagement of RTK in MArSMCs too, although other TFs may be involved. Hence, Sp1 could be the chain link between the nuclear $K_V1.3$ and the downregulation of *Fgfr1* and *Egr1* observed under PAP-1 treatment. In addition, since *Pdgfrb* expression under MTM was performed in MArSMCs stimulated for six hours, which might have led to a negative feedback regulation, further experiments are needed to demonstrate an Sp1-mediated regulation of *Pdgfrb* expression following RTK engagement.

$K_V1.3$ blockade inhibits Sp1 expression in MArSMCs but not in whole collateral arteries

Besides post-translational modifications and protein interactions influencing DNA binding and/or transactivation activity, Sp1 transcription activity can be modulated by Sp1 abundance (Bonello and Khachigian 2004, Tapias, Ciudad et al. 2008, Tan and Khachigian 2009, Azahri, Di Bartolo et al. 2012). Thus, the effect of $K_V1.3$ blockade on Sp1 gene expression was analysed *in vitro* and *in vivo*.

Interestingly, six hours stimulation with GFs-containing SMCGM following a starvation period did not influence Sp1 gene expression in MArSMCs, while $K_V1.3$ blockade with PAP-1 resulted in a significant decline of *Sp1* mRNA levels. In contrast, channel blockade did not influence *Sp1* expression in collateral arteries of occluded hind-limb 12h after FAL compared to their contralateral counterparts in control mice. Moreover, and in contrast to *Egr1*, *Sp1* mRNA levels in control mice were not differentially expressed at this time point neither.

Sp1 plays an important role in cell cycle regulation and its Sp1 abundance is tiny regulated by cell cycle related proteins reaching a peak at the G1 phase (Tapias, Ciudad et al. 2008). Indeed, while ectopic expression of a truncated Sp1 mutant results in growth arrest at the S-phase, its overexpression in several cancer cells leads to an aberrant cell proliferation (Kumar and Butler

1998, Chen, Zhang et al. 2000, Wang, Wei et al. 2003). Expression of Sp1 is mainly regulated by Sp1 itself as well as by other Sp/KLF family members (Nicolas, Noe et al. 2003).

Considering Sp1 downregulation by PAP-1 in MArSMCs, it is conceivable that $K_V1.3$ channel influences Sp1 expression and subsequent transcriptional activity. However, this effect was not detectable in whole collateral artery samples, probably due to the ubiquitous expression of Sp1, unmasking any expression changes in collateral SMCs. Hence, further analysis of Sp1 abundance in collateral SMCs through quantitative immunofluorescence histochemistry would complement *in vitro* data. In addition, Kv1.3 may influence Sp1 post-transcriptional modifications too as observed for p-CREB. Interestingly, post-translational induction of Sp1-DNA binding and not Sp1 abundance induced SMC proliferation in a balloon angioplasty model (Andres, Urena et al. 2001). The proposed model has been pictured in **Figure 4.2**.

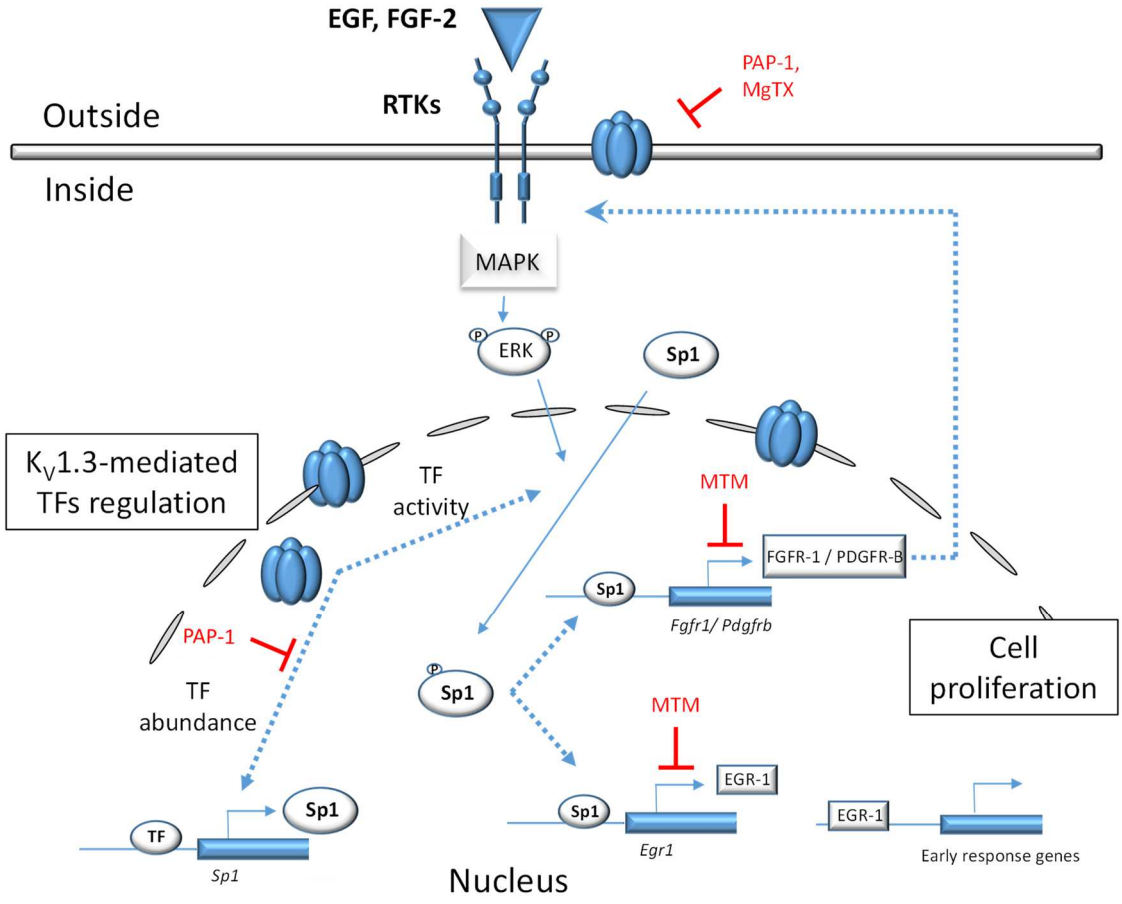

Figure 4.2: Proposed model of K_V1.3-mediated transcription regulation of *Fgfr1* and *Egr1* through the regulation of Sp1 abundance in SMCs

Following RTK engagement and MAPK signalling activation, K_V1.3 channel is recycled to the nucleus and nuclear envelope. There, it might regulate Sp1 gene transcription since K_V1.3 blockade repressed Sp1 expression. In addition, K_V1.3 might also regulate Sp1 post-transcriptional regulation. As demonstrated with the Sp1 inhibitor Mithramycin A (MTM), Sp1 in turns regulates *Fgfr1*, *Egr1* and probably *Pdgfrb* in SMCs, all three genes involved in SMC proliferation. The repression of the TF EGR-1 would lead to the repression of early response genes regulating cell division while FGFR-1 and PDGFR-ß downregulation of the RTK would decline RTK signalling. Both situations would finally lead to less SMC proliferation.

4.2.6. Sp1 does not regulate Kv1.3 expression in MArSMCs

Besides *Fgfr1*, *Pdgfrb* and *Egr1*, Kv1.3 gene expression itself has been reported to be under the transcriptional activity of Sp1, albeit in cancer cells (Jang, Byun et al. 2015). Moreover, the expression of the K_V1.3 highly related channel K_V1.5 is also regulated by Sp1 (Fountain, Cheong et al. 2007).

Interestingly, no effects on Kv1.3 mRNA levels were observed when MArSMCs were treated with MTM following RTK engagement, even if Kv1.3 expression was significantly upregulated following GF stimulation compared to cells cultured further in starvation medium.

This result denotes that $K_V1.3$ gene expression is certainly regulated by TFs activated downstream RTK engagement. Interestingly, FGF-2 and PDGF-B upregulate $K_V1.3$ expression and mitogenesis of cultured oligodendrocyte precursor cells (Chittajallu, Chen et al. 2002). So far, Sp1-mediated $K_V1.3$ and $K_V1.5$ expression regulation has been demonstrated through artificial *in vitro* systems (Fountain, Cheong et al. 2007, Jang, Byun et al. 2015). Thus, the stimulus inducing Sp1-mediated transcription of the $K_V1.3$ gene is still unknown.

4.3. The role of $K_{Ca}3.1$ in arteriogenesis

Similar to $K_V1.3$, the Ca^{2+}-gated K^+ channel $K_{Ca}3.1$ has been related to SMC proliferation *in vitro* and *in vivo* situations of intima hyperplasia. However, its specific role in arteriogenesis and in outward remodelling processes has not been investigated so far.

4.3.1. $K_{Ca}3.1$ expression is induced in early arteriogenesis

Immunofluorescence staining of collateral arteries sections demonstrated the presence of $K_{Ca}3.1$ in collateral SMCs, ECs and perivascular inflammatory cells. Interestingly, a rise in $K_{Ca}3.1$ level was observed in both SMCs and ECs two days after FAL, while seven days after ligation $K_{Ca}3.1$ levels returned to basal values in both cell types.

In SMCs, expression of $K_{Ca}3.1$ was restricted to the proliferative phenotype. While in resting collateral arteries $K_{Ca}3.1$ protein level in SMCs was very low, two days after FAL an upregulation was evident although statistically insignificant. Moreover, $K_{Ca}3.1$ protein level was significantly restrained seven days compared to two days after FAL, time point by which most SMCs have reached again a differentiated phenotype.

This *in vivo* induction of $K_{Ca}3.1$ expression has been reported in situations of neointima hyperplasia at both mRNA and protein levels too (Kohler, Wulff et al. 2003, Tharp, Wamhoff et al. 2008). However, the downregulation of $K_{Ca}3.1$ following a SMC mitogenic phase as observed in growing collaterals has never been described, again reflecting the different regulation mechanisms controlling neointima hyperplasia and arteriogenesis.

$K_{Ca}3.1$ was also expressed in collateral ECs as detected by co-localization with the EC marker CD31. Again, its expression was stronger two days after FAL but very weak in resting and in seven day growing collaterals. Several studies report an upregulation of the channel in ECs when stimulated with the GFs FGF-2, VEGF and EGF. Moreover, through $K_{Ca}3.1$ blockade with TRAM-34, they confirmed a role of the channel in endothelial mitogenesis *in vitro* and in murine models of angiogenesis (Grgic, Eichler et al. 2005, Yang, Li et al. 2013). However, since in our *in vivo* findings, TRAM-34 did not influence ECs proliferation during

arteriogenesis (see below), its role in ECs may have more to do with its function in EDHF-mediated vasodilation. Hence, $K_{Ca}3.1$ expression is induced in ECs exposed to FSS (Brakemeier, Kersten et al. 2003). Since increased FSS is the driving force for EC activation during early arteriogenesis, it might explain its upregulation soon after FAL. Interestingly, the Ca^{2+}-channel transient receptor potential cation channel, subfamily V, member 4 (TRPV4) acts as an mechanotransducer of increased FSS in collateral arteries, being upregulated in ECs as early as 24h after FAL. Upon channel activation a first rise in intracellular Ca^{2+} concentration could lead to activation of $K_{Ca}3.1$ and EDHF-mediated vasodilation while a sustained increased in Ca^{2+} ions would activate Ca^{2+}-dependent TFs (Troidl, Troidl et al. 2009, Troidl, Nef et al. 2010)

Besides SMCs and ECs, fibroblasts and perivascular inflammatory cells were also stained for $K_{Ca}3.1$. The channel has been correlated with migration in macrophages (Chung, Zelivyanskaya et al. 2002, Penna and Stutzin 2015), migration and degranulation in mast cells (Duffy, Cruse et al. 2005), T cell receptor-mediated activation and proliferation in T cells (Ghanshani, Wulff et al. 2000) and proliferation in fibroblasts (Pena and Rane 1999). Since $K_{Ca}3.1$ channel blockade in these cells could influence SMC proliferation, *in vivo* data were contrasted with cultured MArSMCs.

4.3.2. $K_{Ca}3.1$ blockade by TRAM-34 has a mild effect on arteriogenesis

The role of $K_{Ca}3.1$ in arteriogenesis and particularly in SMC proliferation was further investigated in the FAL model, under $K_{Ca}3.1$ blockade with TRAM-34. LDI revealed a tendency to lower perfusion recovery at day three that resulted in a significant impediment in perfusion recovery seven days after FAL in mice treated with the $K_{Ca}3.1$ channel blocker. In contrast, analysis of collateral artery lumen diameters and medial area displayed a regular collateral artery growth. To resolve this incongruency, quantification of SMCs proliferation under $K_{Ca}3.1$ blockade was performed in mice receiving the proliferation marker BrdU. Hence, and consolidating collateral morphometry data, no obvious decrease in medial $BrdU^+$ SMCs numbers were detected in seven days growing collateral arteries when mice were given TRAM-34. In ECs, $K_{Ca}3.1$ blockade had no inhibitory effect in their proliferation neither, since collateral diameters and $BrdU^+$ ECs were normal or even higher than in control collaterals.

The controversial data concerning perfusion recovery and collateral morphometry, might be explained by the well-known function of the $K_{Ca}3.1$ in EDHF-mediated vasodilation that could affect vascular tone (Eichler, Wibawa et al. 2003, Si, Heyken et al. 2006). Indeed, $K_{Ca}3.1$-KO

exhibit 7 mmHg increase in mean arterial blood pressure probably due to impediment of its EDHF-mediated function (Si, Heyken et al. 2006). The effect of endothelial $K_{Ca}3.1$ blockade could influence perfusion of the feet during LDI measurements under heat-induced vasodilation by an increased vascular tone compared to control mice. As mentioned above, a similar effect was observed in eNOS-KO mice (Schaper and Schaper 2004).

In addition, to assess a role of $K_{Ca}3.1$ in PM and soon induction of SMC mitogenesis, gene expression analysis of the contractile marker α-SMA and the RTK FGFR-1 and PDGFR-ß were assessed in whole collateral arteries of mice treated with TRAM-34. 12h after FAL, *aSma* mRNA levels were downregulated in collateral arteries of the occluded hind-limb compared to their contralateral counterparts in both, control and TRAM-34-treated mice. Moreover, $K_{Ca}3.1$ blockade did not affect the expression of the GF receptors *Fgfr1* and *Pdgfrb* neither.

Contrastingly, a downregulation of the contractile markers α-SMA, SMMHC and Smoothelin-B together with a $K_{Ca}3.1$ upregulation has been reported in cultured SMCs under stimulation with PDGF-BB. Moreover, treatment with TRAM-34 was able to downregulate $K_{Ca}3.1$ channel expression and blocked repression of the above-mentioned contractile markers (Tharp, Wamhoff et al. 2006). Together with the later $K_{Ca}3.1$ expression induction following FAL, these findings questioned a role of the channel in the induction of SMC PM and early SMC proliferation during arteriogenesis.

Considering the many reports linking the channel with SMC proliferation and the increased protein levels in collateral SMCs during the active proliferation phase, the low effect of TRAM-34 treatment in arteriogenic SMC proliferation was unexpected. One hypothesis contemplates the absence of phenotype to a suboptimal channel blockade *in vivo*. However, given that the dose of 120 mg/Kg/day used has been reported to be effective in inhibiting SMC proliferation in several *in vivo* studies, this hypothesis seems unlikely. Hence, in a rat model of restenosis, the same dose of TRAM-34 reduced intima hyperplasia by 40 % (Kohler, Wulff et al. 2003), while in an atherogenic mouse model, it led to a significant SMCs inhibition in atherosclerotic lesions in aortic roots (Toyama, Wulff et al. 2008).

Furthermore, $K_{Ca}3.1$ blockade with TRAM-34 did not inhibit EC proliferation neither, as has been reported elsewhere (Grgic, Eichler et al. 2005, Yang, Li et al. 2013). To the contrary, collateral artery diameters in TRAM-34 treated mice were similar or even slightly higher to those of control mice. Moreover, quantification of $BrdU^+$ ECs in seven days growing collateral transversal sections were slightly increased compared to the control group. Interestingly, TRAM-34 has been shown to act as an agonist of the estrogen receptors α and ß and to potentiate

the estrogen-induced *in vitro* proliferation of breast cancer cells at concentrations of 3-10 µM (Roy, Cowley et al. 2010). Moreover, ECs express both receptors and their engagement, together with an eNOS activation and NO-dependent vasodilation, is responsible for estrogen-induced EC proliferation and migration (Haynes, Sinha et al. 2000, Lu, Schnitzler et al. 2016). Contrastingly, estrogen has an inhibitory effect on SMCs migration and proliferation *in vivo* and *in vitro* (Dai-Do, Espinosa et al. 1996, Yue, Vickery-Clark et al. 2000, Pare, Krust et al. 2002).

At this stage, it can be concluded that $K_{Ca}3.1$ plays a mild if not irrelevant role in SMC proliferation during arteriogenesis. Its expression and upregulation in collateral endothelium two days after FAL may reflect a role of the channel in EDHF-mediated vasodilation in early arteriogenesis. In addition, besides its effects on $K_{Ca}3.1$ blockade, TRAM-34 could have act as an estrogen receptor agonist in ECs, slightly stimulating their proliferation and concurring with the reported inhibitory effect on $K_{Ca}3.1$-mediated ECs proliferation.

$K_{Ca}3.1$ localizes in the cell membrane and nuclei of MArSMCs and its blockade inhibits MArSMCs proliferation

Interestingly, $K_{Ca}3.1$ channel staining in MArSMCs depicted a strong localization surrounding the nuclei and at the nuclei together with a much weaker staining at the cytoplasm and cell membrane.

The nuclear localization of $K_{Ca}3.1$ has been reported in airway SMC as well as in placental trophoblasts (Chachi, Shikotra et al. 2013, Diaz, Wood et al. 2014). In spite of the reported $K_{Ca}3.1$ localization at the NE, its function at the NE has not been investigated specifically. As mentioned above, $K_{Ca}1.1$ has also been found in the NE of neurones. Its role has been correlated with Ca^{2+} transients from the NE towards the nucleoplasm and subsequent Ca^{2+}-mediated CREB transcription (Li, Jie et al. 2014). It is therefore possible that, $K_{Ca}3.1$ similar to $K_{Ca}1.1$ influence Ca^{2+}-mediated gene expression, albeit certainly with different activation and regulation mechanisms. Interestingly, Bi et al reported in whole cell lysates an increased phosphorylation of CREB levels and c-fos following stimulation of SMCs with PDGF that was repressed under TRAM-34 treatment or even enhanced in SMCs overexpressing the channel (Bi, Toyama et al. 2013).

Since several studies involve $K_{Ca}3.1$ with SMC proliferation *in vitro*, a BrdU proliferation assay was performed with cultured MArSMCs. After a starvation period of 24h, cells were stimulated with 10% FCS-enriched basal medium in the presence of increasing doses of TRAM-34. Indeed, the specific dose of 100 nM significantly reduced proliferation more than 35 % respect

to control cells. The mitogenic inhibitory effect of 100 nM TRAM-34 in SMCs has also been observed in human coronary SMCs (Toyama, Wulff et al. 2008, Bi, Toyama et al. 2013) and in the cell line A7r5 derived from rat aortic vascular SMCs (Si, Grgic et al. 2006).

Interestingly, since TRAM-34 is a membrane-permeable blocker, a role of the nuclear channel in SMC proliferation through gene expression regulation cannot been discarded. However, as observed *in vivo*, $K_{Ca}3.1$-mediated SMC proliferation seems to be independent of *Fgfr1* and *Pdgfrb* expression regulation, since treatment with TRAM-34, in contrast to the $K_V1.3$ channel blocker PAP-1, did not influence their mRNA levels neither in cultured MArSMCs nor in collateral arteries of mice treated with the channel blocker, 12h after FAL. Accordingly, neither Bi et al could observe any change on *Pdgfrb* expression in human coronary SMCs under $K_{Ca}3.1$ blockade with TRAM-34 and PDGF stimulation. Moreover, as mentioned above $K_{Ca}3.1$-mediated proliferation was dependent on intracellular Ca^{2+} concentrations and CREB, c-fos and neuron-derived orphan receptor 1 (NOR-1) activation (Bi, Toyama et al. 2013).

In conclusion, $K_{Ca}3.1$ induced MArSMCs proliferation as shown be the inhibitory mitogenic effect of its blocker TRAM-34. Furthermore, the strong subcellular localization of the channel in MArSMCs cultured in a GF-enriched growth medium and literature reports make hypothesize that the channel might regulate SMC proliferation through Ca^{2+}-mediated gene expression regulation, as described for the related channel $K_{Ca}1.1$. However, experiments performed in the murine FAL model under channel blockade revealed an irrelevant role of the channel on arteriogenic SMCs proliferation. However, its upregulation in endothelium two days after FAL may indicate a role of the channel in EDHF-mediated vasodilation in early arteriogenesis.

Conclusion

5. Conclusion

The present study demonstrates that the voltage-gated K^+ channel $K_V1.3$, but not the Ca^{2+}-gated K^+ channel $K_{Ca}3.1$, remarkably influences SMC proliferation during arteriogenesis. $K_V1.3$ *in vivo* blockade with PAP-1 resulted in thinner collateral arteries and lower medial $BrdU^+$ SMCs ratios. This restricted SMC proliferation is presumably consequence of an early repression of the receptor tyrosine kinases FGFR-1 and PDGFR-ß as well as the well-known pro-arteriogenic transcription factor EGR-1 observed under $K_V1.3$ blockade.

In MArSMCs, RTK downstream signalling was not affected by $K_V1.3$ blockade as observed by normal ERK phosphorylation following growth factor (GF) stimulation. Together with the strong detection of $K_V1.3$ at the nuclei of MArSMCs cultured in GF-enriched growth medium, these findings argue for a nuclear $K_V1.3$-mediated gene expression regulation. The precise mechanism however remains to be elucidated. As reported in cancer cells, nuclear $K_V1.3$ is able to regulate transcription factor activation and abundance. Sp1, a transcription factor influencing SMC PM and proliferation may mediate this effect. Hence, beside a downregulation of *Fgfr1* and *Egr1* under Sp1 blockade, we detected an *in vitro* repression of Sp1 under treatment with the $K_V1.3$ blocker PAP-1.

These findings, on the one hand, add insight into the role of $K_V1.3$ in SMC proliferation during collateral artery growth, and further support the nuclear localization of the channel as well as its control over gene expression regulation in SMCs. Future investigations on $K_V1.3$ activation mechanisms during arteriogenesis and $K_V1.3$ downstream targets might assist in the identification of new and specific targets for therapeutic arteriogenesis. On the other hand, since $K_{Ca}3.1$ blockade manifested a very mild effect on arteriogenesis, this study further supports $K_{Ca}3.1$ channel blockade as a potential target for neointima hyperplasia therapy.

Summary

6. Summary

Arteriogenesis, i.e. the growth of collateral arteries forming physiological bypasses, represents a physiological alternative to vascular surgery in obstructive diseases, the leading cause of death worldwide. Collateral growth, however, is limited by genetic factors, age and physiological restrictions. Therefore, a better molecular knowledge is necessary in order to identify molecular targets to promote a faster and stronger growth of collateral arteries in patients.

Proliferative smooth muscle cells (SMCs) are key players of collateral enlargement and wall remodelling, and thus interesting targets for therapeutic arteriogenesis. The induction of SMC de-differentiation towards proliferative SMCs is accompanied by changes in K^+ channel composition and activity. The voltage-gated K^+ channel $K_V1.3$ and the Ca^{2+}-gated K^+ channel $K_{Ca}3.1$ are upregulated in cultured SMCs and in proliferative SMCs of neointima hyperplasia models. Moreover, their blockade impairs SMC proliferation. However, their role in arteriogenic SMC proliferation has not been investigated so far. Furthermore, the signalling pathways involved in $K_V1.3$ and $K_{Ca}3.1$-mediated SMC proliferation are still under research.

Using the murine femoral artery ligation (FAL) model of arteriogenesis, the expression of both channels in SMCs of resting and growing collateral arteries of wild type mice was first verified through histological analysis. The specific role of $K_V1.3$ and $K_{Ca}3.1$ channel on arteriogenesis was then investigated employing pharmacological channel blockade with 5-(4-Phenoxybutoxy) psoralen (PAP-1) and TRAM-34 (1-[(2-chlorophenyl)diphenyl-methyl]-1H-pyrazole), respectively, giving a special focus on SMC proliferation. Furthermore, *in vitro* experiments with primary mouse artery SMCs (MArSMCs) were performed in parallel, so as to further investigate channel involvement in receptor tyrosine kinase engagement and downstream mitogen-activated protein kinase (MAPK) signalling pathway.

The results showed that $K_{Ca}3.1$ blockade with TRAM-34 hindered MArSMCs proliferation *in vitro* but hold no significant effects on SMC proliferation in growing collateral arteries *in vivo*. Interestingly, its upregulation in endothelial cells two days after FAL may reflect a role of the channel in endothelial-derived hyperpolarization factor-mediated vasodilation.

In contrast, an impairment on SMCs proliferation both in MArSMCs as well as *in vivo* was detected under $K_V1.3$ blockade with PAP-1. Mice treated with PAP-1 displayed thinner collateral arteries and lower Bromodeoxyuridine $(BrdU)^+$ SMCs ratios seven days after FAL, compared to control mice. Kv1.3 was constantly expressed in resting and growing collateral arteries, however, its function might be regulated at the level of channel activity or subcellular

localization. Moreover, since the channel is expressed in resting collateral arteries and channel blockade resulted in an absence of repression of the contractile marker alpha-smooth muscle actin (α-SMA) as early as 12h after FAL, a role of the channel in SMC phenotypic modulation was hypothesized. Interestingly, at the same time point, a repression at the mRNA level of the growth factor receptors fibroblast growth factor receptor 1 (FGFR-1) and platelet-derived growth factor receptor ß (PDGFR-ß) as well as the pro-mitogenic transcription factor early growth response protein 1 (EGR-1) was stated under $K_V1.3$ blockade with PAP-1. Moreover, this repression was observed in MArSMCs too. Further *in vitro* experiments assessing the possible involvement of $K_V1.3$ on receptor tyrosine kinase (RTK) signalling discarded a role of the channel upstream extracellular signal-regulated kinase (ERK) since ERK phosphorylation was not affected by $K_V1.3$ blockade following stimulation with growth factors-enriched growth medium.

Intriguingly, a strong detection at the nucleus beside its conventional cell membrane localization was noticed in MArSMCs cultured with growth factors-enriched growth medium. Since nuclear $K_V1.3$ is able to regulate transcription factor activation and abundance in cancer cells, a role of the channel in nuclear gene expression regulation was ascribed in MArSMCs too. An *in silico* analysis and literature research revealed the transcription factor Sp1 as a common transcription factor for *Fgfr1*, *Pdgfrb* and *Egr1*. Moreover, Sp1 blockade with Mithramycin A indeed downregulated *Fgfr1* and *Egr1* in MArSMCs following stimulation with growth factors-enriched growth medium. Intriguingly, Kv1.3 blockade with PAP-1 repressed Sp1 expression in MArSMCs. Hence, the transcription factor Sp1 might be behind $K_V1.3$-mediated transcription regulation of at least *Fgfr1* and *Egr1* genes.

7. Zusammenfassung

Arteriogenese bezeichnet das Wachstum von Kollateralarterien zu physiologischen Bypässen und stellt eine natürliche Alternative zur Gefäßchirurgie bei obstruktiven Gefäßerkrankungen dar, die Haupttodesursache weltweit. Allerdings beeinträchtigen genetische Faktoren, Alter und physiologische Einschränkungen das Wachstum von Kollateralarterien in Patienten. Ein besseres molekulares Verständnis der Arteriogenese ist daher notwendig um neue molekulare Angriffspunkte zu identifizieren und ein schnelleres und ausgeprägteres Kollateralwachstum in Patienten zu fördern.

Proliferierende glatte Gefäßmuskelzellen (smooth muscle cells, SMCs) spielen eine Schlüsselrolle bei der Erweiterung und dem Wandaufbau von Kollateralarterien und sind aus diesem Grunde ein interessanter Angriffspunkt für die therapeutische Arteriogenese. Die Induktion der SMC Dedifferenzierung zu proliferierenden SMCs wird unter anderem von Veränderungen in der K^+-Kanalzusammensetzung und -Aktivität begleitet. Der spannungsgesteuerte K^+-Kanal $K_V1.3$ und der Ca^{2+}-gesteuerte K^+-Kanal $K_{Ca}3.1$ sind überexprimiert in kultivierten SMCs sowie in proliferierenden SMCs bei Neointima Hyperplasie Modellen. Ferner beeinträchtigt die Blockierung dieser Kanäle die Proliferation von SMCs. Nichtsdestotrotz wurde ihre Rolle bei der arteriogenen SMC Proliferation bis jetzt nicht erforscht. Des Weiteren sind die Signalwege, die an der $K_V1.3$ and $K_{Ca}3.1$ gesteuerten SMC Proliferation beteiligt sind, noch Gegenstand der aktuellen Forschung.

Unter Verwendung des Arteriogenese-Modells der murinen Femoralarterienligatur (FAL) wurde die Expression der beiden Kanäle in SMCs bei ruhenden und wachsenden Kollateralarterien von Wildtyp-Mäusen durch histologische Analyse überprüft. Die spezifische Rolle von $K_V1.3$ and $K_{Ca}3.1$-Kanälen bei der Arteriogenese wurde dann mittels pharmakologischer Kanalblockierung unter Verwendung von 5-(4-Phenoxybutoxy) psoralen (PAP-1) beziehungsweise TRAM-34 (1-[(2-chlorophenyl)diphenyl-methyl]-1H-pyrazole) mit Fokus auf der SMC Proliferation untersucht. Des Weiteren wurden *in vitro* Experimente mit primären Mausarterien-SMCs (MArSMCs) parallel durchgeführt, um die Beteiligung der Kanäle an den Signalwegen der Tyrosin-Rezeptor-Kinase-Aktivierung (RTK) und der stromabwärts gelegenen Mitogen-aktivierten-Protein-Kinase (MAPK) zu untersuchen.

Die Ergebnisse zeigten, dass obwohl eine $K_{Ca}3.1$ Blockierung mit TRAM-34 die Proliferation von MArSMCs *in vitro* behinderte, kein besonderer Effekt auf die *in vivo* SMC Proliferation bei wachsenden Kollateralarterien beobachtet werden konnte. Interessanterweise könnte die erhörte $K_{Ca}3.1$ Proteinmenge in Endothelzellen zwei Tage nach der FAL auf eine Rolle bei der

durch den endothelialen hyperpolarisierenden Faktor (endothelium-derived hyperpolarizing factor, EDHF) verursachten Vasodilatation hinweisen.

Im Gegensatz dazu konnte eine gestörte SMC Proliferation sowohl in MArSMCs als auch *in vivo* bei der $K_V1.3$ Blockierung mit PAP-1 nachgewiesen werden. Mäuse die mit PAP-1 behandelt wurden zeigten gegenüber den Kontrollmäusen schmalere Kollateralarterien und niedrigere Bromodeoxyuridine $(BrdU)^+$ SMC Verhältnisse sieben Tage nach der FAL. Obwohl $K_V1.3$ in ruhenden und wachsenden Kollateralarterien konstant exprimiert ist, könnte seine Funktion jedoch auf der Ebene der Kanalaktivität oder subzellulärer Orte reguliert sein. Da der Kanal in ruhenden Kollateralarterien exprimiert ist und 12 Stunden nach der FAL die Kanalblockierung nicht zu einem Aussetzen der Repression des kontraktilen Markers alpha-smooth-muscle Aktin (α-SMA) führte, wurde angenommen dass der Kanal bei der phänotypischen Modulation der SMCs eine Rolle spielt. Interessanterweise wurde zur gleichen Zeit eine Repression auf mRNA-Ebene des Fibroblast-Wachstumsfaktor-Rezeptors-1 (FGFR-1) und Plättchen-gebundenen-Wachstumsfaktors-ß (PDGFR-ß) sowie des Pro-Mitogenetischen Transkriptionsfaktors Early Growth Factor 1 (EGR-1) bei einer $K_V1.3$ Blockierung mit PAP-1 festgestellt. Des Weiteren wurde diese Repression auch in MArSMCs beobachtet. Weitere *in vitro* Experimente, die die mögliche Beteiligung von $K_V1.3$ beim Rezeptor-Tyrosin-Kinase (RTK)-Signalweg ermitteln sollten, schlossen eine Rolle der kanalaufwärts gelegenen Extrazellulären-signalregulierten-Kinase (ERK) aus, da die ERK-Phosphorylierung nach Stimulierung mit einem Wachstumsfaktoren-angereicherten Nährmedium durch eine $K_V1.3$ Blockierung nicht beeinträchtigt wurde.

Faszinierenderweise konnte neben der konventionellen Zellmembranlokalisierung des $K_V1.3$ dieser auch im Kern von MArSMCs, die mit Wachstumsfaktoren angereichertem Nährmedium kultiviert wurden, detektiert werden. Da $K_V1.3$ im Zellkern in der Lage ist die Aktivierung und Menge von Transkriptionsfaktoren in Krebszellen zu regulieren, wurde dem Kanal auch eine Rolle bei der Kontrolle der nuklearen Genexpression in MArSMCs zugeschrieben. Eine *in silico* Analyse, sowie eine Literatur-Recherche zeigten, dass Specifity protein 1 (Sp1) ein gemeinsamer Transkriptionsfaktor für *Fgfr1*, *Pdgfrb* und *Egr1* ist. Außerdem verhinderte eine Sp1 Inhibition mit Mithramyzin A tatsächlich *Fgfr1* und *Egr1* Expression in MArSMCs nach Stimulierung mit einem Wachstumsfaktoren-angereichertem Nährmedium. Zudem unterdrückte die $K_V1.3$ Blockierung mit PAP-1 die Sp1 Expression in MArSMCs. Das heißt, dass der Transkriptionsfaktor Sp1 zumindest hinter der $K_V1.3$ gesteuerten Transkriptionsregulierung von *Fgfr1* und *Egr1* Genen stecken könnte.

References

8. References

Adamo, R. F., I. Fishbein, K. Zhang, J. Wen, R. J. Levy, I. S. Alferiev and M. Chorny (2016). "Magnetically enhanced cell delivery for accelerating recovery of the endothelium in injured arteries." J Control Release **222**: 169-175.

Al-Lamee, R., D. Thompson, H. M. Dehbi, S. Sen, K. Tang, J. Davies, T. Keeble, M. Mielewczik, R. Kaprielian, I. S. Malik, S. S. Nijjer, R. Petraco, C. Cook, Y. Ahmad, J. Howard, C. Baker, A. Sharp, R. Gerber, S. Talwar, R. Assomull, J. Mayet, R. Wensel, D. Collier, M. Shun-Shin, S. A. Thom, J. E. Davies and D. P. Francis (2018). "Percutaneous coronary intervention in stable angina (ORBITA): a double-blind, randomised controlled trial." Lancet **391**(10115): 31-40.

Al Ali, J., C. Franck, K. B. Filion and M. J. Eisenberg (2014). "Coronary artery bypass graft surgery versus percutaneous coronary intervention with first-generation drug-eluting stents: a meta-analysis of randomized controlled trials." JACC Cardiovasc Interv **7**(5): 497-506.

Andres, V., J. Urena, E. Poch, D. Chen and D. Goukassian (2001). "Role of Sp1 in the induction of p27 gene expression in vascular smooth muscle cells in vitro and after balloon angioplasty." Arterioscler Thromb Vasc Biol **21**(3): 342-347.

Arras, M., W. D. Ito, D. Scholz, B. Winkler, J. Schaper and W. Schaper (1998). "Monocyte activation in angiogenesis and collateral growth in the rabbit hindlimb." J Clin Invest **101**(1): 40-50.

Azahri, N. S., B. A. Di Bartolo, L. M. Khachigian and M. M. Kavurma (2012). "Sp1, acetylated histone-3 and p300 regulate TRAIL transcription: mechanisms of PDGF-BB-mediated VSMC proliferation and migration." J Cell Biochem **113**(8): 2597-2606.

Azam, P., A. Sankaranarayanan, D. Homerick, S. Griffey and H. Wulff (2007). "Targeting effector memory T cells with the small molecule Kv1.3 blocker PAP-1 suppresses allergic contact dermatitis." J Invest Dermatol **127**(6): 1419-1429.

Baroldi, G., O. Mantero and G. Scomazzoni (1956). "The collaterals of the coronary arteries in normal and pathologic hearts." Circ Res **4**(2): 223-229.

Beech, D. J. (2007). "Ion channel switching and activation in smooth-muscle cells of occlusive vascular diseases." Biochem Soc Trans **35**(Pt 5): 890-894.

Beech, D. J. and A. Cheong (2006). "Potassium channels at the beginnings of cell proliferation." J Physiol **570**(Pt 1): 1.

Bentzon, J. F., F. Otsuka, R. Virmani and E. Falk (2014). "Mechanisms of plaque formation and rupture." Circ Res **114**(12): 1852-1866.

Berry, C., K. P. Balachandran, P. L. L'Allier, J. Lesperance, R. Bonan and K. G. Oldroyd (2007). "Importance of collateral circulation in coronary heart disease." Eur Heart J **28**(3): 278-291.

Bi, D., K. Toyama, V. Lemaitre, J. Takai, F. Fan, D. P. Jenkins, H. Wulff, D. D. Gutterman, F. Park and H. Miura (2013). "The intermediate conductance calcium-activated potassium channel KCa3.1 regulates vascular smooth muscle cell proliferation via controlling calcium-dependent signaling." J Biol Chem **288**(22): 15843-15853.

Blackiston, D. J., K. A. McLaughlin and M. Levin (2009). "Bioelectric controls of cell proliferation: ion channels, membrane voltage and the cell cycle." Cell Cycle **8**(21): 3527-3536.

Blunck, R. and Z. Batulan (2012). "Mechanism of electromechanical coupling in voltage-gated potassium channels." Front Pharmacol **3**: 166.

Blunck, R. and Z. Batulan (2012). "Mechanism of electromechanical coupling in voltage-gated potassium channels." Front Pharmacol **3**(166).

Bonello, M. R. and L. M. Khachigian (2004). "Fibroblast growth factor-2 represses platelet-derived growth factor receptor-alpha (PDGFR-alpha) transcription via ERK1/2-dependent Sp1 phosphorylation and an atypical cis-acting element in the proximal PDGFR-alpha promoter." J Biol Chem **279**(4): 2377-2382.

Bowlby, M. R., D. A. Fadool, T. C. Holmes and I. B. Levitan (1997). "Modulation of the Kv1.3 potassium channel by receptor tyrosine kinases." J Gen Physiol **110**(5): 601-610.

Brakemeier, S., A. Kersten, I. Eichler, I. Grgic, A. Zakrzewicz, H. Hopp, R. Kohler and J. Hoyer (2003). "Shear stress-induced up-regulation of the intermediate-conductance Ca(2+)-activated K(+) channel in human endothelium." Cardiovasc Res **60**(3): 488-496.

Cahalan, M. D. and K. G. Chandy (2009). "The functional network of ion channels in T lymphocytes." Immunol Rev **231**(1): 59-87.

Cai, W. J., E. Kocsis, X. Wu, M. Rodriguez, X. Luo, W. Schaper and J. Schaper (2004). "Remodeling of the vascular tunica media is essential for development of collateral vessels in the canine heart." Mol Cell Biochem **264**(1-2): 201-210.

Cailliau, K., V. Le Marcis, V. Bereziat, D. Perdereau, B. Cariou, J. P. Vilain, A. F. Burnol and E. Browaeys-Poly (2003). "Inhibition of FGF receptor signalling in Xenopus oocytes: differential effect of Grb7, Grb10 and Grb14." FEBS Lett **548**(1-3): 43-48.

Cao, R., E. Brakenhielm, R. Pawliuk, D. Wariaro, M. J. Post, E. Wahlberg, P. Leboulch and Y. Cao (2003). "Angiogenic synergism, vascular stability and improvement of hind-limb ischemia by a combination of PDGF-BB and FGF-2." Nat Med **9**(5): 604-613.

Cao, X., R. Mahendran, G. R. Guy and Y. H. Tan (1993). "Detection and characterization of cellular EGR-1 binding to its recognition site." J Biol Chem **268**(23): 16949-16957.

Cardenas, C., J. L. Liberona, J. Molgo, C. Colasante, G. A. Mignery and E. Jaimovich (2005). "Nuclear inositol 1,4,5-trisphosphate receptors regulate local Ca2+ transients and modulate cAMP response element binding protein phosphorylation." J Cell Sci **118**(Pt 14): 3131-3140.

Cartin, L., K. M. Lounsbury and M. T. Nelson (2000). "Coupling of Ca(2+) to CREB activation and gene expression in intact cerebral arteries from mouse : roles of ryanodine receptors and voltage-dependent Ca(2+) channels." Circ Res **86**(7): 760-767.

Chachi, L., A. Shikotra, S. M. Duffy, O. Tliba, C. Brightling, P. Bradding and Y. Amrani (2013). "Functional KCa3.1 channels regulate steroid insensitivity in bronchial smooth muscle cells." J Immunol **191**(5): 2624-2636.

Chalothorn, D. and J. E. Faber (2010). "Strain-dependent variation in collateral circulatory function in mouse hindlimb." Physiol Genomics **42**(3): 469-479.

Chandraratne, S., M. L. von Bruehl, J. I. Pagel, K. Stark, E. Kleinert, I. Konrad, S. Farschtschi, R. Coletti, F. Gartner, O. Chillo, K. R. Legate, M. Lorenz, S. Rutkowski, A. Caballero-Martinez, R. Starke, A. Tirniceriu, L. Pauleikhoff, S. Fischer, G. Assmann, J. Mueller-Hoecker, J. Ware, B. Nieswandt, W. Schaper, C. Schulz, E. Deindl and S. Massberg (2015). "Critical role of platelet glycoprotein ibalpha in arterial remodeling." Arterioscler Thromb Vasc Biol **35**(3): 589-597.

Checchetto, V., E. Teardo, L. Carraretto, L. Leanza and I. Szabo (2016). "Physiology of intracellular potassium channels: A unifying role as mediators of counterion fluxes?" Biochim Biophys Acta **1857**(8): 1258-1266.

Chen, F., F. Zhang, J. Rao and G. P. Studzinski (2000). "Ectopic expression of truncated Sp1 transcription factor prolongs the S phase and reduces the growth rate." Anticancer Res **20**(2a): 661-667.

Chen, Y., A. Sanchez, M. E. Rubio, T. Kohl, L. A. Pardo and W. Stuhmer (2011). "Functional K(v)10.1 channels localize to the inner nuclear membrane." PLoS One **6**(5): e19257.

Chen, Y. J., J. Lam, C. R. Gregory, S. Schrepfer and H. Wulff (2013). "The Ca(2)(+)-activated K(+) channel KCa3.1 as a potential new target for the prevention of allograft vasculopathy." PLoS One **8**(11): e81006.

Cheong, A., A. M. Dedman and D. J. Beech (2001). "Expression and function of native potassium channel [K(V)alpha1] subunits in terminal arterioles of rabbit." J Physiol **534**(Pt 3): 691-700.

Cheong, A., J. Li, P. Sukumar, B. Kumar, F. Zeng, K. Riches, C. Munsch, I. C. Wood, K. E. Porter and D. J. Beech (2011). "Potent suppression of vascular smooth muscle cell migration and human neointimal hyperplasia by KV1.3 channel blockers." Cardiovasc Res **89**(2): 282-289.

Chillo, O., E. C. Kleinert, T. Lautz, M. Lasch, J. I. Pagel, Y. Heun, K. Troidl, S. Fischer, A. Caballero-Martinez, A. Mauer, A. R. M. Kurz, G. Assmann, M. Rehberg, S. M. Kanse, B. Nieswandt, B. Walzog, C. A. Reichel, H. Mannell, K. T. Preissner and E. Deindl (2016). "Perivascular Mast Cells Govern Shear Stress-Induced Arteriogenesis by Orchestrating Leukocyte Function." Cell Rep **16**(8): 2197-2207.

Chittajallu, R., Y. Chen, H. Wang, X. Yuan, C. A. Ghiani, T. Heckman, C. J. McBain and V. Gallo (2002). "Regulation of Kv1 subunit expression in oligodendrocyte progenitor cells and their role in G1/S phase progression of the cell cycle." Proc Natl Acad Sci U S A **99**(4): 2350-2355.

Chittenden, T. W., J. A. Sherman, F. Xiong, A. E. Hall, A. A. Lanahan, J. M. Taylor, H. Duan, J. D. Pearlman, J. H. Moore, S. M. Schwartz and M. Simons (2006). "Transcriptional profiling in coronary artery disease: indications for novel markers of coronary collateralization." Circulation **114**(17): 1811-1820.

Chung, I., M. Zelivyanskaya and H. E. Gendelman (2002). "Mononuclear phagocyte biophysiology influences brain transendothelial and tissue migration: implication for HIV-1-associated dementia." J Neuroimmunol **122**(1-2): 40-54.

Cidad, P., L. Jimenez-Perez, D. Garcia-Arribas, E. Miguel-Velado, S. Tajada, C. Ruiz-McDavitt, J. R. Lopez-Lopez and M. T. Perez-Garcia (2012). "Kv1.3 channels can modulate cell proliferation during phenotypic switch by an ion-flux independent mechanism." Arterioscler Thromb Vasc Biol **32**(5): 1299-1307.

Cidad, P., A. Moreno-Dominguez, L. Novensa, M. Roque, L. Barquin, M. Heras, M. T. Perez-Garcia and J. R. Lopez-Lopez (2010). "Characterization of ion channels involved in the proliferative response of femoral artery smooth muscle cells." Arterioscler Thromb Vasc Biol **30**(6): 1203-1211.

Cidad, P., L. Novensa, M. Garabito, M. Batlle, A. P. Dantas, M. Heras, J. R. Lopez-Lopez, M. T. Perez-Garcia and M. Roque (2014). "K+ channels expression in hypertension after arterial injury, and effect of selective Kv1.3 blockade with PAP-1 on intimal hyperplasia formation." Cardiovasc Drugs Ther **28**(6): 501-511.

Cook, K. K. and D. A. Fadool (2002). "Two adaptor proteins differentially modulate the phosphorylation and biophysics of Kv1.3 ion channel by SRC kinase." J Biol Chem **277**(15): 13268-13280.

Dai-Do, D., E. Espinosa, G. Liu, T. J. Rabelink, F. Julmy, Z. Yang, F. Mahler and T. F. Luscher (1996). "17 beta-estradiol inhibits proliferation and migration of human vascular smooth muscle cells: similar effects in cells from postmenopausal females and in males." Cardiovasc Res **32**(5): 980-985.

Davies, P. F. (1995). "Flow-mediated endothelial mechanotransduction." Physiol Rev **75**(3): 519-560.

de Groot, D., G. Pasterkamp and I. E. Hoefer (2009). "Cardiovascular risk factors and collateral artery formation." Eur J Clin Invest **39**(12): 1036-1047.

de Marchi, S. F. (2014). "Determinants of human coronary collaterals." Curr Cardiol Rev **10**(1): 24-28.

de Paula, E. V., M. C. Flores-Nascimento, V. R. Arruda, R. A. Garcia, C. D. Ramos, A. T. Guillaumon and J. M. Annichino-Bizzacchi (2009). "Dual gene transfer of fibroblast growth factor-2 and platelet derived growth factor-BB using plasmid deoxyribonucleic acid promotes effective angiogenesis and arteriogenesis in a rodent model of hindlimb ischemia." Transl Res **153**(5): 232-239.

Deaton, R. A., Q. Gan and G. K. Owens (2009). "Sp1-dependent activation of KLF4 is required for PDGF-BB-induced phenotypic modulation of smooth muscle." Am J Physiol Heart Circ Physiol **296**(4): H1027-1037.

Degen, A., D. Millenaar and S. H. Schirmer (2014). "Therapeutic approaches in the stimulation of the coronary collateral circulation." Curr Cardiol Rev **10**(1): 65-72.

Deindl, E., I. E. Hoefer, B. Fernandez, M. Barancik, M. Heil, M. Strniskova and W. Schaper (2003). "Involvement of the fibroblast growth factor system in adaptive and chemokine-induced arteriogenesis." Circ Res **92**(5): 561-568.

Demicheva, E., M. Hecker and T. Korff (2008). "Stretch-induced activation of the transcription factor activator protein-1 controls monocyte chemoattractant protein-1 expression during arteriogenesis." Circ Res **103**(5): 477-484.

Diaz, P., A. M. Wood, C. P. Sibley and S. L. Greenwood (2014). "Intermediate conductance Ca2+-activated K+ channels modulate human placental trophoblast syncytialization." PLoS One **9**(3): e90961.

Doran, A. C., N. Meller and C. A. McNamara (2008). "Role of smooth muscle cells in the initiation and early progression of atherosclerosis." Arterioscler Thromb Vasc Biol **28**(5): 812-819.

Duffy, S. M., G. Cruse, W. J. Lawley and P. Bradding (2005). "Beta2-adrenoceptor regulation of the K+ channel iKCa1 in human mast cells." Faseb j **19**(8): 1006-1008.

Eichler, I., J. Wibawa, I. Grgic, A. Knorr, S. Brakemeier, A. R. Pries, J. Hoyer and R. Kohler (2003). "Selective blockade of endothelial Ca2+-activated small- and intermediate-conductance K+-channels suppresses EDHF-mediated vasodilation." Br J Pharmacol **138**(4): 594-601.

Eitenmuller, I., O. Volger, A. Kluge, K. Troidl, M. Barancik, W. J. Cai, M. Heil, F. Pipp, S. Fischer, A. J. Horrevoets, T. Schmitz-Rixen and W. Schaper (2006). "The range of adaptation by collateral vessels after femoral artery occlusion." Circ Res **99**(6): 656-662.

Epstein, S. E., R. M. Lassance-Soares, J. E. Faber and M. S. Burnett (2012). "Effects of aging on the collateral circulation, and therapeutic implications." Circulation **125**(25): 3211-3219.

Erdogan, A., C. A. Schaefer, M. Schaefer, D. W. Luedders, F. Stockhausen, Y. Abdallah, C. Schaefer, A. K. Most, H. Tillmanns, H. M. Piper and C. R. Kuhlmann (2005). "Margatoxin inhibits VEGF-induced hyperpolarization, proliferation and nitric oxide production of human endothelial cells." J Vasc Res **42**(5): 368-376.

Faber, J. E., W. M. Chilian, E. Deindl, N. van Royen and M. Simons (2014). "A brief etymology of the collateral circulation." Arterioscler Thromb Vasc Biol **34**(9): 1854-1859.

Fadool, D. A., K. Tucker, R. Perkins, G. Fasciani, R. N. Thompson, A. D. Parsons, J. M. Overton, P. A. Koni, R. A. Flavell and L. K. Kaczmarek (2004). "Kv1.3 channel gene-targeted deletion produces "Super-Smeller Mice" with altered glomeruli, interacting scaffolding proteins, and biophysics." Neuron **41**(3): 389-404.

Fadool, D. A., K. Tucker, J. J. Phillips and J. A. Simmen (2000). "Brain insulin receptor causes activity-dependent current suppression in the olfactory bulb through multiple phosphorylation of Kv1.3." J Neurophysiol **83**(4): 2332-2348.

Fanari, Z., S. A. Weiss, W. Zhang, S. S. Sonnad and W. S. Weintraub (2015). "Comparison of percutaneous coronary intervention with drug eluting stents versus coronary artery bypass grafting in patients with multivessel coronary artery disease: Meta-analysis of six randomized controlled trials." Cardiovasc Revasc Med **16**(2): 70-77.

Feletou, M. (2011). Integrated Systems Physiology: from Molecule to Function to Disease. The Endothelium: Part 2: EDHF-Mediated Responses "The Classical Pathway". San Rafael (CA), Morgan & Claypool Life Sciences Publisher

Copyright (c) 2011 by Morgan & Claypool Life Sciences Publisher.

Félétou, M. (2011). "The Endothelium: Part 1: Multiple Functions of the Endothelial Cells—Focus on Endothelium-Derived Vasoactive Mediators." Morgan & Claypool Life Sciences.

Felix, J. P., R. M. Bugianesi, W. A. Schmalhofer, R. Borris, M. A. Goetz, O. D. Hensens, J. M. Bao, F. Kayser, W. H. Parsons, K. Rupprecht, M. L. Garcia, G. J. Kaczorowski and R. S. Slaughter (1999). "Identification and biochemical characterization of a novel nortriterpene inhibitor of the human lymphocyte voltage-gated potassium channel, Kv1.3." Biochemistry **38**(16): 4922-4930.

Fountain, S. J., A. Cheong, R. Flemming, L. Mair, A. Sivaprasadarao and D. J. Beech (2004). "Functional up-regulation of KCNA gene family expression in murine mesenteric resistance artery smooth muscle." J Physiol **556**(Pt 1): 29-42.

Fountain, S. J., A. Cheong, J. Li, N. Y. Dondas, F. Zeng, I. C. Wood and D. J. Beech (2007). "K(v)1.5 potassium channel gene regulation by Sp1 transcription factor and oxidative stress." Am J Physiol Heart Circ Physiol **293**(5): H2719-2725.

Fox, K., M. A. Garcia, D. Ardissino, P. Buszman, P. G. Camici, F. Crea, C. Daly, G. De Backer, P. Hjemdahl, J. Lopez-Sendon, J. Marco, J. Morais, J. Pepper, U. Sechtem, M. Simoons, K. Thygesen, S. G. Priori, J. J. Blanc, A. Budaj, J. Camm, V. Dean, J. Deckers, K. Dickstein, J. Lekakis, K. McGregor, M. Metra, J. Morais, A. Osterspey, J. Tamargo and J. L. Zamorano (2006). "Guidelines on the management of stable angina pectoris: executive summary: The Task Force on the Management of Stable Angina Pectoris of the European Society of Cardiology." Eur Heart J **27**(11): 1341-1381.

Fulton, W. F. (1963). "ARTERIAL ANASTOMOSES IN THE CORONARY CIRCULATION. I. ANATOMICAL FEATURES IN NORMAL AND DISEASED HEARTS DEMONSTRATED BY STEREOARTERIOGRAPHY." Scott Med J **8**: 420-434.

Fung, E. and A. Helisch (2012). "Macrophages in collateral arteriogenesis." Front Physiol **3**: 353.

Garcia-Calvo, M., R. J. Leonard, J. Novick, S. P. Stevens, W. Schmalhofer, G. J. Kaczorowski and M. L. Garcia (1993). "Purification, characterization, and biosynthesis of margatoxin, a component of Centruroides margaritatus venom that selectively inhibits voltage-dependent potassium channels." J Biol Chem **268**(25): 18866-18874.

Garner, M. H. (2002). "Na,K-ATPase in the nuclear envelope regulates Na+: K+ gradients in hepatocyte nuclei." J Membr Biol **187**(2): 97-115.

Ghanshani, S., H. Wulff, M. J. Miller, H. Rohm, A. Neben, G. A. Gutman, M. D. Cahalan and K. G. Chandy (2000). "Up-regulation of the IKCa1 potassium channel during T-cell activation. Molecular mechanism and functional consequences." J Biol Chem **275**(47): 37137-37149.

Gonzalez, C., D. Baez-Nieto, I. Valencia, I. Oyarzun, P. Rojas, D. Naranjo and R. Latorre (2012). "K(+) channels: function-structural overview." Compr Physiol **2**(3): 2087-2149.

Gregg, J. and G. Fraizer (2011). "Transcriptional Regulation of EGR1 by EGF and the ERK Signaling Pathway in Prostate Cancer Cells." Genes Cancer **2**(9): 900-909.

Grgic, I., I. Eichler, P. Heinau, H. Si, S. Brakemeier, J. Hoyer and R. Kohler (2005). "Selective blockade of the intermediate-conductance Ca2+-activated K+ channel suppresses proliferation of microvascular and macrovascular endothelial cells and angiogenesis in vivo." Arterioscler Thromb Vasc Biol **25**(4): 704-709.

Grgic, I., E. Kiss, B. P. Kaistha, C. Busch, M. Kloss, J. Sautter, A. Muller, A. Kaistha, C. Schmidt, G. Raman, H. Wulff, F. Strutz, H. J. Grone, R. Kohler and J. Hoyer (2009). "Renal fibrosis is attenuated by targeted disruption of KCa3.1 potassium channels." Proc Natl Acad Sci U S A **106**(34): 14518-14523.

Grgic, I., H. Wulff, I. Eichler, C. Flothmann, R. Kohler and J. Hoyer (2009). "Blockade of T-lymphocyte KCa3.1 and Kv1.3 channels as novel immunosuppression strategy to prevent kidney allograft rejection." Transplant Proc **41**(6): 2601-2606.

Grundmann, S., J. J. Piek, G. Pasterkamp and I. E. Hoefer (2007). "Arteriogenesis: basic mechanisms and therapeutic stimulation." Eur J Clin Invest **37**(10): 755-766.

Grunnet, M., H. B. Rasmussen, A. Hay-Schmidt, M. Rosenstierne, D. A. Klaerke, S. P. Olesen and T. Jespersen (2003). "KCNE4 is an inhibitory subunit to Kv1.1 and Kv1.3 potassium channels." Biophys J **85**(3): 1525-1537.

Gueguinou, M., A. Chantome, G. Fromont, P. Bougnoux, C. Vandier and M. Potier-Cartereau (2014). "KCa and Ca(2+) channels: the complex thought." Biochim Biophys Acta **1843**(10): 2322-2333.

Gulbins, E., N. Sassi, H. Grassme, M. Zoratti and I. Szabo (2010). "Role of Kv1.3 mitochondrial potassium channel in apoptotic signalling in lymphocytes." Biochim Biophys Acta **1797**(6-7): 1251-1259.

Gulbis, J. M., M. Zhou, S. Mann and R. MacKinnon (2000). "Structure of the cytoplasmic beta subunit-T1 assembly of voltage-dependent K+ channels." Science **289**(5476): 123-127.

Haas, T. L., P. G. Lloyd, H. T. Yang and R. L. Terjung (2012). "Exercise training and peripheral arterial disease." Compr Physiol **2**(4): 2933-3017.

Hakimzadeh, N., H. J. Verberne, M. Siebes and J. J. Piek (2014). "The future of collateral artery research." Curr Cardiol Rev **10**(1): 73-86.

Hammes, M. (2015). Hemodynamic and Biologic Determinates of Arteriovenous Fistula Outcomes in Renal Failure Patients.

Haynes, M. P., D. Sinha, K. S. Russell, M. Collinge, D. Fulton, M. Morales-Ruiz, W. C. Sessa and J. R. Bender (2000). "Membrane estrogen receptor engagement activates endothelial nitric oxide synthase via the PI3-kinase-Akt pathway in human endothelial cells." Circ Res **87**(8): 677-682.

Heil, M., I. Eitenmuller, T. Schmitz-Rixen and W. Schaper (2006). "Arteriogenesis versus angiogenesis: similarities and differences." J Cell Mol Med **10**(1): 45-55.

Heldin, C. H. and B. Westermark (1999). "Mechanism of action and in vivo role of platelet-derived growth factor." Physiol Rev **79**(4): 1283-1316.

Hernandez-Verdun, D. (2011). "Assembly and disassembly of the nucleolus during the cell cycle." Nucleus **2**(3): 189-194.

Herrington, W., B. Lacey, P. Sherliker, J. Armitage and S. Lewington (2016). "Epidemiology of Atherosclerosis and the Potential to Reduce the Global Burden of Atherothrombotic Disease." Circ Res **118**(4): 535-546.

Hjoberg, J., L. Le, A. Imrich, V. Subramaniam, S. I. Mathew, J. Vallone, K. J. Haley, F. H. Green, S. A. Shore and E. S. Silverman (2004). "Induction of early growth-response factor 1 by platelet-derived growth factor in human airway smooth muscle." Am J Physiol Lung Cell Mol Physiol **286**(4): L817-825.

Holmes, T. C., D. A. Fadool and I. B. Levitan (1996). "Tyrosine phosphorylation of the Kv1.3 potassium channel." J Neurosci **16**(5): 1581-1590.

Hua, X., T. Deuse, Y. J. Chen, H. Wulff, M. Stubbendorff, R. Kohler, H. Miura, F. Langer, H. Reichenspurner, R. C. Robbins and S. Schrepfer (2013). "The potassium channel KCa3.1 as new therapeutic target for the prevention of obliterative airway disease." Transplantation **95**(2): 285-292.

Hui, D. Y. (2008). "Intimal hyperplasia in murine models." Curr Drug Targets **9**(3): 251-260.

Jackson, W. F. (2000). "Ion channels and vascular tone." Hypertension **35**(1 Pt 2): 173-178.

Jacobsen, J. C. and N. H. Holstein-Rathlou (2012). "A life under pressure: circumferential stress in the microvascular wall." Basic Clin Pharmacol Toxicol **110**(1): 26-34.

Jang, S. H., J. K. Byun, W. I. Jeon, S. Y. Choi, J. Park, B. H. Lee, J. E. Yang, J. B. Park, S. M. O'Grady, D. Y. Kim, P. D. Ryu, S. W. Joo and S. Y. Lee (2015). "Nuclear localization and functional characteristics of voltage-gated potassium channel Kv1.3." J Biol Chem **290**(20): 12547-12557.

Jang, S. H., S. Y. Choi, P. D. Ryu and S. Y. Lee (2011). "Anti-proliferative effect of Kv1.3 blockers in A549 human lung adenocarcinoma in vitro and in vivo." Eur J Pharmacol **651**(1-3): 26-32.

Jimenez-Perez, L., P. Cidad, I. Alvarez-Miguel, A. Santos-Hipolito, R. Torres-Merino, E. Alonso, M. A. de la Fuente, J. R. Lopez-Lopez and M. T. Perez-Garcia (2016). "Molecular Determinants of Kv1.3 Potassium Channels-induced Proliferation." J Biol Chem **291**(7): 3569-3580.

Kan, X. H., H. Q. Gao, Z. Y. Ma, L. Liu, M. Y. Ling and Y. Y. Wang (2016). "Kv1.3 potassium channel mediates macrophage migration in atherosclerosis by regulating ERK activity." Arch Biochem Biophys **591**: 150-156.

Kaneko, M., W. Yang, Y. Matsumoto, F. Watt and K. Funa (2006). "Activity of a novel PDGF beta-receptor enhancer during the cell cycle and upon differentiation of neuroblastoma." Exp Cell Res **312**(11): 2028-2039.

Kano, M. R., Y. Morishita, C. Iwata, S. Iwasaka, T. Watabe, Y. Ouchi, K. Miyazono and K. Miyazawa (2005). "VEGF-A and FGF-2 synergistically promote neoangiogenesis through enhancement of endogenous PDGF-B-PDGFRbeta signaling." J Cell Sci **118**(Pt 16): 3759-3768.

Kaplan-Albuquerque, N., V. Van Putten, M. C. Weiser-Evans and R. A. Nemenoff (2005). "Depletion of serum response factor by RNA interference mimics the mitogenic effects of platelet derived growth factor-BB in vascular smooth muscle cells." Circ Res **97**(5): 427-433.

Karin, M. (1995). "The regulation of AP-1 activity by mitogen-activated protein kinases." J Biol Chem **270**(28): 16483-16486.

Klemm, D. J., P. A. Watson, M. G. Frid, E. C. Dempsey, J. Schaack, L. A. Colton, A. Nesterova, K. R. Stenmark and J. E. Reusch (2001). "cAMP response element-binding protein content is a molecular determinant of smooth muscle cell proliferation and migration." J Biol Chem **276**(49): 46132-46141.

Kohl, T., E. Lorinczi, L. A. Pardo and W. Stuhmer (2011). "Rapid internalization of the oncogenic K+ channel K(V)10.1." PLoS One **6**(10): e26329.

Kohler, R., H. Wulff, I. Eichler, M. Kneifel, D. Neumann, A. Knorr, I. Grgic, D. Kampfe, H. Si, J. Wibawa, R. Real, K. Borner, S. Brakemeier, H. D. Orzechowski, H. P. Reusch, M. Paul, K. G. Chandy and J. Hoyer (2003). "Blockade of the intermediate-conductance calcium-activated potassium channel as a new therapeutic strategy for restenosis." Circulation **108**(9): 1119-1125.

Koni, P. A., R. Khanna, M. C. Chang, M. D. Tang, L. K. Kaczmarek, L. C. Schlichter and R. A. Flavella (2003). "Compensatory anion currents in Kv1.3 channel-deficient thymocytes." J Biol Chem **278**(41): 39443-39451.

Kotecha, S. A. and L. C. Schlichter (1999). "A Kv1.5 to Kv1.3 switch in endogenous hippocampal microglia and a role in proliferation." J Neurosci **19**(24): 10680-10693.

Kuang, Q., P. Purhonen and H. Hebert (2015). "Structure of potassium channels." Cell Mol Life Sci **72**(19): 3677-3693.

Kuhbandner, S., S. Brummer, D. Metzger, P. Chambon, F. Hofmann and R. Feil (2000). "Temporally controlled somatic mutagenesis in smooth muscle." Genesis **28**(1): 15-22.

Kumar, A. P. and A. P. Butler (1998). "Serum responsive gene expression mediated by Sp1." Biochem Biophys Res Commun **252**(2): 517-523.

Labro, A. J. and D. J. Snyders (2012). "Being flexible: the voltage-controllable activation gate of kv channels." Front Pharmacol **3**: 168.

Lallet-Daher, H., M. Roudbaraki, A. Bavencoffe, P. Mariot, F. Gackiere, G. Bidaux, R. Urbain, P. Gosset, P. Delcourt, L. Fleurisse, C. Slomianny, E. Dewailly, B. Mauroy, J. L. Bonnal, R. Skryma and N. Prevarskaya (2009). "Intermediate-conductance Ca2+-activated K+ channels (IKCa1) regulate human prostate cancer cell proliferation through a close control of calcium entry." Oncogene **28**(15): 1792-1806.

Lasch, M., A. Caballero-Martinez, K. Troidl, I. Schloegl, T. Lautz and E. Deindl (2016). "Arginase inhibition attenuates arteriogenesis and interferes with M2 macrophage accumulation." Lab Invest **96**(8): 830-838.

Lazarous, D. F., M. Scheinowitz, M. Shou, E. Hodge, S. Rajanayagam, S. Hunsberger, W. G. Robison, Jr., J. A. Stiber, R. Correa, S. E. Epstein and et al. (1995). "Effects of chronic systemic administration of basic fibroblast growth factor on collateral development in the canine heart." Circulation **91**(1): 145-153.

Leanza, L., B. Henry, N. Sassi, M. Zoratti, K. G. Chandy, E. Gulbins and I. Szabo (2012). "Inhibitors of mitochondrial Kv1.3 channels induce Bax/Bak-independent death of cancer cells." EMBO Mol Med **4**(7): 577-593.

Leanza, L., E. Venturini, S. Kadow, A. Carpinteiro, E. Gulbins and K. A. Becker (2015). "Targeting a mitochondrial potassium channel to fight cancer." Cell Calcium **58**(1): 131-138.

Ledoux, J., M. E. Werner, J. E. Brayden and M. T. Nelson (2006). "Calcium-activated potassium channels and the regulation of vascular tone." Physiology (Bethesda) **21**: 69-78.

Li, B., W. Jie, L. Huang, P. Wei, S. Li, Z. Luo, A. K. Friedman, A. L. Meredith, M. H. Han, X. H. Zhu and T. M. Gao (2014). "Nuclear BK channels regulate gene expression via the control of nuclear calcium signaling." Nat Neurosci **17**(8): 1055-1063.

Li, Y., P. Wang, J. Xu and G. V. Desir (2006). "Voltage-gated potassium channel Kv1.3 regulates GLUT4 trafficking to the plasma membrane via a Ca2+-dependent mechanism." Am J Physiol Cell Physiol **290**(2): C345-351.

Limbourg, A., T. Korff, L. C. Napp, W. Schaper, H. Drexler and F. P. Limbourg (2009). "Evaluation of postnatal arteriogenesis and angiogenesis in a mouse model of hind-limb ischemia." Nat Protoc **4**(12): 1737-1746.

Lu, Q., G. R. Schnitzler, K. Ueda, L. K. Iyer, O. I. Diomede, T. Andrade and R. H. Karas (2016). "ER Alpha Rapid Signaling Is Required for Estrogen Induced Proliferation and Migration of Vascular Endothelial Cells." PLoS One **11**(4): e0152807.

Mack, C. P. (2011). "Signaling mechanisms that regulate smooth muscle cell differentiation." Arterioscler Thromb Vasc Biol **31**(7): 1495-1505.

MacKinnon, R. (2003). "Potassium channels." FEBS Lett **555**(1): 62-65.

Martínez-Mármol, R., N. Comes, K. Styrczewska, M. Pérez-Verdaguer, R. Vicente, L. Pujadas, E. Soriano, A. Sorkin and A. Felipe (2016). "Unconventional EGF-induced ERK1/2-mediated Kv1.3 endocytosis." Cellular and molecular life sciences : CMLS **73**(7): 1515-1528.

Mayer, S. I., G. B. Willars, E. Nishida and G. Thiel (2008). "Elk-1, CREB, and MKP-1 regulate Egr-1 expression in gonadotropin-releasing hormone stimulated gonadotrophs." J Cell Biochem **105**(5): 1267-1278.

McCormack, T., K. McCormack, M. S. Nadal, E. Vieira, A. Ozaita and B. Rudy (1999). "The effects of Shaker beta-subunits on the human lymphocyte K+ channel Kv1.3." J Biol Chem **274**(29): 20123-20126.

Meier, P., J. Antonov, R. Zbinden, A. Kuhn, S. Zbinden, S. Gloekler, M. Delorenzi, R. Jaggi and C. Seiler (2009). "Non-invasive gene-expression-based detection of well-developed collateral function in individuals with and without coronary artery disease." Heart **95**(11): 900-908.

Meier, P., H. Hemingway, A. J. Lansky, G. Knapp, B. Pitt and C. Seiler (2012). "The impact of the coronary collateral circulation on mortality: a meta-analysis." Eur Heart J **33**(5): 614-621.

Meier, P., S. H. Schirmer, A. J. Lansky, A. Timmis, B. Pitt and C. Seiler (2013). "The collateral circulation of the heart." BMC Med **11**: 143.

Merchant, J. L., M. Du and A. Todisco (1999). "Sp1 phosphorylation by Erk 2 stimulates DNA binding." Biochem Biophys Res Commun **254**(2): 454-461.

Miguel-Velado, E., A. Moreno-Dominguez, O. Colinas, P. Cidad, M. Heras, M. T. Perez-Garcia and J. R. Lopez-Lopez (2005). "Contribution of Kv channels to phenotypic remodeling of human uterine artery smooth muscle cells." Circ Res **97**(12): 1280-1287.

Millership, J. E., D. C. Devor, K. L. Hamilton, C. M. Balut, J. I. Bruce and I. M. Fearon (2011). "Calcium-activated K+ channels increase cell proliferation independent of K+ conductance." Am J Physiol Cell Physiol **300**(4): C792-802.

Mitchell, D. L. and J. X. DiMario (2010). "AP-2 alpha suppresses skeletal myoblast proliferation and represses fibroblast growth factor receptor 1 promoter activity." Exp Cell Res **316**(2): 194-202.

Mobius-Winkler, S., M. Uhlemann, V. Adams, M. Sandri, S. Erbs, K. Lenk, N. Mangner, U. Mueller, J. Adam, M. Grunze, S. Brunner, T. Hilberg, M. Mende, A. P. Linke and G. Schuler (2016). "Coronary Collateral Growth Induced by Physical Exercise: Results of the Impact of Intensive Exercise Training on Coronary Collateral Circulation in Patients With Stable Coronary Artery Disease (EXCITE) Trial." Circulation **133**(15): 1438-1448; discussion 1448.

Mochizuki, S., B. Brassart and A. Hinek (2002). "Signaling pathways transduced through the elastin receptor facilitate proliferation of arterial smooth muscle cells." J Biol Chem **277**(47): 44854-44863.

Molander, C., A. Hackzell, M. Ohta, H. Izumi and K. Funa (2001). "Sp1 is a key regulator of the PDGF beta-receptor transcription." Mol Biol Rep **28**(4): 223-233.

Morales, P., L. Garneau, H. Klein, M. F. Lavoie, L. Parent and R. Sauve (2013). "Contribution of the KCa3.1 channel-calmodulin interactions to the regulation of the KCa3.1 gating process." J Gen Physiol **142**(1): 37-60.

Murrant, C. L. (2008). "Structural and functional limitations of the collateral circulation in peripheral artery disease." The Journal of Physiology **586**(Pt 24): 5845-5845.

Napoli, C., G. Paolisso, A. Casamassimi, M. Al-Omran, M. Barbieri, L. Sommese, T. Infante and L. J. Ignarro (2013). "Effects of nitric oxide on cell proliferation: novel insights." J Am Coll Cardiol **62**(2): 89-95.

Neylon, C. B., R. J. Lang, Y. Fu, A. Bobik and P. H. Reinhart (1999). "Molecular cloning and characterization of the intermediate-conductance Ca(2+)-activated K(+) channel in vascular smooth muscle: relationship between K(Ca) channel diversity and smooth muscle cell function." Circ Res **85**(9): e33-43.

Nguyen, H. M., C. A. Galea, G. Schmunk, B. J. Smith, R. A. Edwards, R. S. Norton and K. G. Chandy (2013). "Intracellular Trafficking of the K(V)1.3 Potassium Channel Is Regulated by the Prodomain of a Matrix Metalloprotease." The Journal of Biological Chemistry **288**(9): 6451-6464.

Nicolas, M., V. Noe and C. J. Ciudad (2003). "Transcriptional regulation of the human Sp1 gene promoter by the specificity protein (Sp) family members nuclear factor Y (NF-Y) and E2F." Biochem J **371**(Pt 2): 265-275.

Nugent, H. M., C. Rogers and E. R. Edelman (1999). "Endothelial implants inhibit intimal hyperplasia after porcine angioplasty." Circ Res **84**(4): 384-391.

Owens, G. K., M. S. Kumar and B. R. Wamhoff (2004). "Molecular regulation of vascular smooth muscle cell differentiation in development and disease." Physiol Rev **84**(3): 767-801.

Pagel, J. I., T. Ziegelhoeffer, M. Heil, S. Fischer, B. Fernandez, W. Schaper, K. T. Preissner and E. Deindl (2012). "Role of early growth response 1 in arteriogenesis: impact on vascular cell proliferation and leukocyte recruitment in vivo." Thromb Haemost **107**(3): 562-574.

Parakati, R. and J. X. DiMario (2002). "Sp1- and Sp3-mediated transcriptional regulation of the fibroblast growth factor receptor 1 gene in chicken skeletal muscle cells." J Biol Chem **277**(11): 9278-9285.

Parakati, R. and J. X. DiMario (2013). "Repression of myoblast proliferation and fibroblast growth factor receptor 1 promoter activity by KLF10 protein." J Biol Chem **288**(19): 13876-13884.

Pardo, L. A. (2004). "Voltage-gated potassium channels in cell proliferation." Physiology (Bethesda) **19**: 285-292.

Pare, G., A. Krust, R. H. Karas, S. Dupont, M. Aronovitz, P. Chambon and M. E. Mendelsohn (2002). "Estrogen receptor-alpha mediates the protective effects of estrogen against vascular injury." Circ Res **90**(10): 1087-1092.

Patel, S. D., M. Waltham, A. Wadoodi, K. G. Burnand and A. Smith (2010). "The role of endothelial cells and their progenitors in intimal hyperplasia." Ther Adv Cardiovasc Dis **4**(2): 129-141.

Patel, S. G. and J. X. DiMario (2001). "Two distal Sp1-binding cis-elements regulate fibroblast growth factor receptor 1 (FGFR1) gene expression in myoblasts." Gene **270**(1-2): 171-180.

Pena, T. L. and S. G. Rane (1999). "The fibroblast intermediate conductance K(Ca) channel, FIK, as a prototype for the cell growth regulatory function of the IK channel family." J Membr Biol **172**(3): 249-257.

Penna, A. and A. Stutzin (2015). "KCa3.1-Dependent Hyperpolarization Enhances Intracellular Ca2+ Signaling Induced by fMLF in Differentiated U937 Cells." PLoS One **10**(9): e0139243.

Pereira, L. E., F. Villinger, H. Wulff, A. Sankaranarayanan, G. Raman and A. A. Ansari (2007). "Pharmacokinetics, toxicity, and functional studies of the selective Kv1.3 channel blocker 5-(4-phenoxybutoxy)psoralen in rhesus macaques." Exp Biol Med (Maywood) **232**(10): 1338-1354.

Pfaffl, M. W. (2001). "A new mathematical model for relative quantification in real-time RT-PCR." Nucleic Acids Res **29**(9): e45.

Pipp, F., S. Boehm, W. J. Cai, F. Adili, B. Ziegler, G. Karanovic, R. Ritter, J. Balzer, C. Scheler, W. Schaper and T. Schmitz-Rixen (2004). "Elevated fluid shear stress enhances postocclusive collateral artery growth and gene expression in the pig hind limb." Arterioscler Thromb Vasc Biol **24**(9): 1664-1668.

Plane, F., R. Johnson, P. Kerr, W. Wiehler, K. Thorneloe, K. Ishii, T. Chen and W. Cole (2005). "Heteromultimeric Kv1 channels contribute to myogenic control of arterial diameter." Circ Res **96**(2): 216-224.

Pongs, O. and J. R. Schwarz (2010). "Ancillary subunits associated with voltage-dependent K+ channels." Physiol Rev **90**(2): 755-796.

Quesada, I., J. M. Rovira, F. Martin, E. Roche, A. Nadal and B. Soria (2002). "Nuclear KATP channels trigger nuclear Ca(2+) transients that modulate nuclear function." Proc Natl Acad Sci U S A **99**(14): 9544-9549.

Resnick, N., H. Yahav, A. Shay-Salit, M. Shushy, S. Schubert, L. C. Zilberman and E. Wofovitz (2003). "Fluid shear stress and the vascular endothelium: for better and for worse." Prog Biophys Mol Biol **81**(3): 177-199.

Rissanen, T. T., J. E. Markkanen, K. Arve, J. Rutanen, M. I. Kettunen, I. Vajanto, S. Jauhiainen, L. Cashion, M. Gruchala, O. Narvanen, P. Taipale, R. A. Kauppinen, G. M. Rubanyi and S. Yla-Herttuala (2003). "Fibroblast growth factor 4 induces vascular permeability, angiogenesis and arteriogenesis in a rabbit hindlimb ischemia model." Faseb j **17**(1): 100-102.

Roy, J. W., E. A. Cowley, J. Blay and P. Linsdell (2010). "The intermediate conductance Ca2+-activated K+ channel inhibitor TRAM-34 stimulates proliferation of breast cancer cells via activation of oestrogen receptors." Br J Pharmacol **159**(3): 650-658.

Saito, H., H. Kouhara, S. Kasayama, T. Kishimoto and B. Sato (1992). "Characterization of the promoter region of the murine fibroblast growth factor receptor 1 gene." Biochem Biophys Res Commun **183**(2): 688-693.

Sakamoto, K. M., C. Bardeleben, K. E. Yates, M. A. Raines, D. W. Golde and J. C. Gasson (1991). "5' upstream sequence and genomic structure of the human primary response gene, EGR-1/TIS8." Oncogene **6**(5): 867-871.

Santiago, F. S., H. C. Lowe, F. L. Day, C. N. Chesterman and L. M. Khachigian (1999). "Early growth response factor-1 induction by injury is triggered by release and paracrine activation by fibroblast growth factor-2." Am J Pathol **154**(3): 937-944.

Schaper, W. (2009). "Collateral circulation: past and present." Basic Res Cardiol **104**(1): 5-21.

Schaper, W., M. De Brabander and P. Lewi (1971). "DNA synthesis and mitoses in coronary collateral vessels of the dog." Circ Res **28**(6): 671-679.

Schaper, W. and J. Schaper (2004). "Arteriogenesis." Springer US.

Schaper, W. and D. Scholz (2003). "Factors regulating arteriogenesis." Arterioscler Thromb Vasc Biol **23**(7): 1143-1151.

Schirmer, S. H., J. O. Fledderus, P. T. Bot, P. D. Moerland, I. E. Hoefer, J. Baan, Jr., J. P. Henriques, R. J. van der Schaaf, M. M. Vis, A. J. Horrevoets, J. J. Piek and N. van Royen (2008). "Interferon-beta signaling is enhanced in patients with insufficient coronary collateral artery development and inhibits arteriogenesis in mice." Circ Res **102**(10): 1286-1294.

Schirmer, S. H., F. C. van Nooijen, J. J. Piek and N. van Royen (2009). "Stimulation of collateral artery growth: travelling further down the road to clinical application." Heart **95**(3): 191-197.

Schmitz, A., A. Sankaranarayanan, P. Azam, K. Schmidt-Lassen, D. Homerick, W. Hansel and H. Wulff (2005). "Design of PAP-1, a selective small molecule Kv1.3 blocker, for the suppression of effector memory T cells in autoimmune diseases." Mol Pharmacol **68**(5): 1254-1270.

Scholz, D., W. Ito, I. Fleming, E. Deindl, A. Sauer, M. Wiesnet, R. Busse, J. Schaper and W. Schaper (2000). "Ultrastructure and molecular histology of rabbit hind-limb collateral artery growth (arteriogenesis)." Virchows Arch **436**(3): 257-270.

Scholz, D., T. Ziegelhoeffer, A. Helisch, S. Wagner, C. Friedrich, T. Podzuweit and W. Schaper (2002). "Contribution of arteriogenesis and angiogenesis to postocclusive hindlimb perfusion in mice." J Mol Cell Cardiol **34**(7): 775-787.

Schwachtgen, J. L., C. J. Campbell and M. Braddock (2000). "Full promoter sequence of human early growth response factor-1 (Egr-1): demonstration of a fifth functional serum response element." DNA Seq **10**(6): 429-432.

Seyed, M. and J. X. Dimario (2007). "Sp1 is required for transcriptional activation of the fibroblast growth factor receptor 1 gene in neonatal cardiomyocytes." Gene **400**(1-2): 150-157.

Shepherd, M. C., S. M. Duffy, T. Harris, G. Cruse, M. Schuliga, C. E. Brightling, C. B. Neylon, P. Bradding and A. G. Stewart (2007). "KCa3.1 Ca2+ activated K+ channels regulate human airway smooth muscle proliferation." Am J Respir Cell Mol Biol **37**(5): 525-531.

Si, H., I. Grgic, W. T. Heyken, T. Maier, J. Hoyer, H. P. Reusch and R. Kohler (2006). "Mitogenic modulation of Ca2+ -activated K+ channels in proliferating A7r5 vascular smooth muscle cells." Br J Pharmacol **148**(7): 909-917.

Si, H., W. T. Heyken, S. E. Wolfle, M. Tysiac, R. Schubert, I. Grgic, L. Vilianovich, G. Giebing, T. Maier, V. Gross, M. Bader, C. de Wit, J. Hoyer and R. Kohler (2006). "Impaired endothelium-derived hyperpolarizing factor-mediated dilations and increased blood pressure in mice deficient of the intermediate-conductance Ca2+-activated K+ channel." Circ Res **99**(5): 537-544.

Siddiqui-Jain, A., C. L. Grand, D. J. Bearss and L. H. Hurley (2002). "Direct evidence for a G-quadruplex in a promoter region and its targeting with a small molecule to repress c-MYC transcription." Proc Natl Acad Sci U S A **99**(18): 11593-11598.

Simons, M., B. H. Annex, R. J. Laham, N. Kleiman, T. Henry, H. Dauerman, J. E. Udelson, E. V. Gervino, M. Pike, M. J. Whitehouse, T. Moon and N. A. Chronos (2002). "Pharmacological treatment of coronary artery disease with recombinant fibroblast growth factor-2: double-blind, randomized, controlled clinical trial." Circulation **105**(7): 788-793.

Sole, L., S. R. Roig, A. Vallejo-Gracia, A. Serrano-Albarras, R. Martinez-Marmol, M. M. Tamkun and A. Felipe (2016). "The C-terminal domain of Kv1.3 regulates functional interactions with the KCNE4 subunit." J Cell Sci **129**(22): 4265-4277.

Sole, L., M. Roura-Ferrer, M. Perez-Verdaguer, A. Oliveras, M. Calvo, J. M. Fernandez-Fernandez and A. Felipe (2009). "KCNE4 suppresses Kv1.3 currents by modulating trafficking, surface expression and channel gating." J Cell Sci **122**(Pt 20): 3738-3748.

Sprossmann, F., P. Pankert, U. Sausbier, A. Wirth, X. B. Zhou, J. Madlung, H. Zhao, I. Bucurenciu, A. Jakob, T. Lamkemeyer, W. Neuhuber, S. Offermanns, M. J. Shipston, M. Korth, A. Nordheim, P. Ruth and M. Sausbier (2009). "Inducible knockout mutagenesis reveals compensatory mechanisms elicited by constitutive BK channel deficiency in overactive murine bladder." Febs j **276**(6): 1680-1697.

Stabile, E., T. Kinnaird, A. la Sala, S. K. Hanson, C. Watkins, U. Campia, M. Shou, S. Zbinden, S. Fuchs, H. Kornfeld, S. E. Epstein and M. S. Burnett (2006). "CD8+ T lymphocytes regulate the arteriogenic response to ischemia by infiltrating the site of collateral vessel development and recruiting CD4+ mononuclear cells through the expression of interleukin-16." Circulation **113**(1): 118-124.

Stefanini, G. G. and D. R. Holmes, Jr. (2013). "Drug-eluting coronary-artery stents." N Engl J Med **368**(3): 254-265.

Straub, S. V., S. M. Perez, B. Tan, K. A. Coughlan, C. E. Trebino, P. Cosgrove, J. M. Buxton, J. M. Kreeger and V. M. Jackson (2011). "Pharmacological inhibition of Kv1.3 fails to modulate insulin sensitivity in diabetic mice or human insulin-sensitive tissues." Am J Physiol Endocrinol Metab **301**(2): E380-390.

Su, X. L., Y. Wang, W. Zhang, L. M. Zhao, G. R. Li and X. L. Deng (2011). "Insulin-mediated upregulation of K(Ca)3.1 channels promotes cell migration and proliferation in rat vascular smooth muscle." J Mol Cell Cardiol **51**(1): 51-57.

Sullivan, C. J., T. Doetschman and J. B. Hoying (2002). "Targeted disruption of the Fgf2 gene does not affect vascular growth in the mouse ischemic hindlimb." J Appl Physiol (1985) **93**(6): 2009-2017.

Takeda, Y., S. Costa, E. Delamarre, C. Roncal, R. Leite de Oliveira, M. L. Squadrito, V. Finisguerra, S. Deschoemaeker, F. Bruyere, M. Wenes, A. Hamm, J. Serneels, J. Magat, T. Bhattacharyya, A. Anisimov, B. F. Jordan, K. Alitalo, P. Maxwell, B. Gallez, Z. W. Zhuang, Y. Saito, M. Simons, M. De Palma and M. Mazzone (2011). "Macrophage skewing by Phd2 haplodeficiency prevents ischaemia by inducing arteriogenesis." Nature **479**(7371): 122-126.

Tan, N. Y. and L. M. Khachigian (2009). "Sp1 phosphorylation and its regulation of gene transcription." Mol Cell Biol **29**(10): 2483-2488.

Tang, Y., S. Yu, Y. Liu, J. Zhang, L. Han and Z. Xu (2017). "MicroRNA-124 controls human vascular smooth muscle cell phenotypic switch via Sp1." Am J Physiol Heart Circ Physiol **313**(3): H641-h649.

Tapias, A., C. J. Ciudad, I. B. Roninson and V. Noe (2008). "Regulation of Sp1 by cell cycle related proteins." Cell Cycle **7**(18): 2856-2867.

Tashiro, E., H. Maruki, Y. Minato, Y. Doki, I. B. Weinstein and M. Imoto (2003). "Overexpression of cyclin D1 contributes to malignancy by up-regulation of fibroblast growth factor receptor 1 via the pRB/E2F pathway." Cancer Res **63**(2): 424-431.

Tharp, D. L., B. R. Wamhoff, J. R. Turk and D. K. Bowles (2006). "Upregulation of intermediate-conductance Ca2+-activated K+ channel (IKCa1) mediates phenotypic modulation of coronary smooth muscle." Am J Physiol Heart Circ Physiol **291**(5): H2493-2503.

Tharp, D. L., B. R. Wamhoff, H. Wulff, G. Raman, A. Cheong and D. K. Bowles (2008). "Local delivery of the KCa3.1 blocker, TRAM-34, prevents acute angioplasty-induced coronary smooth muscle phenotypic modulation and limits stenosis." Arterioscler Thromb Vasc Biol **28**(6): 1084-1089.

Tian, Y., X. Yue, D. Luo, R. Wazir, J. Wang, T. Wu, L. Chen, B. Liao and K. Wang (2013). "Increased proliferation of human bladder smooth muscle cells is mediated by physiological cyclic stretch via the PI3KSGK1Kv1.3 pathway." Mol Med Rep **8**(1): 294-298.

Toyama, K., H. Wulff, K. G. Chandy, P. Azam, G. Raman, T. Saito, Y. Fujiwara, D. L. Mattson, S. Das, J. E. Melvin, P. F. Pratt, O. A. Hatoum, D. D. Gutterman, D. R. Harder and H. Miura (2008). "The intermediate-conductance calcium-activated potassium channel KCa3.1 contributes to atherogenesis in mice and humans." J Clin Invest **118**(9): 3025-3037.

Troidl, C., G. Jung, K. Troidl, J. Hoffmann, H. Mollmann, H. Nef, W. Schaper, C. W. Hamm and T. Schmitz-Rixen (2013). "The temporal and spatial distribution of macrophage subpopulations during arteriogenesis." Curr Vasc Pharmacol **11**(1): 5-12.

Troidl, C., H. Nef, S. Voss, A. Schilp, S. Kostin, K. Troidl, S. Szardien, A. Rolf, T. Schmitz-Rixen, W. Schaper, C. W. Hamm, A. Elsasser and H. Mollmann (2010). "Calcium-

dependent signalling is essential during collateral growth in the pig hind limb-ischemia model." J Mol Cell Cardiol **49**(1): 142-151.

Troidl, C., K. Troidl, W. Schierling, W. J. Cai, H. Nef, H. Mollmann, S. Kostin, S. Schimanski, L. Hammer, A. Elsasser, T. Schmitz-Rixen and W. Schaper (2009). "Trpv4 induces collateral vessel growth during regeneration of the arterial circulation." J Cell Mol Med **13**(8b): 2613-2621.

Ungricht, R. and U. Kutay (2015). "Establishment of NE asymmetry-targeting of membrane proteins to the inner nuclear membrane." Curr Opin Cell Biol **34**: 135-141.

Unthank, J. L., J. C. Nixon and M. C. Dalsing (1996). "Inhibition of NO synthase prevents acute collateral artery dilation in the rat hindlimb." J Surg Res **61**(2): 463-468.

Urrego, D., A. P. Tomczak, F. Zahed, W. Stuhmer and L. A. Pardo (2014). "Potassium channels in cell cycle and cell proliferation." Philos Trans R Soc Lond B Biol Sci **369**(1638): 20130094.

van Varik, B. J., R. J. Rennenberg, C. P. Reutelingsperger, A. A. Kroon, P. W. de Leeuw and L. J. Schurgers (2012). "Mechanisms of arterial remodeling: lessons from genetic diseases." Front Genet **3**: 290.

Vaziri, C. and D. V. Faller (1995). "Repression of platelet-derived growth factor beta-receptor expression by mitogenic growth factors and transforming oncogenes in murine 3T3 fibroblasts." Mol Cell Biol **15**(3): 1244-1253.

Vicente, R., A. Escalada, M. Coma, G. Fuster, E. Sanchez-Tillo, C. Lopez-Iglesias, C. Soler, C. Solsona, A. Celada and A. Felipe (2003). "Differential voltage-dependent K+ channel responses during proliferation and activation in macrophages." J Biol Chem **278**(47): 46307-46320.

Vogel, S., T. Kubin, D. von der Ahe, E. Deindl, W. Schaper and R. Zimmermann (2006). "MEK hyperphosphorylation coincides with cell cycle shut down of cultured smooth muscle cells." J Cell Physiol **206**(1): 25-34.

Wang, D. Z. and E. N. Olson (2004). "Control of smooth muscle development by the myocardin family of transcriptional coactivators." Curr Opin Genet Dev **14**(5): 558-566.

Wang, J., H. Dai, N. Yousaf, M. Moussaif, Y. Deng, A. Boufelliga, O. R. Swamy, M. E. Leone and H. Riedel (1999). "Grb10, a positive, stimulatory signaling adapter in platelet-derived growth factor BB-, insulin-like growth factor I-, and insulin-mediated mitogenesis." Mol Cell Biol **19**(9): 6217-6228.

Wang, L., D. Wei, S. Huang, Z. Peng, X. Le, T. T. Wu, J. Yao, J. Ajani and K. Xie (2003). "Transcription factor Sp1 expression is a significant predictor of survival in human gastric cancer." Clin Cancer Res **9**(17): 6371-6380.

Wang, Y. N., H. Yamaguchi, J. M. Hsu and M. C. Hung (2010). "Nuclear trafficking of the epidermal growth factor receptor family membrane proteins." Oncogene **29**(28): 3997-4006.

Wang, Z., D. Z. Wang, D. Hockemeyer, J. McAnally, A. Nordheim and E. N. Olson (2004). "Myocardin and ternary complex factors compete for SRF to control smooth muscle gene expression." Nature **428**(6979): 185-189.

Wang, Z. H., B. Shen, H. L. Yao, Y. C. Jia, J. Ren, Y. J. Feng and Y. Z. Wang (2007). "Blockage of intermediate-conductance-Ca(2+) -activated K(+) channels inhibits progression of human endometrial cancer." Oncogene **26**(35): 5107-5114.

Weekes, D., T. G. Kashima, C. Zandueta, N. Perurena, D. P. Thomas, A. Sunters, C. Vuillier, A. Bozec, E. El-Emir, I. Miletich, A. Patino-Garcia, F. Lecanda and A. E. Grigoriadis (2016).

"Regulation of osteosarcoma cell lung metastasis by the c-Fos/AP-1 target FGFR1." Oncogene **35**(22): 2852-2861.

WHO (2015). "World-Health-Organisation. Who fact sheet n°317. Cardiovascular diseases (cvds). 2015."

Wright, S. H. (2004). "Generation of resting membrane potential." Adv Physiol Educ **28**(1-4): 139-142.

Wulff, H. and N. A. Castle (2010). "Therapeutic potential of KCa3.1 blockers: recent advances and promising trends." Expert Rev Clin Pharmacol **3**(3): 385-396.

Wulff, H., M. J. Miller, W. Hansel, S. Grissmer, M. D. Cahalan and K. G. Chandy (2000). "Design of a potent and selective inhibitor of the intermediate-conductance Ca2+-activated K+ channel, IKCa1: a potential immunosuppressant." Proc Natl Acad Sci U S A **97**(14): 8151-8156.

Xu, J., P. A. Koni, P. Wang, G. Li, L. Kaczmarek, Y. Wu, Y. Li, R. A. Flavell and G. V. Desir (2003). "The voltage-gated potassium channel Kv1.3 regulates energy homeostasis and body weight." Hum Mol Genet **12**(5): 551-559.

Yang, H., X. Li, J. Ma, X. Lv, S. Zhao, W. Lang and Y. Zhang (2013). "Blockade of the intermediate-conductance Ca(2+)-activated K+ channel inhibits the angiogenesis induced by epidermal growth factor in the treatment of corneal alkali burn." Exp Eye Res **110**: 76-87.

Yang, H. T., M. R. Deschenes, R. W. Ogilvie and R. L. Terjung (1996). "Basic fibroblast growth factor increases collateral blood flow in rats with femoral arterial ligation." Circ Res **79**(1): 62-69.

Yang, X. W., J. W. Liu, R. C. Zhang, Q. Yin, W. Z. Shen and J. L. Yi (2013). "Inhibitory effects of blockage of intermediate conductance Ca(2+)-activated K (+) channels on proliferation of hepatocellular carcinoma cells." J Huazhong Univ Sci Technolog Med Sci **33**(1): 86-89.

Yoshida, T., S. Sinha, F. Dandre, B. R. Wamhoff, M. H. Hoofnagle, B. E. Kremer, D. Z. Wang, E. N. Olson and G. K. Owens (2003). "Myocardin is a key regulator of CArG-dependent transcription of multiple smooth muscle marker genes." Circ Res **92**(8): 856-864.

Yuan, X. J., J. Wang, M. Juhaszova, V. A. Golovina and L. J. Rubin (1998). "Molecular basis and function of voltage-gated K+ channels in pulmonary arterial smooth muscle cells." Am J Physiol **274**(4 Pt 1): L621-635.

Yue, T. L., L. Vickery-Clark, C. S. Louden, J. L. Gu, X. L. Ma, P. K. Narayanan, X. Li, J. Chen, B. Storer, R. Willette, K. A. Gossett and E. H. Ohlstein (2000). "Selective estrogen receptor modulator idoxifene inhibits smooth muscle cell proliferation, enhances reendothelialization, and inhibits neointimal formation in vivo after vascular injury." Circulation **102**(19 Suppl 3): Iii281-288.

Zakrzewicz, A., T. W. Secomb and A. R. Pries (2002). "Angioadaptation: keeping the vascular system in shape." News Physiol Sci **17**: 197-201.

Ziegler, M. A., M. R. Distasi, R. G. Bills, S. J. Miller, M. Alloosh, M. P. Murphy, A. G. Akingba, M. Sturek, M. C. Dalsing and J. L. Unthank (2010). "Marvels, Mysteries, and Misconceptions of Vascular Compensation to Peripheral Artery Occlusion." Microcirculation (New York, N.Y. : 1994) **17**(1): 3-20.

Zuleger, N., N. Korfali and E. C. Schirmer (2008). "Inner nuclear membrane protein transport is mediated by multiple mechanisms." Biochem Soc Trans **36**(Pt 6): 1373-1377.

9. Abbreviations

Ab	Antibody
α-SMA	Alpha smooth muscle actin
ANOVA	Analysis of variance
AP-1	Activator protein-1
BC	Bundle crossing
BrdU	Bromodeoxyuridine
BSA	Bovine serum albumin
Ca^{2+}	Calcium ion
CaM	Calmodulin
CaMBD	Calmodulin binding domain
cAMP	Cyclic adenosine monophosphate
CD31	Cluster of differentiation 31
cDNA	Complementary DNA
CHD	Coronary heart disease
Cl^-	Chloride ion
Con	Control
CREB	cAMP response element-binding protein
CVD	Cardiovascular disease
CWS	Circumferential wall stress
DAB	3,3'-diaminobenzidine
DNA	Deoxyribonucleic acid
DAPI	4',6-diamidino-2-phenylindole
DES	Drug-eluting stent
DMEM	Dulbecco's modified Eagle's medium
DMSO	Dimethyl sulfoxide
eag	Éther-a-gogo
EC	Endothelial cell
ECM	Extracellular matrix
EDHF	Endothelium-derived hyperpolarization factor
EDTA	Ethylenediaminetetraacetic acid
EEL	Externa elastic lamina
EGF	Epidermal growth factor
EGFR	EGF receptor
EGR-1	Early growth response 1

eNOS	Endothelial nitric oxide synthase
ER	Endoplasmic reticulum
ERK	Extracellular-signal regulated kinase
Ets	E26 transformation-specific
FAK	Focal adhesion kinase
FAL	Femoral artery ligation
FCS	Foetal calf serum
FGF	Fibroblast growth factor
FGFR-1	Fibroblast growth factor receptor 1
FN	Fibronectin
FSS	Fluid shear stress
GF	Growth factor
HEK	Human embryonic kidney cells
HRP	Horseradish peroxidase
HUVECs	Human umbilical vein ECs
i.p.	Intraperitoneally
ICAM-1	Intercellular adhesion molecule 1
IEL	Internal elastic lamina
INM	Inner nuclear membrane
K^+	Potassium ion
K2P	Tandem pore domain K^+ channel
$K_{Ca}1.1$	Ca^{2+}-gated K^+ channel subfamily M, alpha member 1
$K_{Ca}3.1$	Ca^{2+}-gated K^+ channel subfamily N, member 4
KCNE4	Potassium voltage-gated channel subfamily E member 4
K_{ir}	Inwardly rectifying K^+ channel
K_{ligand}	Ligand-activated K^+ channels
KO	Knockout
K_V	Voltage-gated K^+ channel
$K_V1.10$	Voltage-gated K^+ channel subfamily H member 10
$K_V1.3$	Voltage-gated K^+ channel subfamily A member 1
LDI	Laser Doppler imaging
MAPK	Mitogen-activated protein kinase
MArSMCs	Mouse artery SMCs
MCP-1	Monocyte chemoattractant protein 1
MEJ	Myoendothelial junctions
MgTX	Margatoxin

mmHg	Millimeter of mercury
MMP	Matrix metalloproteinase
MP	Membrane potential
mRNA	Messenger RNA
MRTF	Myocardin related transcription factor
MTM	Mithramycin A
Na^+	Sodium ion
NE	Nuclear envelope
NLS	Nuclear localization signal
NO	Nitric oxide
NPC	Nuclear pore complexes
occ	Occluded
ONM	Outer nuclear membrane
PAD	Peripheral artery disease
PBS	Phosphate-buffered saline
PBST	Phosphate-buffered saline 1 % tween 20
PCR	Polymerase chain reaction
PDGF-BB	Platelet-derived growth factor ß
PDGFR	Platelet-derived growth factor receptor
p-ERK	Phosphorylated ERK
PFA	Paraformaldehyde
PM	Phenotypic modulation
qPCR	Quantitative polymerase chain reaction
RNA	Ribonucleic acid
rRNA	Ribosomal RNA
RT	Room temperature
RTK	Receptor tyrosine kinase
SDS	Sodium dodecyl sulfate
SDS-PAGE	Sodium dodecyl sulfate-polyacrylamide gel electrophoresis
SEM	Standard error of the mean
SF	Selectivity filter
siRNA	Small interference RNA
SM22-α	Smooth muscle 22 alpha
SMC	Smooth muscle cell
SMCGM	SMC growth medium
SMMHC	Smooth muscle myosin heavy chain

Sp/KLF	Specificity protein/Krüppel like factor family
Sp1	Specificity protein 1
SRF	Serum response factor
TBST	Tris-buffered saline 1 % tween 20
TCF	Ternary complex factor
TF	Transcription factor
TGF-ß	Tumor growth factor-ß
TRPV4	Ca^{2+}-channel transient receptor potential cation channel, subfamily V, member 4
UBTF1	Upstream binding transcription factor 1
VCAM-1	Vascular cell adhesion molecule 1
VEGF-A	Vascular endothelial growth factor
VSD	Voltage-sensing domain
WHO	World Health Organisation

Acknowledgments

I am indebted to my supervisor PD Dr rer. nat. Elisabeth Deindl for giving me the chance to complete my PhD in such an exciting field of cardiovascular physiology. I appreciate her scientific advice and the freedom she gave me to pursue own ideas. I am also grateful for the helpful suggestions regarding the writing of this manuscript.

I would like to thank Prof Dr Ulrich Pohl for his manifested interest in this project and for allowing me to perform the experiments at the Walter Brendel-Centre.

To Prof Dr Klaus T. Preissner from the Justus-Liebig-University in Giessen for the financial support at the end of the experimental work.

I would like to extend my gratitude to all my colleagues in the lab for the work together and the nice atmosphere these years! I thoroughly enjoyed learning from Dr Omary Chillo the femoral artery ligation model and LDI technique and passing this knowledge to the new PhD students. To Manuel Lasch, Thomas Lautz and Dr Eike Kleinert for offering assistance whenever needed it. I am also grateful to Christine Csapò for her technical assistance and for taking care of so many organization things. A special thanks to Dr Eike Kleinert for his encouragement and support.

I strongly profited from the cooperative, friendly and international atmosphere at the WBC and I would like to say thank you to many people: Claudia Faney for her technical advices at the cell culture, Dr Michael Lorenz and Stefan Schmitt, for answering so many technical questions, Dr Julian Kirsch and Dr Holger Schneider for the scientific discussions and finally Dr Bettina Pitter, Dr Katharina Nekolla, Dr Sabine Sellner, Dr. Gabriele Zuchtriegel, Dr Louise Ince and Justin Chen for their help and encouragement.

I am deeply grateful to Alba de Juan, not only for her help with fluorescence microscopy but even more for the many scientific discussions, for being there in the bad moments and enjoying the good results as if they were her own ones. For making Mondays more exciting and for the therapeutic swimming hours!

Special thanks to Dr Xiaoling Liang for her personal support and encouragement before and during the thesis. For our cooking times together and long dinner conversations, and phone calls! I am indebted to her for the valuable suggestions regarding the writing of this thesis.

I would like to thank my closest friends in Munich, at home and abroad for their invaluable support.

Finally, I want to thank the most important people in my life, my family. A mis padres, hacia los que siento un inmenso agradecimiento por enseñarme, alentarme y apoyarme incondicionalmente. My parents, my siblings and brother's family have always been a source of love, wellness and trust. Without this fortifying family entourage, I would not be where I am.

My children have been a source of energy and inspiration during the writing of this thesis. But this end would not have been possible without the comprehension, generosity and love of my husband, Markus. To him, to our family, I dedicate this work.

Eidesstattliche Versicherung

Caballero Martínez, Amelia

Name, Vorname

Ich erkläre hiermit an Eides statt,

dass ich die vorliegende Dissertation mit dem Thema

The role of the potassium channels KV1.3 and KCa3.1 in arteriogenic smooth muscle cell proliferation

selbständig verfasst, mich außer der angegebenen keiner weiteren Hilfsmittel bedient und alle Erkenntnisse, die aus dem Schrifttum ganz oder annähernd übernommen sind, als solche kenntlich gemacht und nach ihrer Herkunft unter Bezeichnung der Fundstelle einzeln nachgewiesen habe.

Ich erkläre des Weiteren, dass die hier vorgelegte Dissertation nicht in gleicher oder in ähnlicher Form bei einer anderen Stelle zur Erlangung eines akademischen Grades eingereicht wurde.

München, 06.06.2018

Ort, Datum

Amelia Caballero Martínez

Unterschrift Doktorandin/Doktorand